1988

Developing a procedure to reduce thermal shock influence in a steam turbine due to cold start

Ching-Po Liu

DEVELOPING A PROCEDURE TO REDUCE THERMAL SHOCK INFLUENCE IN A STEAM TURBINE DUE TO COLD START

BY

CHING-PO LIU

A THESIS SUBMITTED
IN
PARTIAL FULFILLMENT
OF THE
REQUIREMENTS FOR THE DEGREE OF
MASTER OF SCIENCE
IN
MECHANICAL ENGINEERING

APPROVED BY:

PROFESSOR_____
(THESIS ADVISOR)

PROFESSOR_____

PROFESSOR_____

PROFESSOR P. Marletcar
(DEPARTMENT HEAD)

DEPARTMENT OF MECHANICAL ENGINEERING
COLLEGE OF ENGINEERING
ROCHESTER INSTITUTE OF TECHNOLOGY
ROCHESTER, NEW YORK
FEBRUARY, 1988

Revised sample statement for granting or denying permission to reproduce an RIT thesis.

Title of Thesis Developing a Procedure to Reduce Thermal Shock of a Steam Turbine

---

I Ching-Po Liu **hereby (grant, deny) permission to the Wallace Memorial Library, of R.I.T., to reproduce my thesis in whole or in part. Any reproduction will not be for commercial use or profit.**

Or

I _____ **prefer to be contacted each time a request for reproduction is made. I can be reached at the following address.** _____

_____

Date May 10, 1988

ABSTRACT

An improved procedure is developed to reduce the thermal shock influence in a steam turbine due to a cold start operation. Thermal shock, a term used to describe the sudden imposition of a large heat flux and temperature gradient on a material surface, is a potential damage mechanism if its intensity is sufficiently high. For the case of a turbine cold start, the thermal shock intensity depends on the film coefficient and the initial temperature difference between the steam and the rotor surface. Reduction of thermal shock intensity can be achieved in several ways, such as lengthening the transit time, lowering the film coefficient, and reducing the temperature difference between the steam and the rotor surface.

One of the most efficient procedures employed to control the thermal shock influence is to increase the heating steps and warm up time. A case studied in this project, the normal two-step heating operation causes a very high compressive stress, 437 MPA, on the platform during the first heating step. Sometimes its magnitude is two or three times greater than the compressive stresses during second heating step. In this two-step heating operation the first heating temperature was 204C and the total operating time for the first heating step was 75 seconds. An improved procedure, a three-step heating operation, was developed to make the stresses caused by each heating step uniform. The first heating step of the two-step heating operation was substituted by the first two heating steps of the three-step heating

operation. The maximum thermal stress as a result of the improved operation was 358 MPA and the total operating time of the first two steps was 22.5 minutes. Under the 22.5 minutes operating time the optimum temperature for the first heating step was 162C, followed by another temperature increment to 204C.

Another study was conducted to study the effects of thermal stresses on different film coefficients (heat transfer coefficients). Under the same operating conditions the stress did not change significantly for the film coefficients from 50% to 150% of the normal operating value of 10,000 W/m^2K.

The thermal behavior obtained in this project will be useful for a turbine designer to ensure that no propagating crack would be formed within the life-time of the design machine. It is obvious that the longer the warm up time, the lower the thermal shock will be. From an economic point of view, longer warm up times are undesirable. A turbine designer needs to consider both these aspects before arriving at a strategy for the cold start.

NOMENCLATURE

C_p - Specific heat at constant pressure, J/kgK

HF (h) - Film coefficient (Convective heat transfer coefficient), W/m^2-K

C - Temperature, degrees Celsius, $^{\circ}C$

E - Young's modulus of elasticity, N/m^2

g - Acceleration due to gravity, m/s^2

k - Thermal conductivity, W/m-K

r - Radius, m

Re - Reynolds number, dimensionless

S_u - Ultimate strength, N/m

$\overline{T}$ - Mean Temperature, $^{\circ}C$

T_s - Surface Temperature, $^{\circ}C$

α - Thermal diffusivity, m^2/s

β - Coefficient of thermal expansion, K^{-1}

μ - Viscosity, Kg/ms

ν - Kinematic Viscosity, m^2/s

ρ - Density, Kg/m^3

τ - Shear stress, N/m^2

σ_M - Mean stress, N/m^2

σ_v - Dynamic stress, N/m^2

Listing of Figures and Tables

TABLE OF CONTENTS

1.0 INTRODUCTION

During the nineteenth century a number of attempts were made to design a practical steam turbine, and several famous engineers attempted to solve this problem. A good historical review of the steam turbine evolution is given by Storer (1969). According to this source Richard Trevithick patented a 'whirling engine' in 1815 and then proceeded to build a full-sized unit. Steam jets were installed at the ends of arms, 15 feet in diameter, and the people who worked on it thought it to be a device for launching missiles at the French. Although it was undoubtedly impressive, it was not a practical project, and Trevithick abandoned it. Other engineers, including John Ericsson, James Nasmyth and Timothy Burstall, turned their attention to the problem of making a steam turbine. Neither these turbines, nor those built by several concurrent inventors, advanced beyond the experimental stage, and it was not until the 1880s that a practical working turbine came into view. When this happened two completely different designs were produced, one in England and the other in Sweden. The Hon. Charles Algernon Parsons (later Sir Charles Parsons) patented his first reaction turbine in 1884, while his Swedish counterpart Carl Gustaf Patrik de Laval was developing an impulse-type of steam turbine.

Despite its very short period of development, Parsons' turbine and dynamo were very successful and the unit remained in service for about sixteen years. Steam at 80 psig was supplied to the turbine, which drove the dynamo at a speed of 18,000 revolutions per minute and produced electrical power equivalent to about 5 horse-power. It was

not as efficient as Parsons had expected, and he immediately started work on improved turbines. His original example is kept in the Science Museum in London.

During the early years of the twentieth century, many different turbines were built uniting improvements in design and combining different types of turbine into one set. Some very complex designs were produced by mixing the impulse and reaction principles together with the alternative methods of compounding and the two types of flow, axial and radial.

The design of reliable, efficient steam turbines requires the application of many diverse areas of technology. There are many competing design and material requirements that must be thoroughly evaluated, so that optimum trade-offs can be achieved. As new design requirements are imposed and as in-service problems occur, the turbine-manufacturer must possess the technical competence to reconcile them quickly and effectively.

The most up-to-date available technology is employed in the design of steam turbines. For example, finite element methods are used for calculating stresses, vibratory frequencies, mode shapes, and temperatures. Fracture mechanics technology is used to evaluate the ability of turbine components to tolerate flaws of various types. Where currently available technology is inadequate for evaluating the turbine design, more advanced technology is developed to meet this need.

The axial flow steam turbines have been built for power stations for many years. Turbines derive their power from a moving substance which

has kinetic energy, determined by two factors - the weight of the substance together with its speed. Water, being heavy, can store considerable energy when travelling at moderate speeds, but steam is very light and must therefore travel much faster than water in order to store the same energy. A turbine converts this store of energy into useful work, and so a steam turbine must rotate at speeds far in excess of its water - driven counterpart. Here comes a problem in steam turbine when starting a 'cold' turbine or during other changes of operation. The sudden application of hot steam to cold turbine surfaces will cause a 'Thermal Shock'.

Before discussing the thermal shock problem, a term called "low cycle fatigue" is worth discussing. The subject of cyclic creep plays a major role in the low cycle fatigue analysis which has been discussed by many investigators including Puglia and Manfredi (1978) and Manson (1966). This is one of a number of challenging tasks that confront researchers in solid mechanics.

Steam turbines are expected to operate under high temperature and pressure conditions for an extended period of time of weeks or months before they are shut down for maintenance or other repairs. During this long period of operation, little variation of temperature and stress conditions in the structure is expected. It is often referred to as the "hold" time in the study of the low cycle fatigue of materials. The significance of the "hold" time in power cycles has been recognized by engineers for a long time. However, very little information is available for the quantitative analysis of its effect on the overall thermomechanical behavior of the structure.

An approach to the low cycle thermomechanical behavior of structure was proposed by Liu and Hsu (1982) with the TEPSAC code, using the kinematic hardening scheme. The rationale was that the thermoelastic-plastic part of the analysis can be used for the start-up and shut-down portions of the load cycles whereas the thermal-creep part of the TEPSAC code can analyze the structure behavior during the long "hold" time.

Analyses of thermal stresses usually are based on conditions of initial and final thermal equilibrium, such as uniform temperature or steady-state heat flow. In practice, however, thermal stresses can arise due to sudden changes in the ambient thermal conditions (temperature, heat flux, etc.) at an instant in time when the component or structure is not at thermal equilibrium. This situation, for instance, is expected to be the case for components of internal combustion or turbine engines. Let us consider a body being heated or cooled from a condition of initial uniform temperature, with the heating or cooling interrupted prior to reaching final thermal equilibrium. In this case, it is reflected that the magnitude of peak stress is a function not only of the values of the Biot numbers for heating or cooling, but also a function of the time at which the heating or cooling is interrupted, i.e., the appropriate Fourier number. In practice, such an effect could arise during thermal fatigue testing of components, such as turbine blades or vanes, for which the time periods of heating and cooling may be chosen such that no thermal equilibrium is achieved within each cycle.

For a long circular cylinder subjected to sudden surface temperature change the thermal stresses consist of radial, tangential and axial

stresses. The first one is zero while the other two are equal at the surface (r=R).

The tangential and axial stresses are given in Boley and Wiener, 19

$$\sigma_z = \sigma_t = \frac{E\alpha}{1-\nu}\,(T_0 - T_{r=R}) \qquad (1)$$

Throughout the volume of the cylinder the axial stress exceeds the tangential stress and is of primary interest.

$$\sigma_z = \frac{\alpha E}{1-\nu}\left[\frac{2}{R^2}\int_0^R T(r',t)r'dr' - T(r,t)\right] \qquad (2)$$

By thermal shock is meant the generation of non-inertial thermal stresses by rapid changes in the temperature distribution in a body. Thermal shock is often produced by the sudden application of a hot or cold fluid to the surface of a structure.

It can be shown (refer to Manson (1966) and Stodola and Loewenstein (1945)) that a thick homogeneous plate in which there is a temperature variation T = T(z) normal to the surface, and which does not undergo bending deformation, will develop surface stresses of high magnitude.

$$\sigma = \frac{E\alpha}{1-\nu}\,(\bar{T} - T) \qquad (3)$$

where $\bar{T}$ is the mean temperature.

In a thick-walled structure of an arbitrary shape, in each the temperature variations are confined to the region close to the surface, the state of stress near the surface will be two-dimensional, and equation (1) will apply. Generally the location at which the greatest difference between T and $\bar{T}$ occurs, is at the surface, so that the magnitude of the stress due to the thermal shock experienced at

the surface becomes

$$\sigma = -\frac{E\alpha}{1-\nu}(\overline{T} - T_s) \qquad (4)$$

where T_s is the surface temperature.

In the case of a heavy-walled structure originally at uniform temperature, the mean temperature $\overline{T}$ may be taken as zero, and the stress due to thermal shock as

$$\sigma = -\frac{E\alpha}{1-\nu} T_s \qquad (5)$$

In the most severe case, in which the film coefficient is essentially infinity the stress due to thermal shock becomes

$$\sigma = -\frac{E\alpha}{1-\nu} T_f \qquad (6)$$

where T_f is the temperature of the fluid in contact with the surface. As a rule the temperature change at a surface is not instantaneous but takes place over a period of time. In thick-walled structures the mean temperature, $\overline{T}$, would not change significantly as a result of the local change in the vicinity of the surface, and even a moderate rate of temperature change would produce a surface stress as given by equations (5) or (6). Thermal "shields" or thermal "sleeves" are sometimes installed in heavy-walled structures and in pipes which are exposed to sudden temperature changes. The thermal shields are thin-walled structural elements whose mean temperatures change rapidly and thereby keep $T-T_s$, in the sleeves, at a low value. The installation of thermal shields on vulnerable components is good

design practice since the thermal stresses are reduced, and the possible generation of fatigue cracks of thermal sleeves due to repeated shock does not represent as critical a hazard as thermal shock and possible fracture of a major structural component.

A problem that is often encountered is that of a plate, tube, or shell having one surface subjected to a large linear temperature increment, with the other surface is insulated. It is clear that the steeper the applied temperature increment and the lower the conductivity of the structural material, the greater will be the resulting thermal stress. Similarly, the greater the specific heat C , the film coefficient h, and the thickness, L, of the plate or shell, the larger will be the thermal stress. The variations of the peak stresses with these parameters are shown in Fig. 1. The maximum stresses occur at the termination of the transient.

When the thermal shock occurs at the surface of a thick-walled structure, the parameter $kt_o/\rho C_p L^2$ is essentially equal to zero, and the uppermost curve of Fig. 1 applies. The parameter k/hL, which is the abscissa in Fig.1 is also approximately zero. In the case of a heavy-walled structure, since L is very large, it is observed in Fig. 1 that under a very severe thermal shock, the maximum stress approaches $\frac{E \alpha \Delta T_o}{1-\nu}$.

From the above introduction it is clear that large stresses can develop due to a thermal shock in the steam turbine. For the case of a turbine cold start, the thermal shock intensity depends on the film coefficient and the initial temperature difference between the steam and the rotor surface.

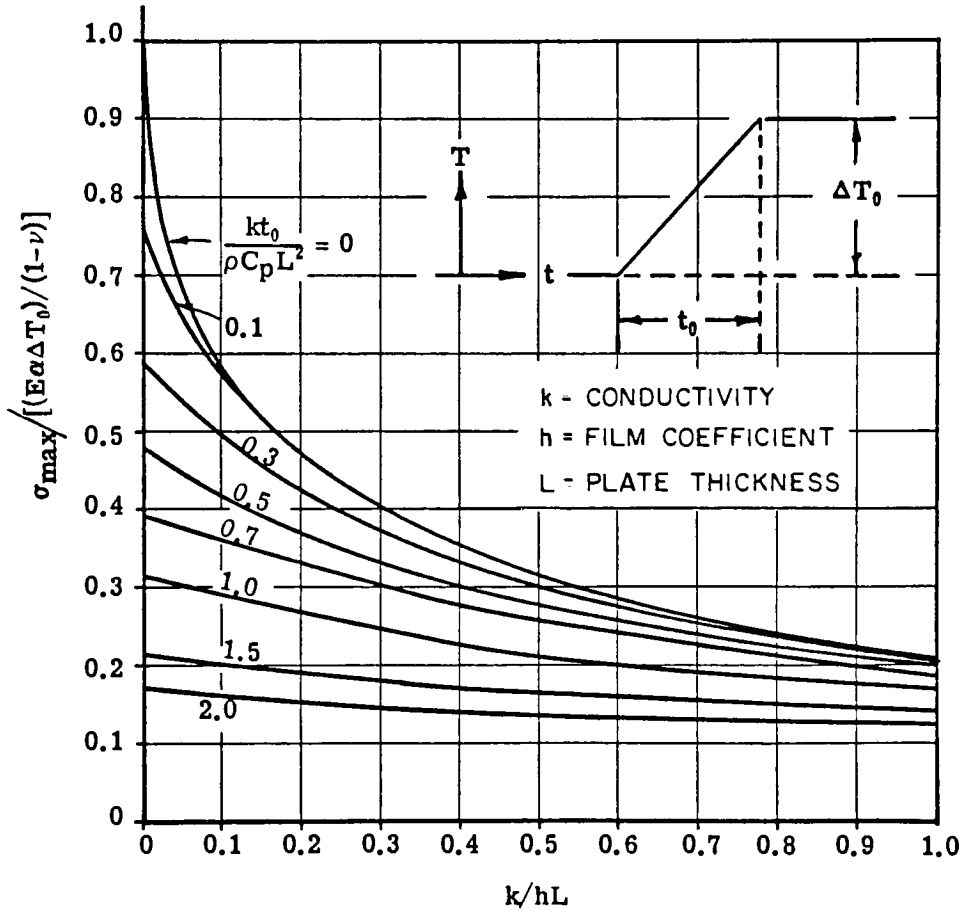
1.0
0.9
0.8
0.7
0.6
0.5
0.4
0.3
0.2
0.1
0
0 0.1 0.2 0.3 0.4 0.5 0.6 0.7 0.8 0.9 1.0
k/hL
σmax/[(EαΔT0)/(1-ν)]
kt0/ρCpL2 = 0
0.1
0.3
0.5
0.7
1.0
1.5
2.0
T
t
t0
ΔT0
k - CONDUCTIVITY
h = FILM COEFFICIENT
L - PLATE THICKNESS

Fig. 11

9

2.0 LITERATURE SEARCH

Literature search was conducted to identify the previous work done on the cold start thermal shock problem in a steam turbine.

Stress Technology Incorporated (STI), a consulting firm in Rochester New York, performed a Brown Boveri Corporation's (BBC) control stage L-2 design analysis in 1984 by using ANSYS finite element analysis program. BBC is a Swiss steam turbine manufacturer. ANSYS is a universal computer program which has been developed and annually updated by Swanson Analysis Systems, Inc. for the last seventeen years. The most recent version of ANSYS program is 4.3 and its education version is available on the Rochester Institute of Technology (RIT) VAX computer system since October 1987.

Figure 2.1 shows the BBC's entire high pressure rotor grid-work used in the analysis by STI. The mesh size was comparatively finer near the rotor surface and at the shaft portion of the control stage where temperature and stresses were expected to experience large spatial variations. Appropriate boundary conditions were imposed on the rotor model surfaces. Surfaces from the shaft ends to the labyringth glands were assigned a prescribed temperature of 80 C. Surfaces in contact with steam were designated as convective and were assigned appropriate values of the heat transfer coefficient and steam bulk temperature using client-provided data. Rotor and blade temperature were initially prescribed at 20 C. Figure 2.2 shows a grid-work for the control stage single blade model. Figure 2.3 shows a single blade substructure for 360° blade-disk model.

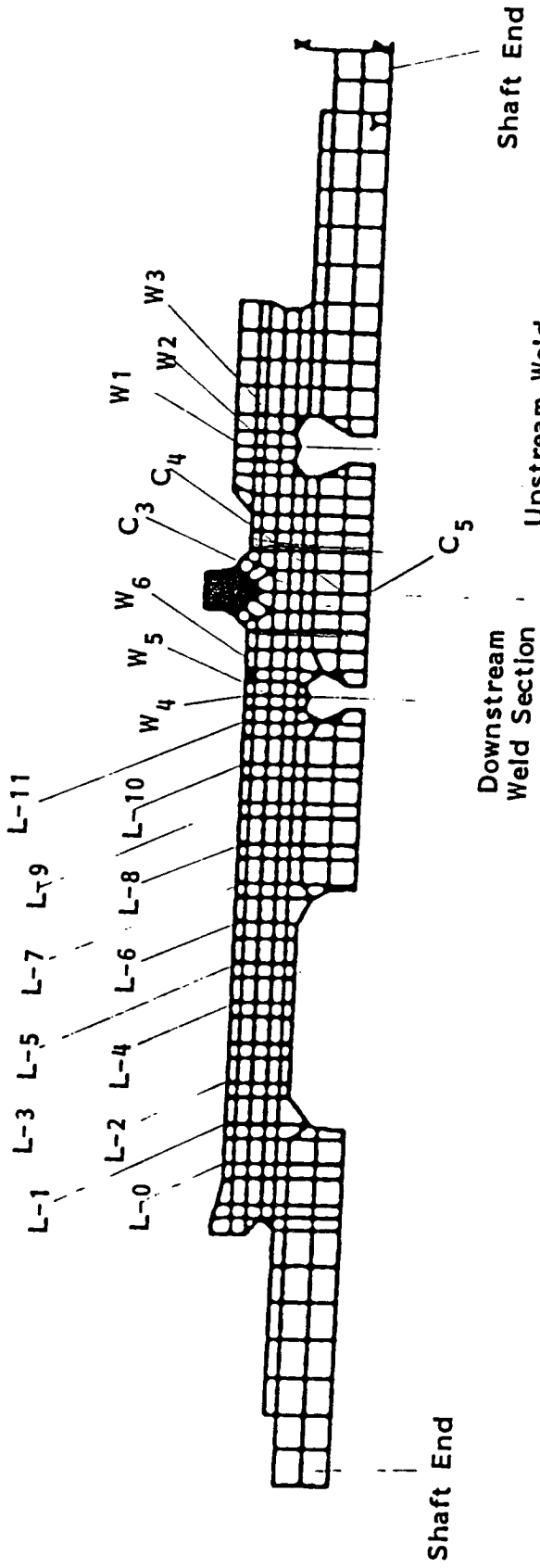

Figure 2.1 Locations of Designated Points in the Rotor Model

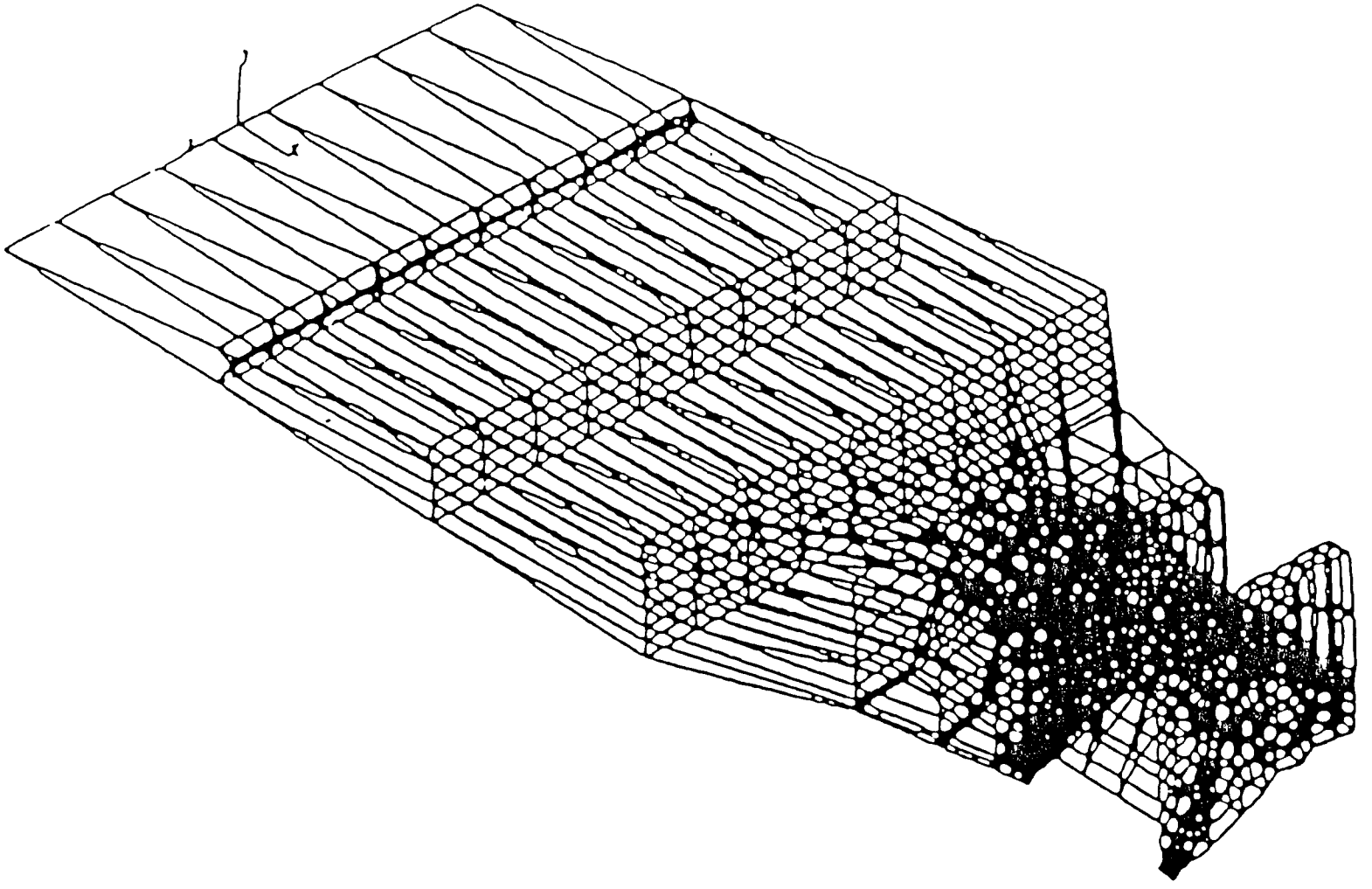

Figure 2.1 Grid-work for the Control Stage Single Blade Model

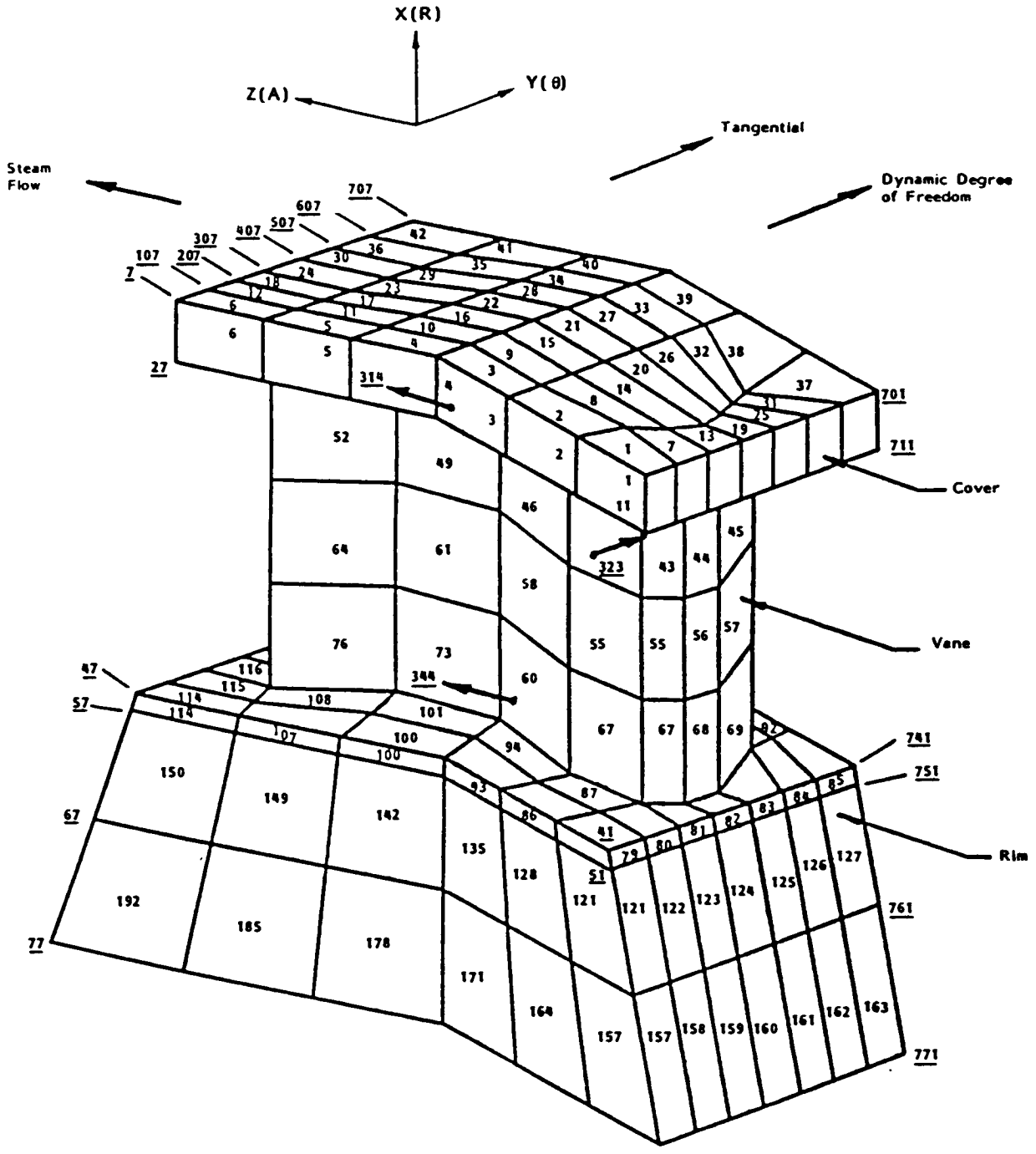

Figure 2.3 Single Blade Substructure for 360° Blade-Disk Model, Element Numbering

In this turbine design analysis 28C used a one step heating process in the first 75 seconds with inlet steam temperature at 204 C followed by another heating process with inlet steam temperature at 510 C. From STI's analysis, the largest compressive stress occurred at 23.4 seconds from the initialization and its magnitude was 564.7 MPA. This high compressive stress was due to the thermal shock problem. Figure 2.4 shows the platform thermal stress distribution at 23.4 seconds. The second largest compressive stress occurred at 3560 seconds from the start and its magnitude was 252 MPA. The second peak was due to the temperature difference between the platform and the rotor center. The steady state would be reached after five hours from the starting point with a maximum tensile stress of 250 MPA. The rotor material had a higher thermal expansion coefficient than the blade material resulting in the tensile stresses. Figure 2.5 shows the variation of the temperature and the film coefficient with time.

A transit time of 5 seconds for steam to fill the rotor passages was assumed (step 1 time interval). Within the step 1 the steam bulk temperature and the associated film coefficient were increased linearly from 20 C to 204 C and from 0 to 10,000 W/m^2-K, respectively. The large magnitude for the film coefficient was attributed to steam condensation on the cold metal surfaces of the rotor and blades. This assumed condensation of steam continued until the metal temperature at the rotor surface reached 150 C. This heating process took approximately 14.5 seconds (step 2 time interval). Since the condensation of pure steam at isobaric condition is an isothermal process, the film coefficient was taken as a constant at $10,000W/m^2-K$ while the temperature increased linearly with time within the second

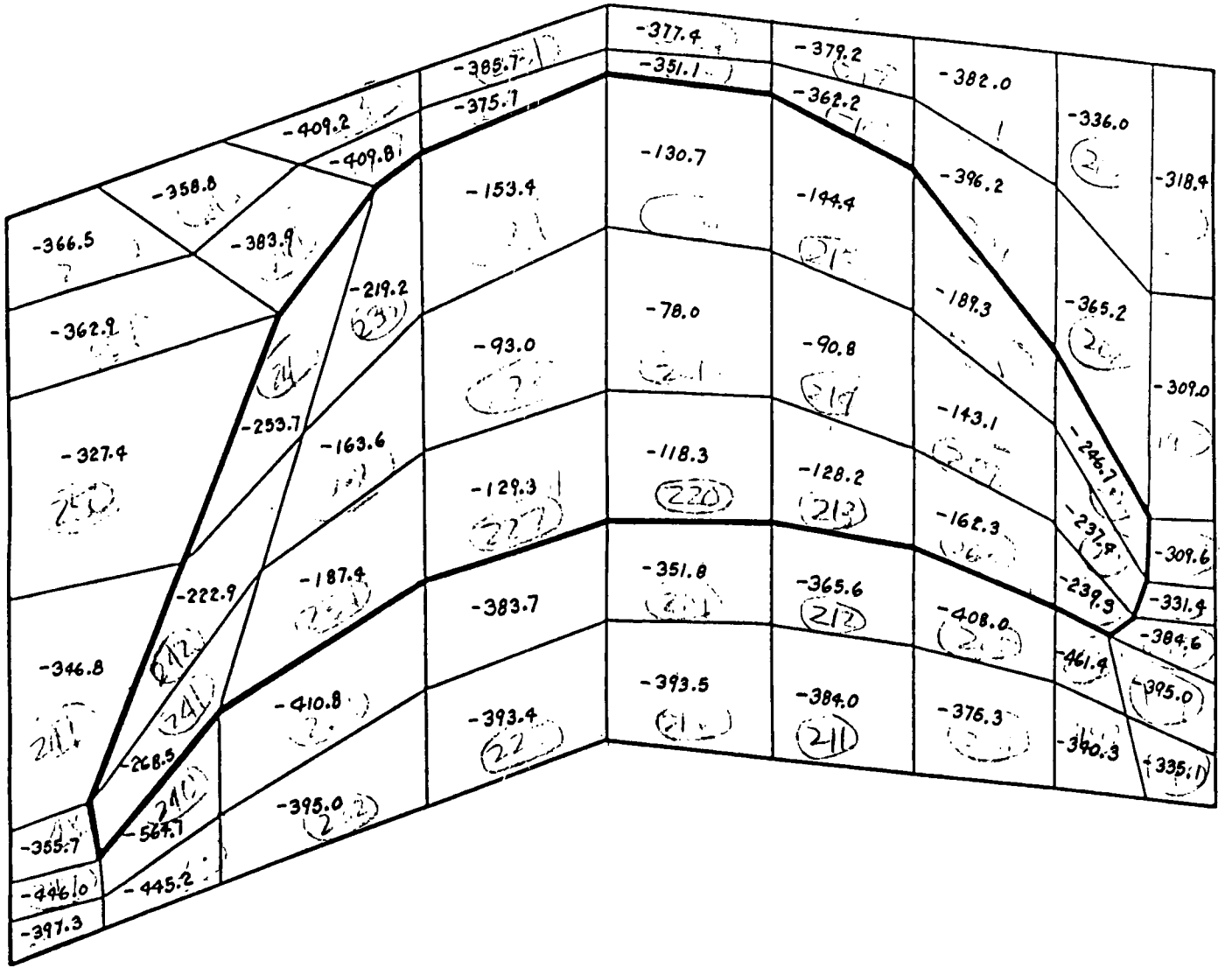

Figure 2.4 Thermal Hoop Stress Distribution for the Layer of Elements Forming the Upper Surface of the Platform - time = 23.4 seconds.

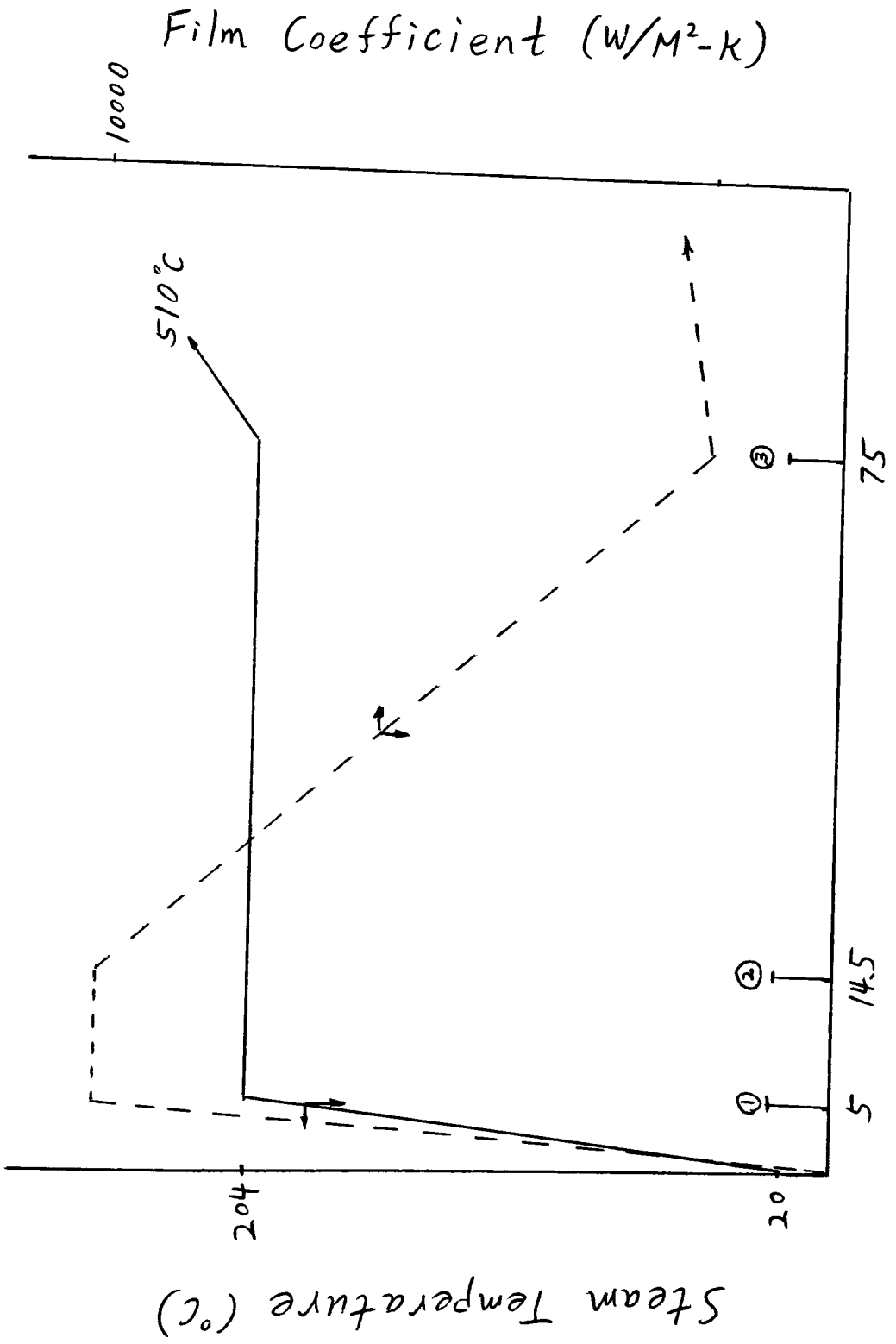

Fig. 2.5 Steam Temperature and Film Coefficient Variation With Time. (First Three Load Steps)

time interval. The diminishing steam condensation and the corresponding decrease in the film coefficient for time greater than 14.5 seconds was modelled as a linear reduction through the step 3 time interval, which spanned from 14.5 to 75 seconds.

One item that deserves clarification is the spatial variation of the steam bulk temperature and film coefficient from the control stage to the exhaust chamber. In the analysis, it was felt that the simplest and yet most reasonable assumption was a linear variation. Figure 2.6 shows stress-time relationship.

2.2 Life Prediction Methodology

To accurately predict the life of any turbine engine component, analysis must be conducted to determine the stress-strain relationships (hysteresis) for the operating cycle. For advanced components, this typically requires the determination of both time dependent and independent local inelastic effects. The turbine blade structural design problem typically contains a collection of the most difficult problems in hysteresis analysis. Throughout a typical mission, a rotor will be subjected to a wide range of tensile and compressive stresses and at some point in its history will experience both time dependent and independent effects.

Many techniques for determining these inelastic effects have been proposed. A review of those procedures which bear directly on the turbine blade design problem is conducted here. As a brute-force technique, a three-dimensional inelastic analysis can be performed on the component for the engine duty cycle, provicing a complete stress-strain history. This complex analysis procedure requires a

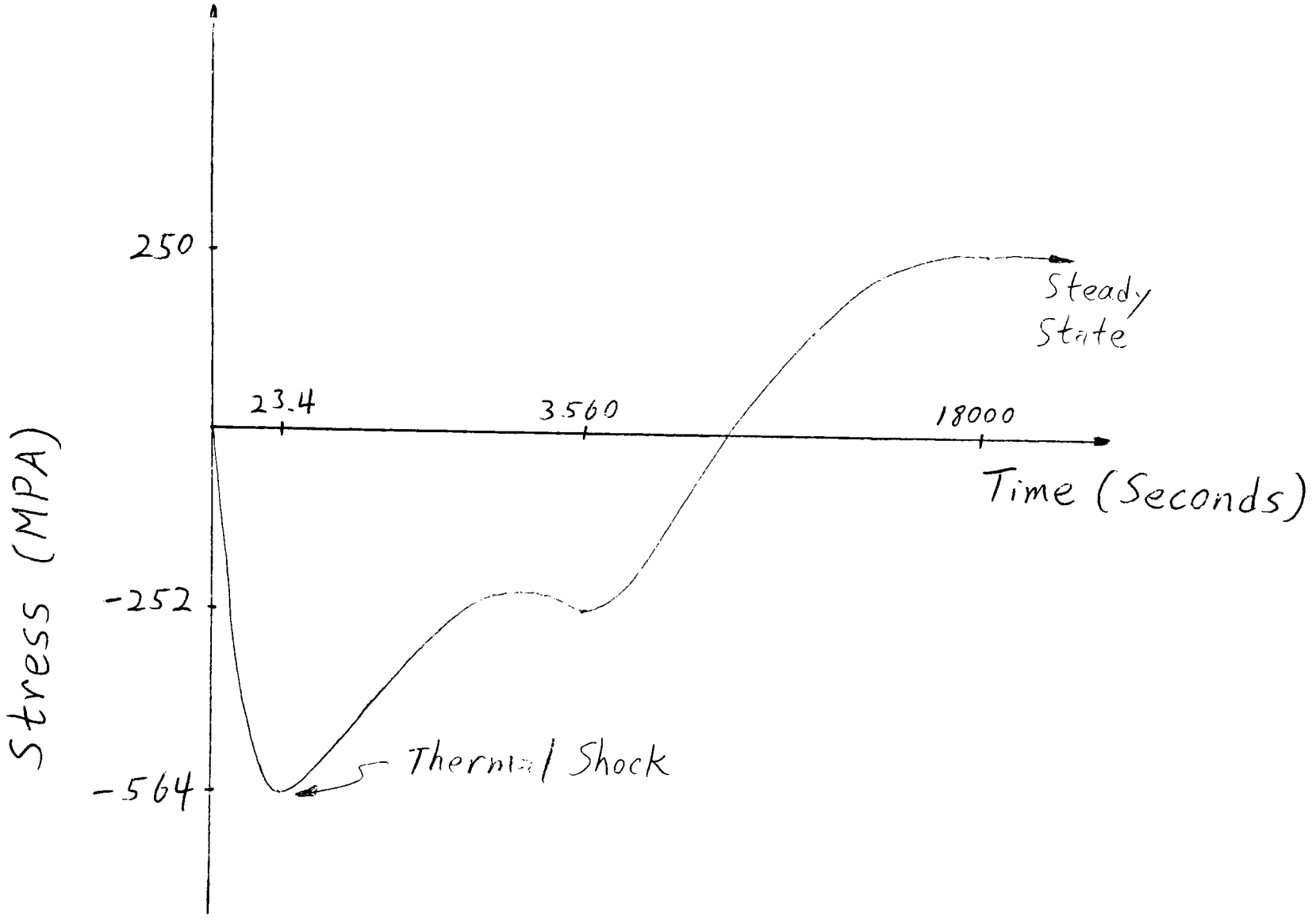

Fig. 2.6 Control Stage Platform Stress Variation with Time. (2-Step Heating)

large amount of model preparation and computer solution time and is not practical in the primary design stages. Additionally, state-of-the-art constitutive modeling in many hot section materials does not justify this effort. One- or two-dimensional inelastic analysis can be more easily performed but the resulting stress field can be substantially in error if multiaxial stress fields exist at the life critical locations.

The method that best lends itself to design analysis is the local pseudo-inelastic approach, which is based on the elastically calculated stresses at the operating conditions in the engine cycle. If the local inelasticity is due to a stress riser, the well known Neuber rule can be used to perform the inelastic analysis for the time independent stress-strain response. Many references in the literature treat the use of the Neuber rule for isothermal, low temperature, cyclic analysis applications (Socie (1977), Walcher et al. (1979), Wetzell (1971), Walcher and Finnerty (1982)). However, the use of the Neuber rule at high temperatures where creep can occur is not well documented. In the absence of notched behavior, an elastic strain invariance method can be used to perform the hysteresis analysis when thermal stresses predominate.

Lockheed-Georgia (1978) reports on extensive tests performed at Lockheed-Georgia on two "calibrated models" made from 7075-T651 aluminum. These tests provided constitutive data for use in the formulation of a hysteresis model for stress risers, including the effects of creep. The Neuber rule was found to overpredict stress and strain at the root of a notch. A correction procedure was presented which could be applied to any material once the correct empirical

constants are determined from test data. Other Neuber corrections are available, such as that derived during the Structural Life Prediction/Correlation (SLP/C) Program conducted at TCAE (Walcher et al. (1979)). This correction method is formulated to be material independent, with the correction factor obtained directly from test data or an inelastic analysis.

The TCF (Time and Cycle Fraction) approach is probably the most widely used method, and has been shown to produce good results for some applications. This approach uses generally available materials data. Possible sources of errors associated with the method includes the treatment of compressive creep damage, the non-linearity of the creep-fatigue damage mechanism, and the treatment of damage predictions for thermal-mechanical cycling. The accuracy of the method is improved if cyclic creep data are used rather than the static creep rates.

The SRP (Strain Range Partitioning) approach is the newest of the listed methods. In its early development, it did not treat the effects of mean stress, but this capability has recently been added. Since only closed hysteresis loops are treated, the application of the method requires partitioning complex cycles from actual engine operation into generic closed hysteresis loops. Difficulties occur with the method when inelastic strains are small because the life for each of the generic hysteresis loops are related to inelastic strain range. Additional work is needed to make the SRP method a general turbine engine design tool.

2.3 Thermal Prediction Methodology:

There is a general agreement in the literature that the limiting factor in the accurate prediction of turbine rotor life is the quality of the metal temperature predictions. Experience has indicated that local errors of 94 C or greater are commonplace for new designs. In the thermal prediction process, the hot side heat transfer coefficients represent the single largest area of uncertainty. Although analytical means of predicting the heat transfer coefficients exist, extensive measured temperature characterization testing remains necessary to achieve an acceptable confidence level in the temperature predictions. Obtaining high quality temperature data used in the calibration of predictive capabilities also presents a challenge due to the complexities of high temperature rotating measurements.

The approach used at TCAE for turbine blade heat transfer analysis is a three dimensional, lumped parameter finite difference method. The modeling concerns which must be addressed involve mesh generation and boundary conditions. The boundary conditions of primary concern are the external heat transfer coefficients, the external gas temperature definition, the internal or blade- to-coolant heat transfer coefficient, the internal coolant temperature definition, the heat exchanged between the airfoil hub and the attachment areas and the airfoil tip heat exchange. Phenomena which contribute to uncertainty include the locations and amounts of turbulence in the hot gas stream, the location of separation and re-attachment of the boundary layer, and the locations of the transition point from laminar to turbulent flow.

The development of improved modeling methods have been accomplished through the extensive use of test data in a correlation/revision process. Thermovision and 5X model testing have been used to enhance the heat transfer modeling process. Engine temperature measurements have been performed on various turbine blades using chromel-alumel thermocouples and a high response infrared probe. Considering the local aerodynamic and heat transfer effects of the ceramic coated cases, reasonable correlation between these measurement techniques has been achieved.

Several papers have been published (Stepha (1980), Akles et al. (1967), and Crane (1973)) which delineate the difficulties of blade metal temperature predictions. These sources conclude that the current knowledge of the factors which influence blade metal temperature results in an uncertainty of analytical studies for uncoated metal airfoils of 7.5 percent. Turbine blade temperature predictions for a calibrated thermal model of an advanced cooled turbine blade have been shown, through measurement accuracy studies, to be reliable within 44 C. Thin film thermocouples and a structured approach to the utilization of the large amounts of heat transfer data generated in testing are required to improve the state-of -the-art in metal temperature prediction.

3.0 PROBLEM FORMULATION

3.1 Problem description:

Chapter 1 is an introduction to the problem of thermal shock. Chapter 2 is a study of the thermal and structural analyses of a steam turbine cold start operation which was conducted by Stress Technology Incorporated (STI).

From STI's analysis, a normal two-step heating process causes a very high compressive hoop stress on the platform during the first heating step. Sometimes the first heating step hoop stress is two times greater than the second step's. Figure 2.6 shows the STI's analysis of stress vs time. For the case of a turbine cold start, the thermal shock intensity depends on the film coefficient and the initial temperature difference between the steam and the rotor surface.

Steam condensation on a cold control stage platform causes a large heat flux to the surface and this situation causes an enormous compressive stress which might create a propagating crack in the platform. Eventually, a catastrophic disaster could occur. The cold start thermal stress problem is a kind of low cycle fatigue. The objective of this project is to develop a procedure to reduce the thermal shock problem of a steam turbine control stage during cold start.

Reduction of thermal shock intensity can be achieved in several ways. Three ways to reduce thermal shock intensity are lengthening the

transit time, lowering the film coefficient, and reducing the temperature difference between the steam and the rotor surface.

The problem of the conventional two-step heating process is the very high compressive thermal stress which occurs in the first step. This kind of high thermal stress is called thermal shock. It occurs only in the beginning of a steam turbine cold start procedure. This is attributed to the rapid change in film coefficient (heat transfer coefficient) introduced by the initiation of steam condensation. Very large heat flux and temperature gradient at the rotor surfaces shortly after the initiation of steam flow causes such high stresses.

An improved procedure, three-step heating process, will be developed to make the stresses caused by each heating step uniform. The thermal shock problem will also be solved. The first two steps of the modified three-step heating process are to be substituted for the first step of the conventional two-step heating process.

In order to perform the comparison, the first and second heating steps of the three-step heating process used the same operating conditions as the first step of the two-step heating process. The difference between these two processes is that the first heating temperature is chosen randomly as 142 C instead of 204 C. There is a ten minute warm up period between the first and second heating steps. Figure 3.1 shows the three-step heating process temperature and film coefficient vs time diagram.

Chapter 4 will do a theoretical analysis of the first part of the two-step heating process. It will also develop a three-step heating process to significantly reduce the thermal shock problem of the

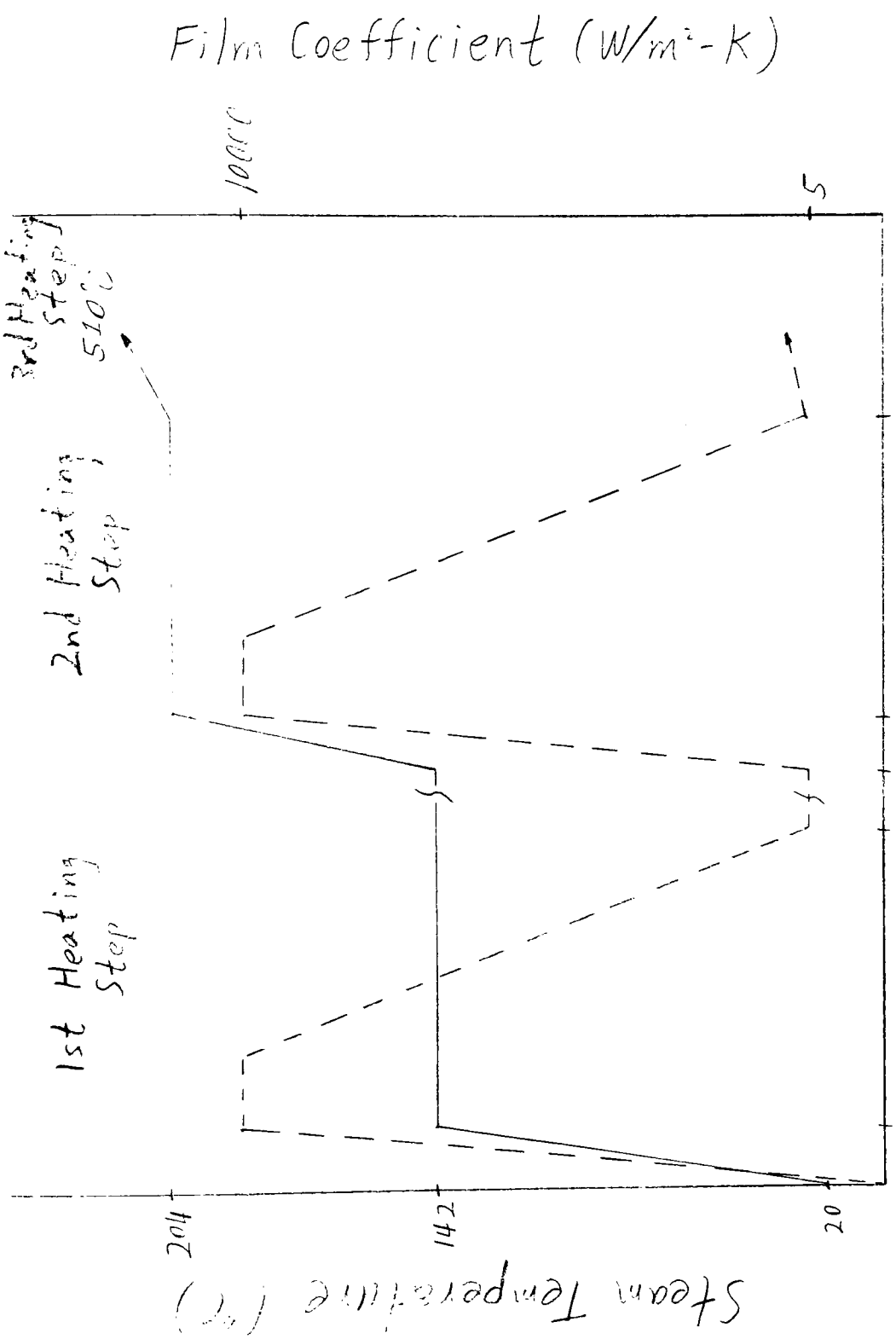

Fig. 3.1 Three-Step Heating Process Temperature and Film Coefficient VS Time Diagram.

two-step process presently in use. Finally, Chapter 4 will present a study of the thermal stress and how it is affected by different film coefficients.

Chapter 5 is an extension of Chapter 4. It will investigate the possible advantages of a longer warm-up time for the steam turbine with the cold start procedure. Finally, Chapter 5 will strive to find the optimum heating temperature to reduce the severity of thermal shock.

3.2 A simplified model of a control stage

In the course of this investigation, the finite element program ANSYS was used to perform all heat transfer analyses and stress calculations. During the study, a simplified three dimensional finite element model was developed to calculate the temperature and stresses for different forcing functions.

A control stage blade model consisting of a cover, vane, platform, disk rim, and portion of the shaft is developed. Only one blade and a wedge segment of the rotor were required in order to perform detailed calculations in this model. The control stage consists of 44 blades. Since all 44 blades are identical, analysis of only one is necessary. Suitable boundary conditions were applied to the edges of the blade model to insure true representation of a 360 degree continuous structure. The segment gridwork consisted of 92 three-dimensional isoparametric elements, ANSYS Element Type STIF 70, and approximately 200 nodes. Figure 3.2 gives a three dimensional view of this model with an extended shaft. Figure 3.3 gives an X-Z view of this model

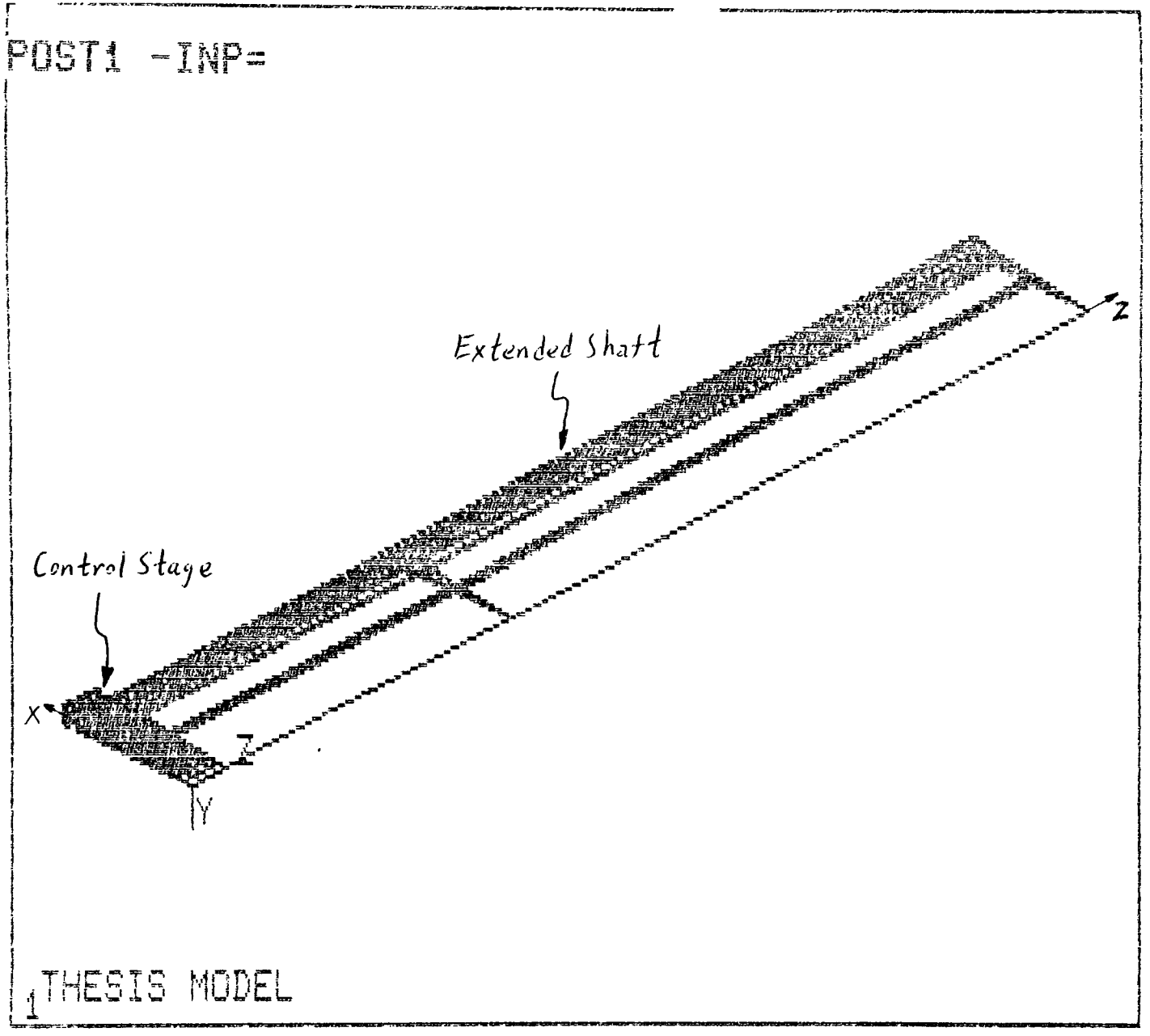

Fig. 3.2 3-D View of Control Stage with Extended Shaft.

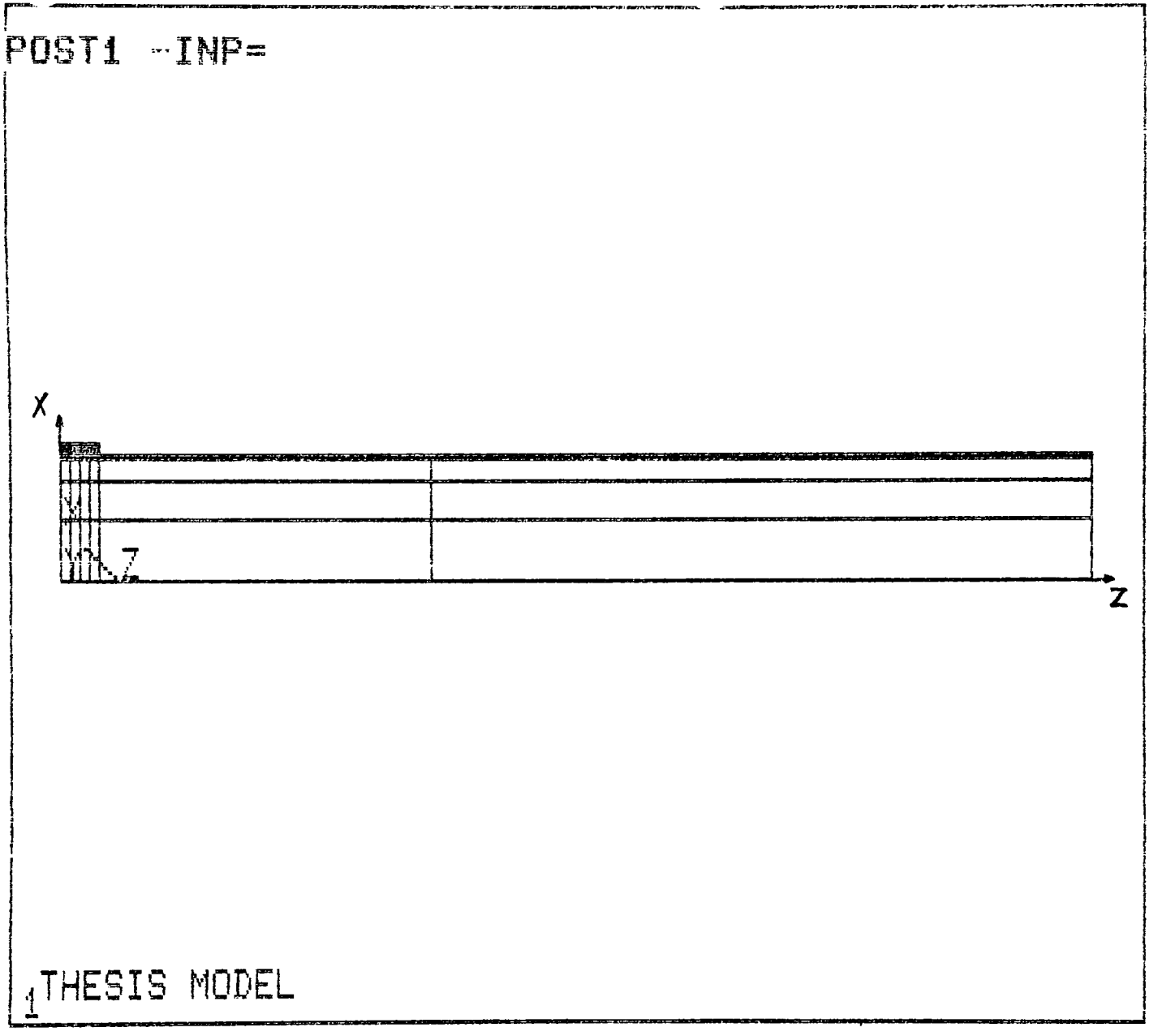

Fig. 3.3 X-Z View of Control Stage with Extended Shaft.

with an extended shaft. Figure 3.4 gives an X-Y view of this model with an extended shaft. Figure 3.5 gives a three dimensional view of the simplified model without the extended shaft. Figure 3.6 gives an X-Z view of the simplified model without the extended shaft. Figures 3.7 to 3.10 give cover, vane, platform, and wedge shaped rotor node and element numbering.

Comparison between STI's actual model with the simplified model.

	Elements	Nodes
STI's actual model	675	1000
Simplified model	92	200

Due to the limitations of the ANSYS university version, the model used in this project was a simplified version of the STI model so further research is needed to complete precise analyses. Analyses in this project are for a comparative nature only.

The simplified model is constructed of two different materials. Blade material is used for the cover, vane and platform. Rotor material is used for the wedge shaped segment of the shaft. Mechanical properties of blade material and rotor material were given as a function of temperature. Table 3.1 and 3.2 summerized the material properties.

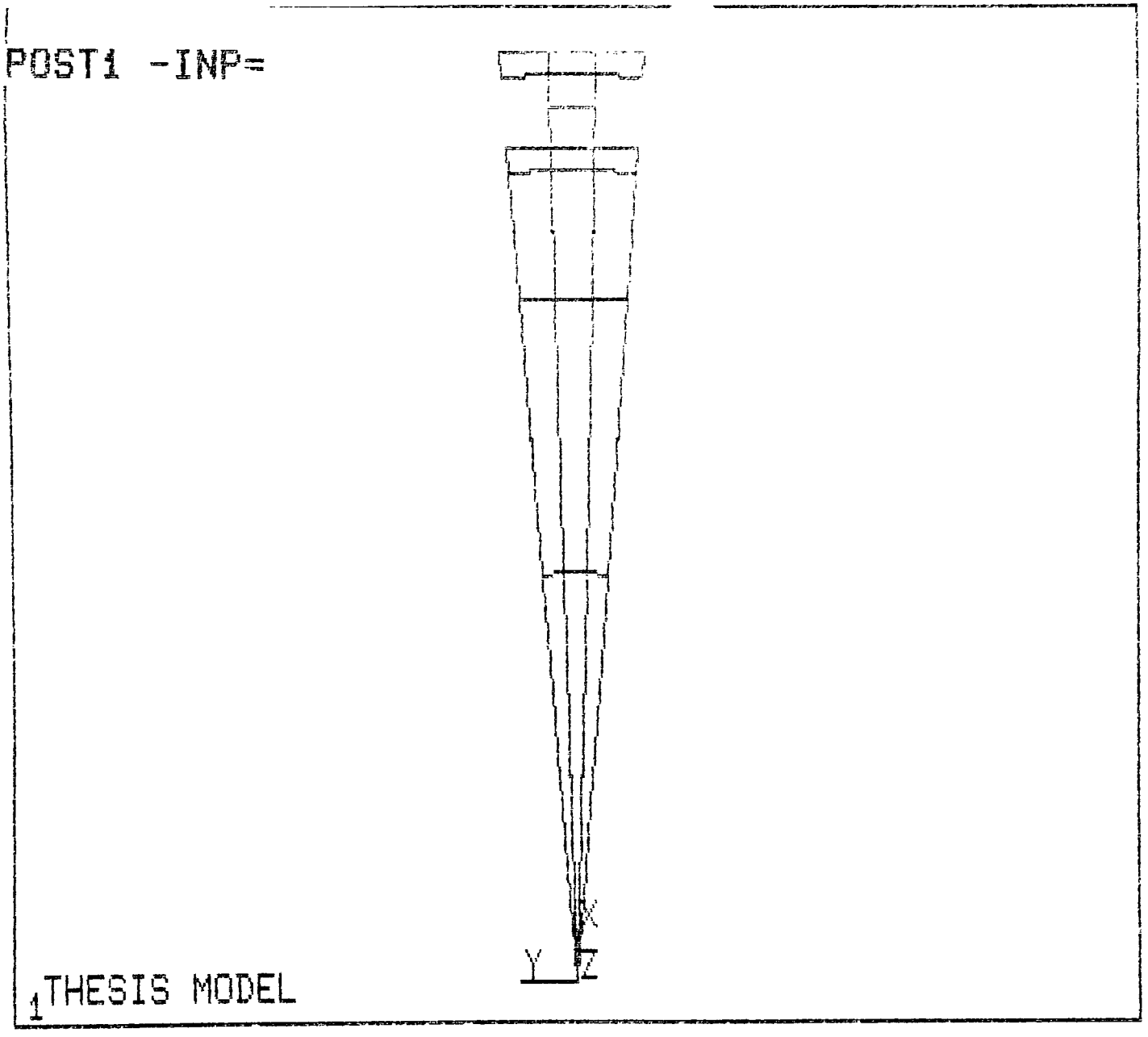

Fig. 3.4 X-Y View of Control Stage Model.

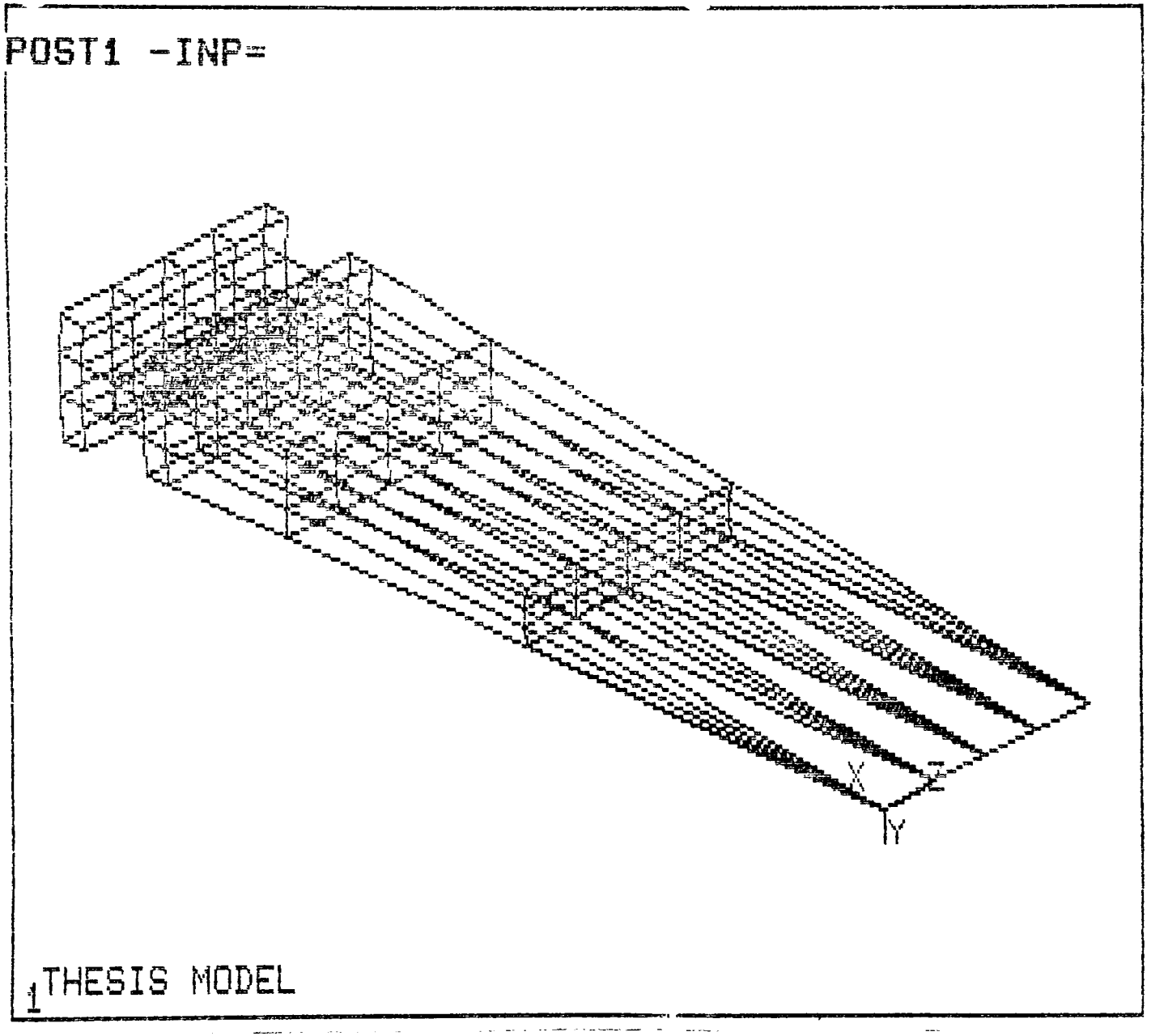

Fig. 3.5 3-D View of Control Stage Model.

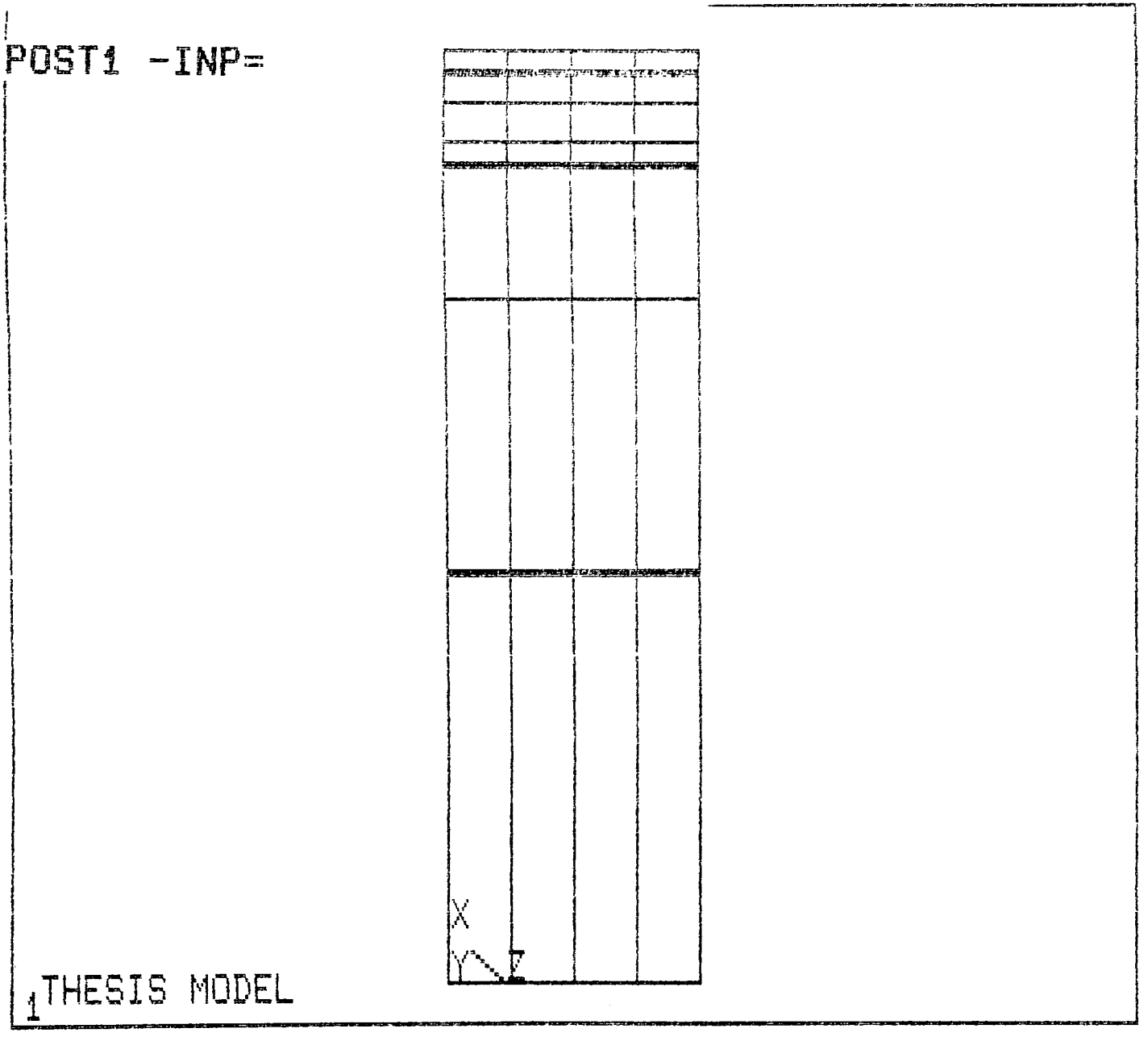

Fig. 3.6 X-Z View of Control Stage Model.

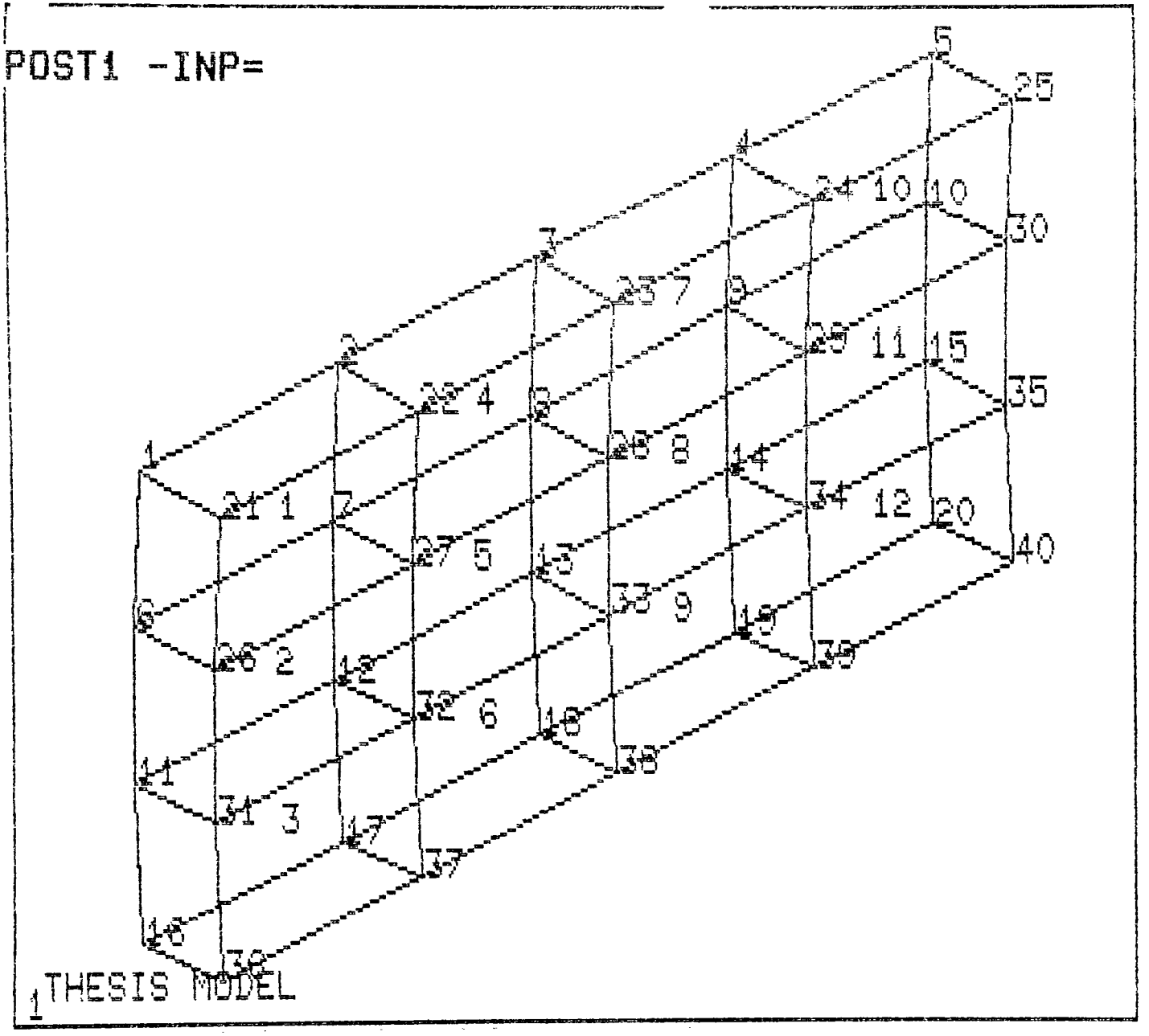

Fig. 3.7 Cover Node and Element Numbering.

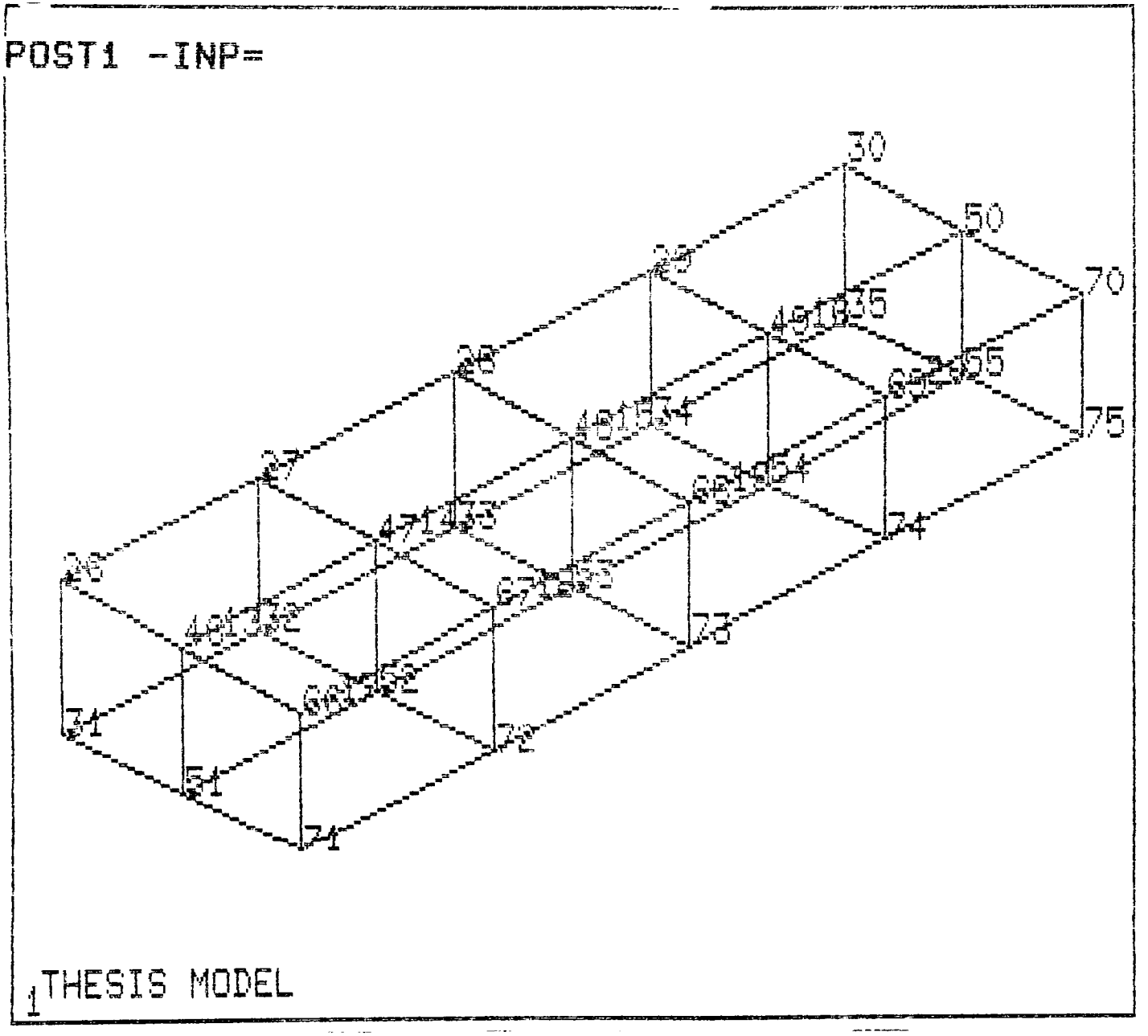

Fig. 3.8 Vane Node and Element Numbering.

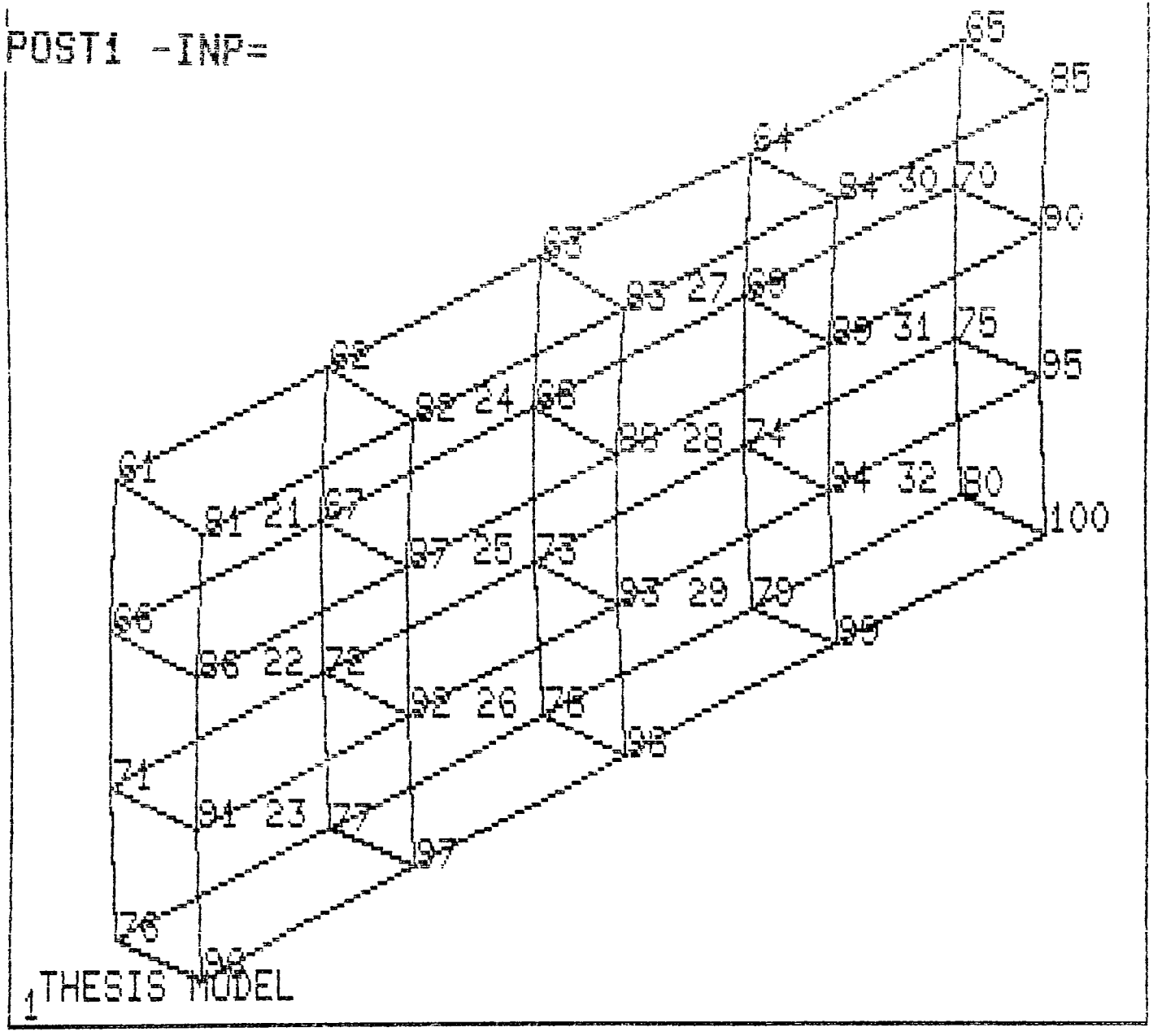

Fig. 3.9 Platform Node and Element Numbering.

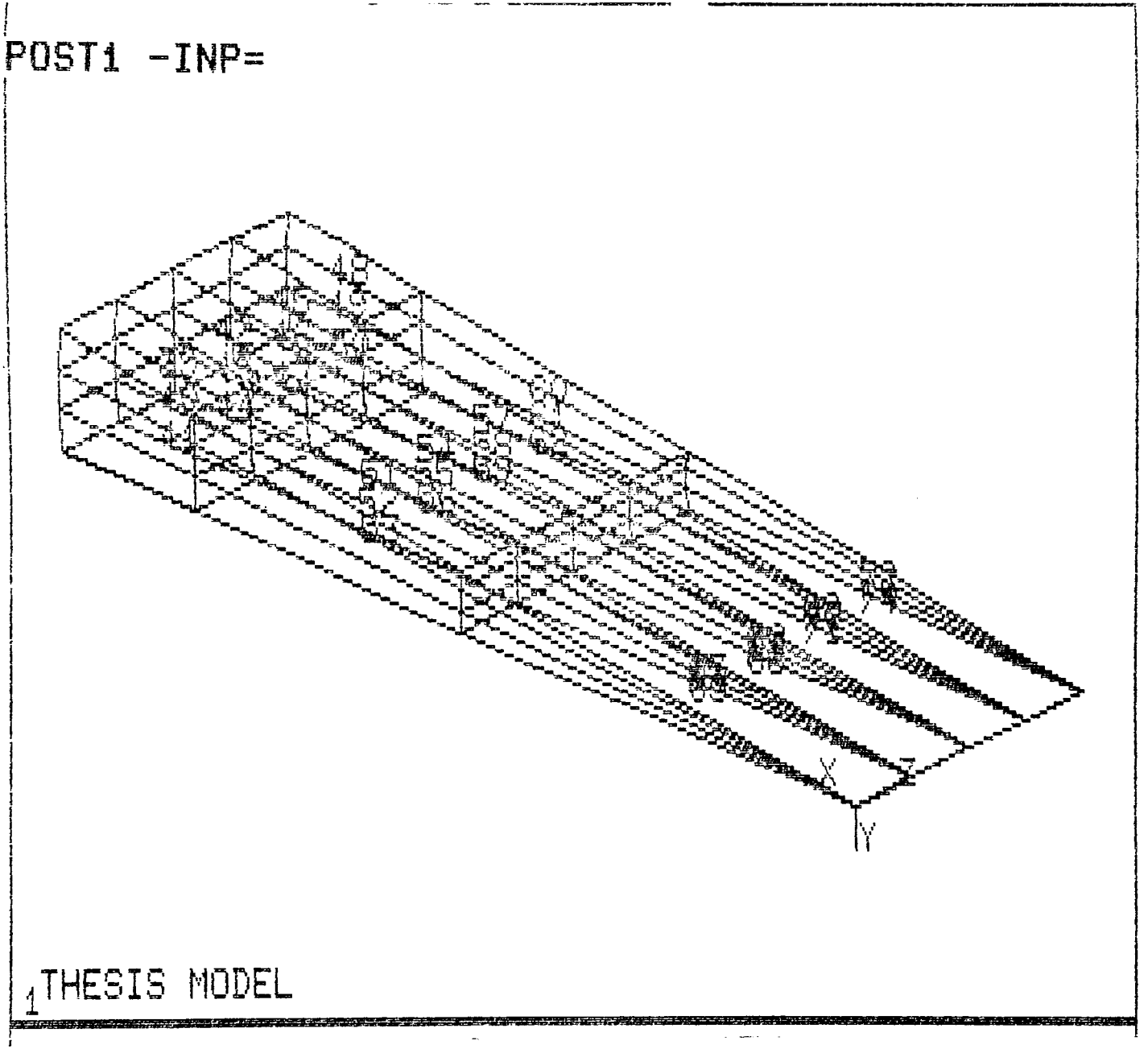

Fig. 3.10 Wedge Shaped Rotor Element Numbering.

Table 3.1 Mechanical Properties of Blade Material

Temperature	Young's Modulus		Thermal Expansion Coefficient	Thermal Conductivity	Specific Heat Capacity	Density
	Static 10^9 N/M^2	Dynamic 10^9 N/M^2	10^{-6}/°C	W/M°C	J/kg°C	kg/M^3
20	219	219			460	
100	214	214	10.1		480	
200	208	208	10.5		520	
300	200	200	10.9		560	
400	188	191	11.2	27	580	7750
450	181	185	11.3		600	
500	169	181	11.5		620	
550	153	174	11.6		650	
600	129	167	11.7		700	
650	113	159	11.75		750	

Table 3.2 Mechanical Properties of Rotor Material

Temperature	Young's Modulus		Thermal Expansion Coefficient	Thermal Conductivity	Specific Heat Capacity	Density
	Static 10^9 N/M^2	Dynamic 10^9 N/M^2	10^{-6}/°C	W/M°C	J/kg°C	kg/M^3
20	211	211		44	460	
100	207	207	11.0	43	480	
200	200	200	12.0	42	520	
300	193	193	12.75	40	560	7850
350	189	189	13.0	38	580	
400	183	184	13.2	37	600	
450	177	180	13.3	36	620	
500	168	175	13.5	34	650	
550	157	170	13.6	33	700	
600	142	164	13.7	31	750	

4.0 THEORETICAL ANALYSIS

4.1 Purpose of work:

This chapter will follow the same procedure of the first part of the two-step heating process analysis which has been used by Stress Technology Incorporated (STI). The thermal shock problem occurred only in the first step. The results will be compared with STI's and if both results are within ±25% error then the simplified model and the analytical method will be assumed to be reliable.

Secondly, this chapter will discuss the simplified model as applied to the improved procedure (the three-step heating process) which can reduce the thermal shock problem significantly. Only the first two steps of the three-step heating process will be analysed. Because the third step is identical with the second step of the two-step heating process.

Finally, this chapter will study the thermal stress affected by different film coefficients which are 1000, 5000, 10000, and 15000 W/m^2-K. These results can be compared with the results of the three-step heating process. It will be made clear which way would be better to reduce thermal shock, i.e., either decrease the film coefficient or extend the number of heating steps.

4.2 Two-step heating process:

The maximum compressive thermal stress which occurs in the first step of the two-step heating process will be obtained for comparison with STI's results.

4.2.1 Thermal analysis:

A three dimensional thermal and stress analysis was performed utilizing the control stage model, Fig. 4.1. This model consisted of a cover, vane, platform, disk rim, a wedge shaped segment of the rotor and an extended shaft. Figs. 3.2 to 3.10 give various perspective views of the simplified model. The mesh size was comparatively finer near the rotor surface and at the shaft portion of the control stage where temperature and stresses were expected to experience large spatial variation.

Appropriate boundary conditions were imposed on the model surfaces. Surface of the shaft end were assigned a prescribed temperature of 80 degree Celsius. Surfaces in contact with steam were designated as convective and were assigned appropriate values of the film coefficient (heat transfer coefficient) and steam bulk temperature using STI's data (refer to Chapter 2). These included surfaces in the control stage cover, vane, and platform. The surface in the downstream shaft end was assumed adiabatic for simplicity. Lateral surfaces (shaded in Fig. 4.2) of the cover, platform and rotor segment were taken as adiabatic in view of the periodic nature of the boundary conditions and structural geometry in the circumferential

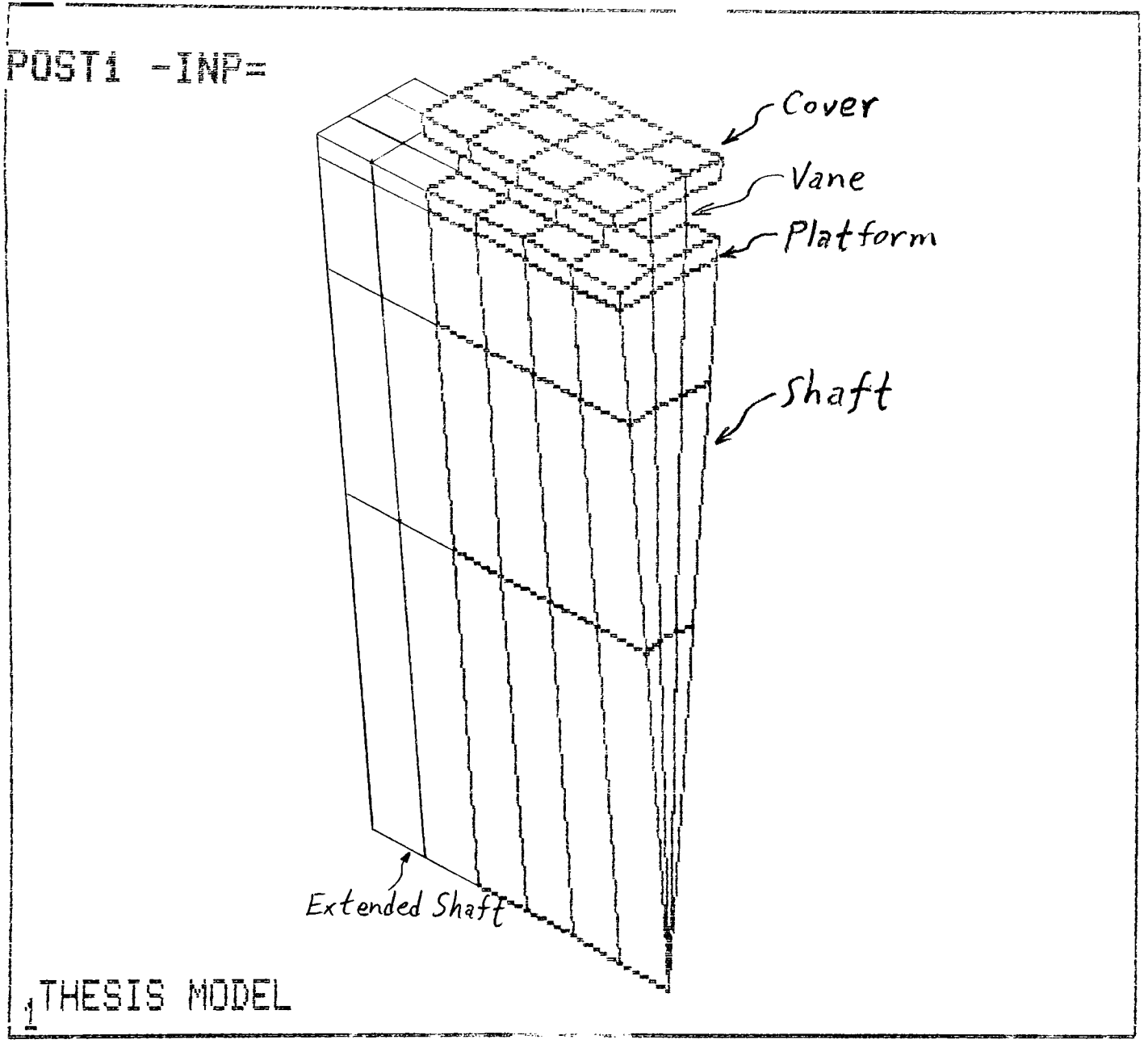

Fig. 4.1 Control Stage Model With Extended Shaft.

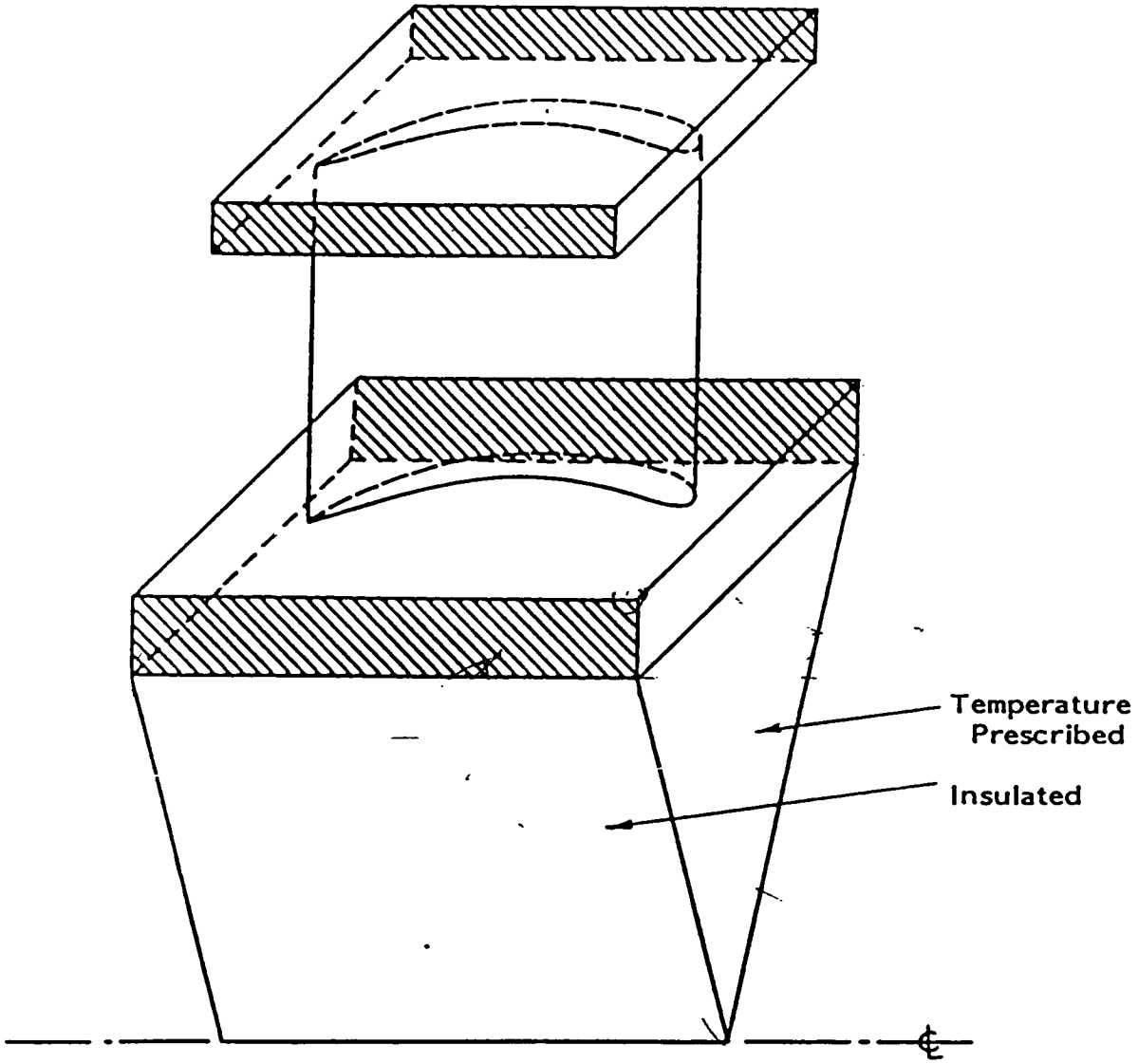

Figure 4.2 Schematic Diagram for the Control Stage Single Blade Model

direction.

4.2.2 Forcing functions:

The thermal response of the rotor and blade stages depend on the thermal forcing functions. For the case at hand, the transient forcing functions were steam bulk temperature and the associated film coefficient (heat transfer coefficient). Both these two variables were functions of time. To characterize the time dependency in the analysis, the steam bulk temperature and film coefficient were specified at selected instances in time. The resulting sets of values are referred to herein as load steps. Intermediate values between load steps were generated automatically by linear interpolation.

Load steps can be selected in an arbitrary fashion. In general, they are chosen in such a way as to give an acceptable if not exact representation of the actual forcing functions. Three load steps were used in the present analysis. Fig. 2.5 depicts the forcing functions and the three load steps.

Rotor and blade temperatures were initially prescribed at 20 C. When steam flow was initiated, a short period of time elapses before the steam completely fills the rotor passages. The exact amount of time needed to achieve this state is usually a complicated function of rotor geometry, steam flow rate, as well as steam thermodynamic properties. In the absence of a detailed data, a transit time of 5 seconds for steam to fill the rotor passages was assumed (time interval 1). Within time interval 1 the steam bulk temperature and the associated film coefficient were increased linearly from 20 C to

204 C and from 0 to 10,000 W/m^2K, respectively. The large magnitude for the film coefficient was attributed to steam condensation on the cold metal surfaces of the rotor and blades. This assumed condensation of steam continued until the metal temperature at the rotor surface reached 150C. This heating process took approximately 14.5 seconds (refers to STI's work).

Since the condensation of pure steam at isobaric condition is an isothermal process, the film coefficient was taken as a constant of $10,000W/m^2K$ while the temperature increased linearly with time within the second time step. The diminishing steam condensation and the corresponding decrease in the film coefficient for time greater than 14.5 seconds was modelled as a linear reduction through the time step 3, which spanned from 14.5 to 75 seconds.

One item that deserves clarification is the spatial variation of the steam bulk temperature and film coefficient from the control stage to the exhaust chamber, i.e. the shaft end of the simplified model. In the analysis, it was felt that the simplest and yet most reasonable assumption was a linear variation.

4.2.3 ANSYS thermal program analysis:

The PREP 7 was chosen as the preprocessing routine to analyse the thermal problem. For thermal analysis the KAN,-1 module type was chosen. There were two different materials in this model and both used three dimensional isoparametric elements so the element type used was STIF 70. The mechanical properties of blade material and rotor material given in table 3.1 and 3.2 were also generated in this

program. Cylindrical coordinate system was chosen for the entire model. There were 92 elements and approximately 200 nodes have been generated. Initial rotor temperature was taken as 20 C. The shaft end surface was assumed to be at 80 C and it acted like a heat sink for all the steam convective heat transfer into cover, vane, platform and the shaft. Four time intervals were taken in this program and their time periods are as follows:

Time Interval	from	to	
1	0.0	0.5	(seconds)
2	0.5	5.0	
3	5.0	14.5	
4	14.5	75.0	

The steam temperature vs time diagram is shown in Fig. 2.5.
The recommended time interval size (Δt) for a transient analysis is related to element conduction length and material properties. The larger the thermal gradient, the smaller the t and element length should be. The recommended time interval is:

$$\Delta t \leq \frac{\delta^2}{10\,\alpha}$$

Where: α = thermal diffusivity, $K/\rho Cp$ m^2/s

δ = conducting length, m

K = conductivity, W/m-K

ρ = mass density, Kg/m^3

c = specific heat, J/Kg-K

From the above equation, the recommended time interval for this analysis would be five seconds. In order to get more accurate data, the first time intrval was 0.5 seconds instead of 5 seconds. The program consists of three load steps from 0.0 to 75 seconds. It is listed in the appendix as Program 1. In Program 1, the film coefficient is a function of time and it is a linear variation between each load step. The film coefficients and time steps relationship are as follow:

Time interval	Time (Seconds)	Film Coefficient (W/m^2-K)
1	0-0.5	1000
2	0.5-5.0	10000
3	5.0-14.5	15000
4	14.5-75.0	5

Another ANSYS technique that has been used in this analysis is the time interval optimization. In many transient problems the user can decrease the computational resources by requesting time interval optimization, which is activated by:

```
ITER,-NITTER,...      *negative nitter activates optimizer
    or
CONV,1                *key to activate optimizer
```

The integration time step (ITS) may be increased or decreased based on the quantity,

T^d = maximum over all nodes $\left| -\frac{d^2T}{dt^2} (\Delta t)^2 \right|$

= transient optimization value

T^d is a measure of the "smoothness" of the response. A small T^d indicates that the radius of curvature of the temperature vs. time curve is large. Therefore, the response is smoothing out and hence a larger time interval can be employed.

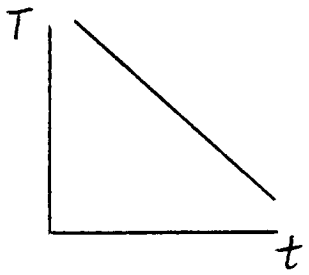

can increase time step

cannot increase time step

Where,

t = time

T = temperature

The transient optimization value, T , is calculated by the finite difference approximation,

$$T^d = \left(\frac{T_n - T_{n-1}}{\Delta t_n} - \frac{T_{n-1} - T_{n-2}}{\Delta t_{n-1}} \right)_{\substack{MAX. \\ Over \\ All\ Nodes}} \frac{2}{(\Delta t_n + \Delta t_{n+1})} (\Delta t_n)^2$$

The goal of the optimization procedure is to keep the transient

optimization value as close as possible to the user-defined transient optimization criterion (T^{cr}) by adjusting the integration time interval.

A trial value for the next time interval can be obtained from the equation:

$$\frac{T^{d}}{(\Delta t_n)^2} = \frac{T^{cr}}{(\Delta t_{n+1})^2}$$

therefore,

$$\Delta t_{n+1} = \Delta t_n \left(\frac{T^{cr}}{T^{d}} \right)^{\frac{1}{2}}$$

where Δt = time interval of previous iteration

T^{cr} = user-supplied optimization criterion

T^{d} = calculated (max.) optimization value for previous iteration

The trial time interval, ΔT_{n+1}, must satisfy various criteria associated with an element changing status (bilinear) or an integration point passing through a phase change boundary.

In addition, Δt must be adjusted so that:

(A) $4\Delta t \geq \Delta t_{n+1} \geq 1/4\Delta t_n$

(B) Δt_{n+1} is an integer multiple of minimum time step

(C) time at last iteration must be the user-specified value

T^{cr} defaults to 10 degree. The user changes the optimization criterion

by giving the new value as the second parameter on the CNVR command.

4.2.4 ANSYS structural program analysis:

Temperatures obtained in a thermal analysis may be input to a structural analysis. This can be done for compatible thermal/structural models. Model that covers the same geometry and the mesh in the thermal model is the same with the mesh in the structural model. An interface file (file 4) contains nodal temperatures which are written at every iteration during the thermal analysis. KTEMP command (lopt module) in the structural analysis defines which load step and iteration of the thermal analysis is to be used to define the temperature distribution in the stress model.

Program 2, in appendix, is the structural analysis program which accompanied with Program 1 would solve thermal stress problem of the three load steps. The KAN,0 module was chosen for structural analysis. The segment gridwork consisted of 92 three dimensional isoparametric elements and STIF45 was chosen in both element type one and element type two. KTEMP,3,50 is shown in program three, i.e., the time at 14.5 seconds thermal analysis may be input to this structural analysis. Constraints were applied on the rotor center line and lateral surfaces of the cover, platform and rotor segment. These details of the constraints are given in the Program 2.

4.2.5 Results of two-step heating process:

Fig. 4.3 shows the thermal response at selected points in the rotor.

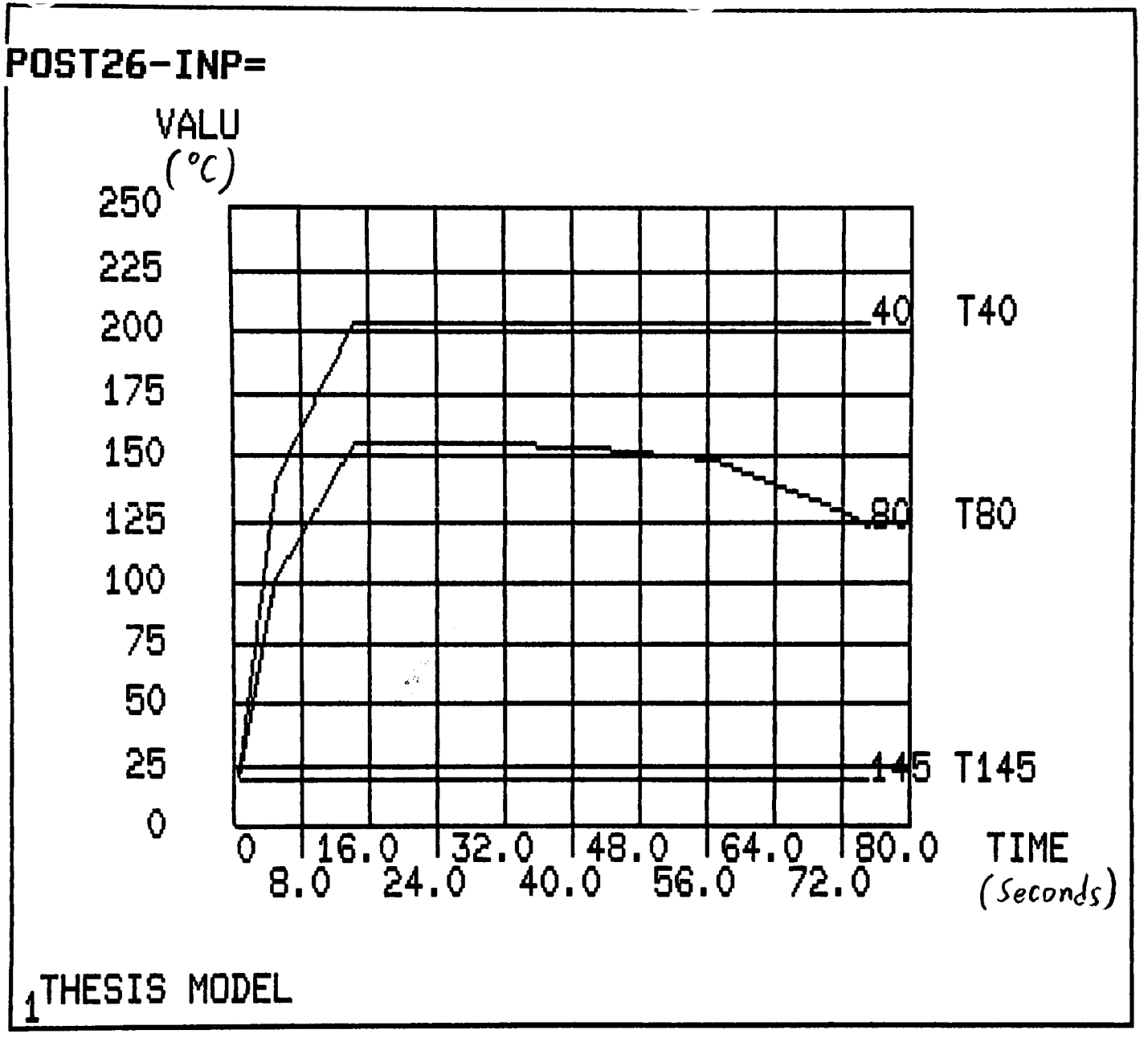

Fig. 4.3 Transient Temperature Distribution of Nodes 40, 80, and 145. (2-step)

The respective position of each point, node 40, 80, and 145, on the control stage model is identified in Fig. 3.7, 3.9, and 3.10. Node 40 is on the inner surface of the cover, node 80 is on the upper surface of the platform and node 145 is on the center of the rotor. A sharp increase in temperature within short period of time was found to be typical for the points on the rotor surface in direct contact with the steam. This is attributed to the rapid change in film coefficient, and the rapid change in the steam temperature.

Fig. 4.4 shows the temperature differentials between points in the control stage at the upper surface of the platform and the center of the rotor, i.e., node 80 and node 145. The peak temperature difference between node 80 and 145 occurred at approximately 23 seconds.

Solution of the stress analysis was handled in a similar manner as its temperature counterpart. First, the stress analysis was preformed for the entire rotor using the same control stage model employed in the thermal analysis. Fig. 4.5 shows the thermal equivalent stress distribution for the layer of elements forming the upper surface of the platform. Very large values of compressive thermal stress were obtained at small values of time, e.g., at 56.9 seconds 437 MPA on the edge of the platform. Such high stresses are attributed to the large heat flux and temperature gradient at the rotor surfaces shortly afar the initiation of steam flow. At 56.9 seconds, the temperature distribution of the platform is shown in Fig. 4.6.

The comparisons between STI's actual model and the simplified model are as follows:

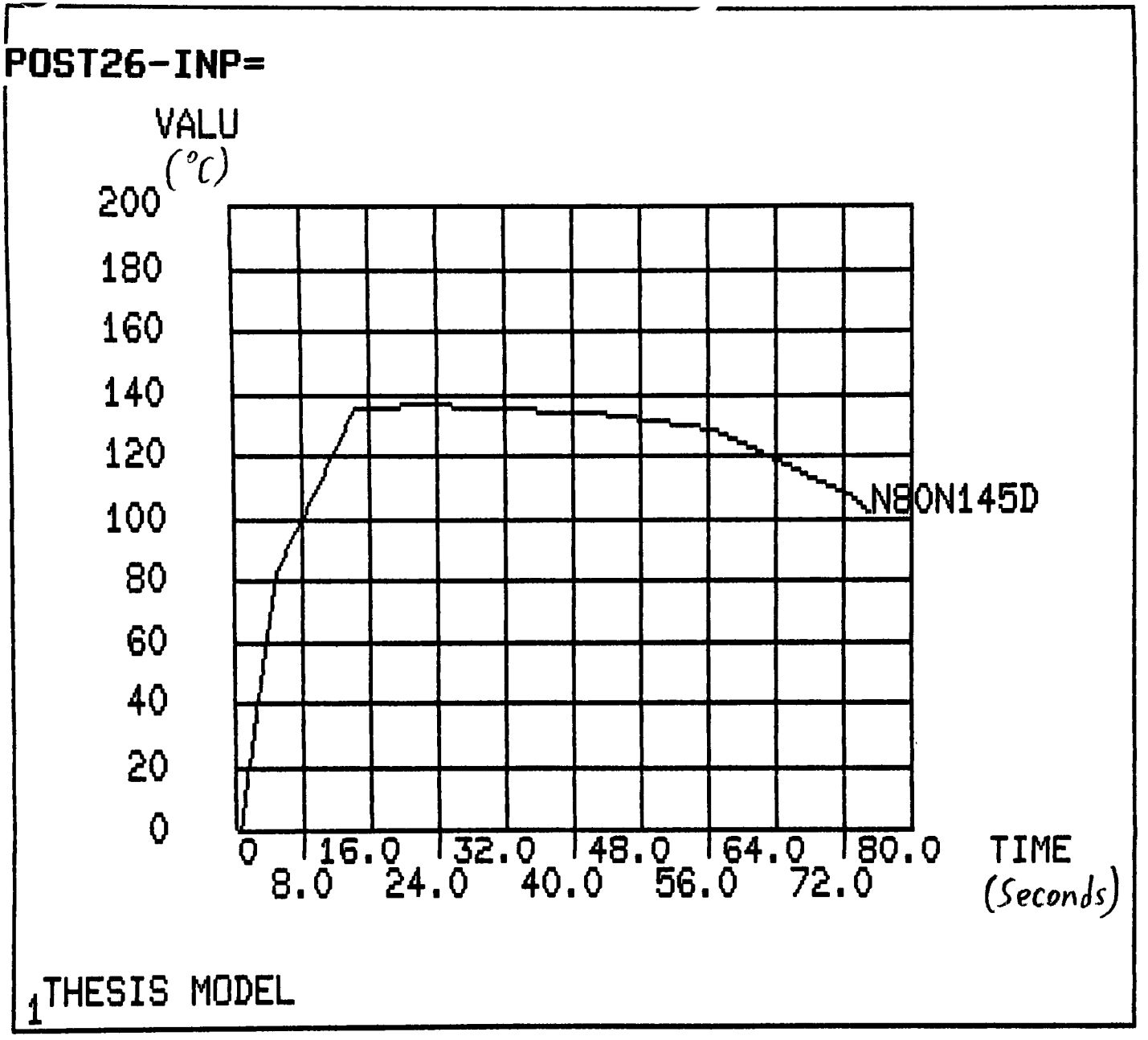

ANSYS 4.3
JAN 17 1988
22:47:00
POST26

ZV=1
DIST=1.48

Fig. 4.4 Temperature Difference Between Nodes 80 and 145. (2-step)

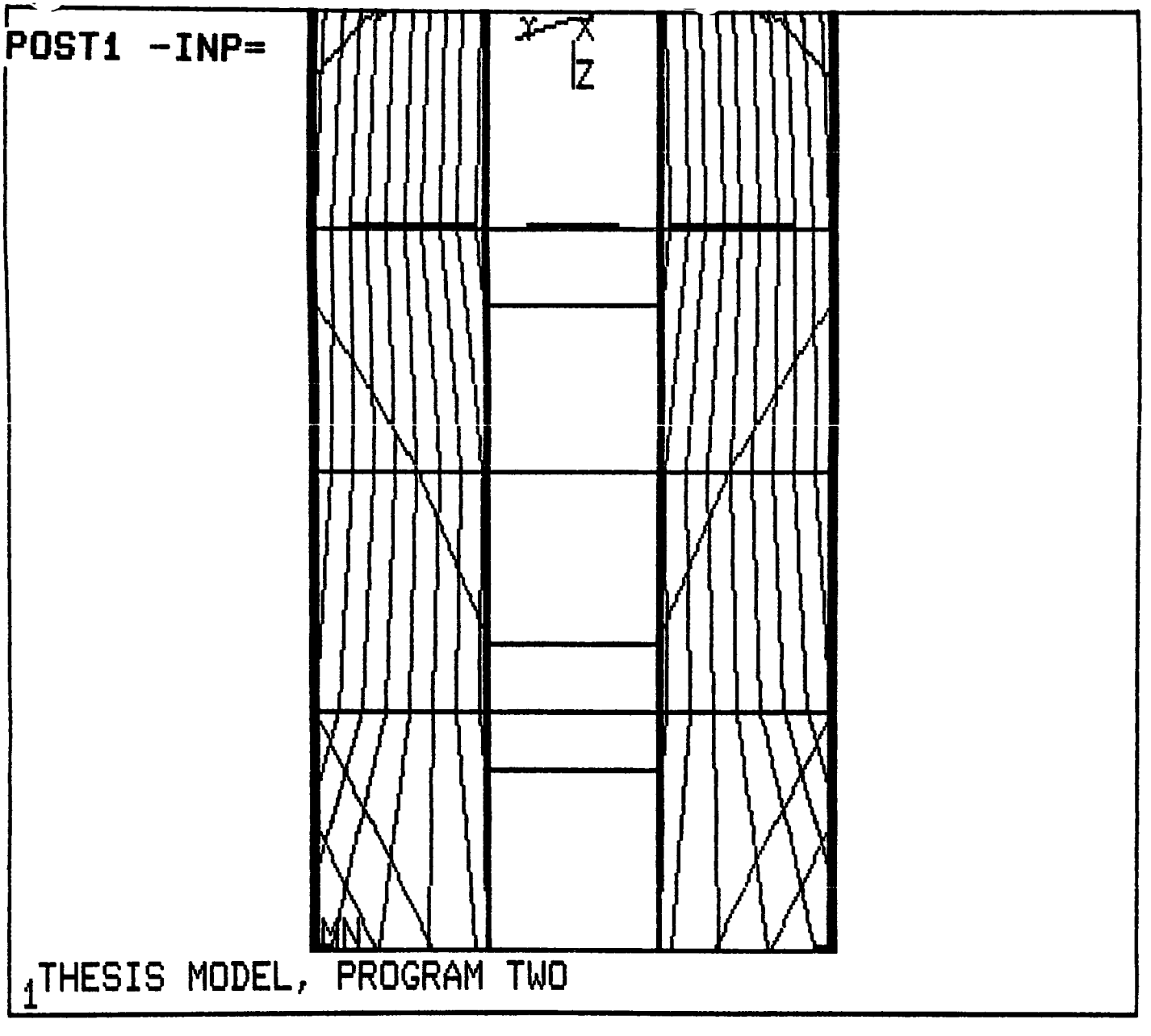

Fig. 4.5 Platform Stress Distribution, Maximum Thermal Stress = 437 MPA, time = 56.9sec., HF = 10000W/m-K

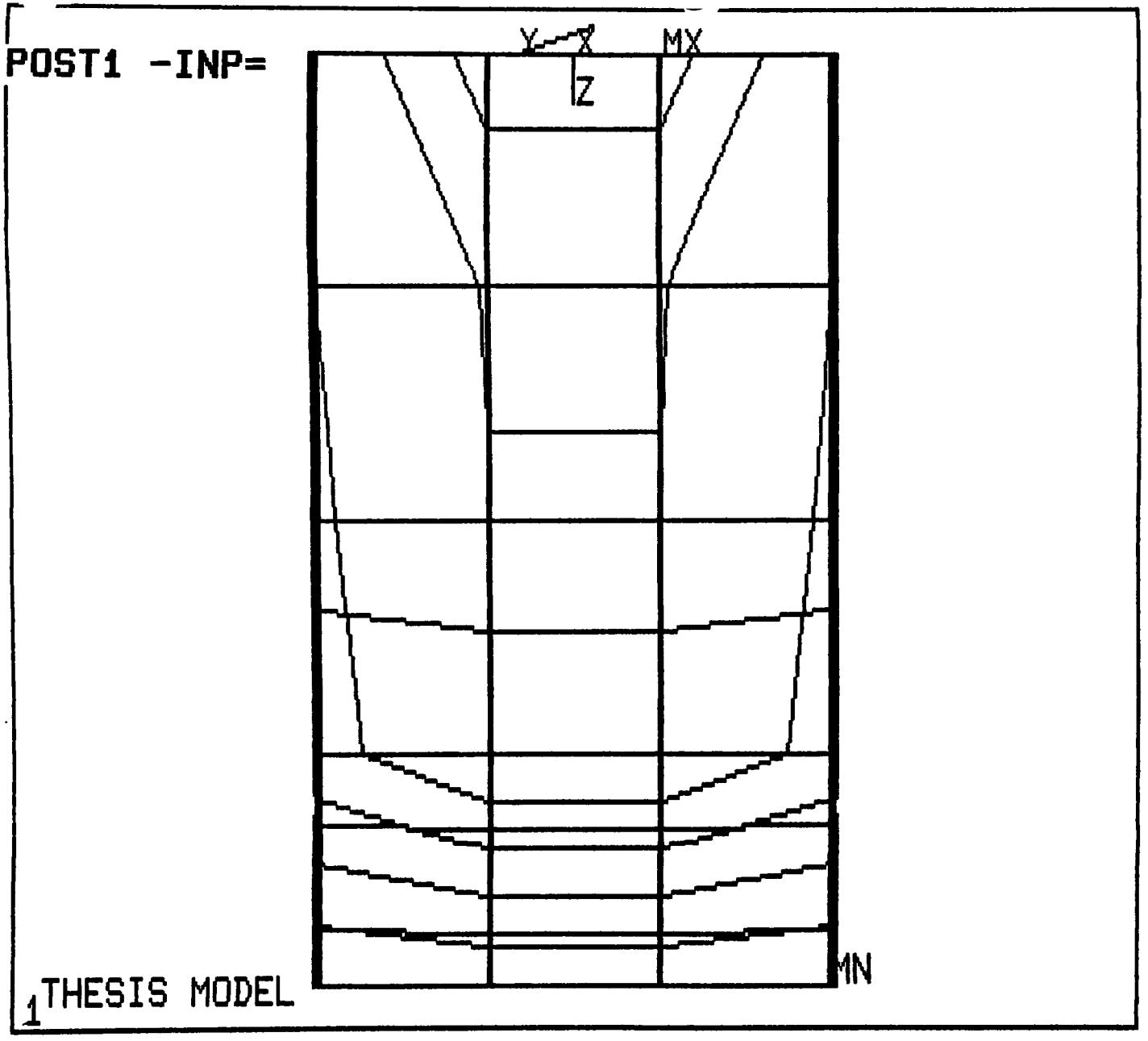

Fig. 4.6 Platform Temperature Distribution, time = 56.9 sec.,

HF = 10000W/m-K. (2-step)

	Maximum Stress (MPA)	Time (Seconds)
Actual Model	565	23.4
Simplified Model	437	56.9

The maximum thermal stress which compared with the STI's results has approximately 22.7% error. This situation was attributed to the smooth surface and thicker layer of the platform which was constructed in this simplified model. The same reason can be applied to explain why the maximum stress happened at 56.9 seconds which was 33.5 seconds later than STI's results. The simplified model employs smaller number of nodes resulting in a substantial reduction in computer time and storage requirements. As seen from the above comparison, the simplified model gives reasonably accurate results. It could therefore be employed as a tool during preliminary optimization to obtain appropriate time steps and intermediate steam temperatures.

4.3 Three-step heating process:

Three dimensional thermal and stress analyses were performed utilizing the same control stage model as employed in the two-step heating process (see Fig. 4.1). In this analysis there are nine time intervals which are as follow:

Time Step	From	To	
1	0.0	0.5	(seconds)
2	0.5	5.0	

3	5.0	14.5
4	14.5	75.0
5	75.0	675.0
6	675.0	675.5
7	675.5	680.0
8	680.0	689.5
9	689.5	750.0

The fifth time interval is ten minutes long during which time the entire rotor warms up. The compressive thermal stress at the platform and cover relaxed (becomes less compressive) with time as the rotor material adjusted to the imposed thermal conditions.

4.3.1 Thermal analysis:

The ANSYS thermal analysis program is in the appendix as Program 3. Basically, Program 3 is similar with Program 2. The difference between these two programs is the arrangement of time steps and temperature rising among every time interval. The rear part of Program 3 shows the arrangement clearly.

The boundary conditions for the control stage model of this analysis were specified in the same manner as for the two-step heating process analysis. The differences between these two analyses are the temperature and time steps. The following table shows the relationship among time, temperature and film coefficient.

Time	Temperature	Film Coefficient

(seconds)	(C)	(W/m^2-K)
0.5	32.2	1000
5.0	142.0	10000
14.5	142.0	10000
75.0	142.0	5
675.0	142.0	5
675.5	148.2	1000
680.0	204.0	10000
689.5	204.0	10000
750.0	204.0	5

Fig. 4.7 shows the same relationship which is given in the above table. The time step arrangements of step 1 to 4 and step 5 to 9 are identical with the arrangement of Fig. 2.5. The only difference being in the warm up time which is now increased to 10 minutes, starting at 75 sec. and continuing up to 675 sec.

In the analysis, it was felt that the simplest and yet most reasonable assumption was a linear variation of the steam bulk temperature and film coefficient among every load step. Consequently, both the steam bulk temperature and film coefficient were assumed to result in a linear variation from the control stage to the shaft end.

Fig. 4.8 shows the transient temperature distribution of the inner surface of the cover, the upper surface of the platform, and the rotor center axis, i.e., nodes 40, 80, and 145. The respective position of each point on the control stage model are identified in Figs. 3.7, 3.9, and 3.10. A sharp increase in temperature followed by an equally rapid decrease within short period of time was found to be typical for

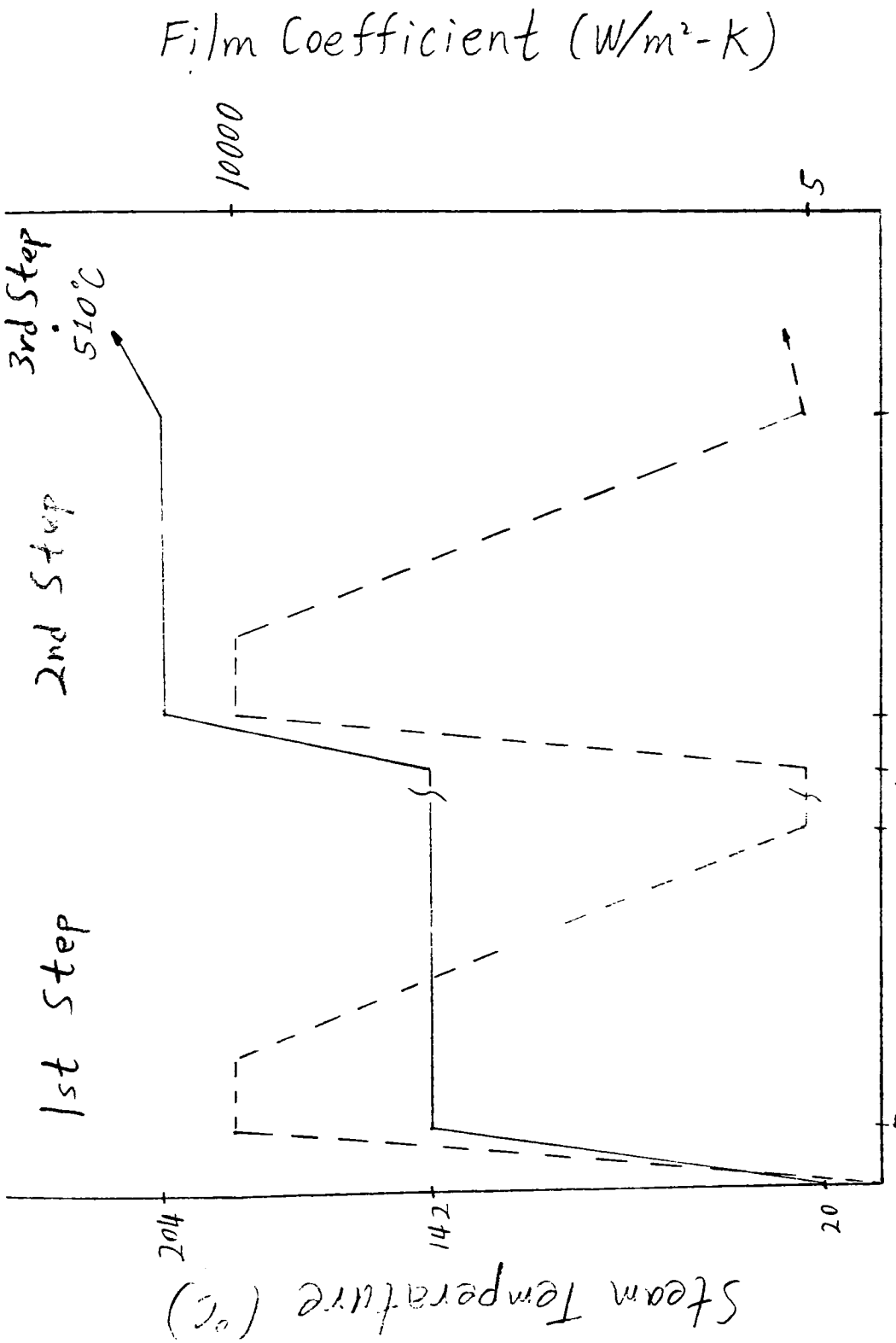

Figure 4.7 Three-Step heating Process Temperature and Film Coefficient VS Time Diagram

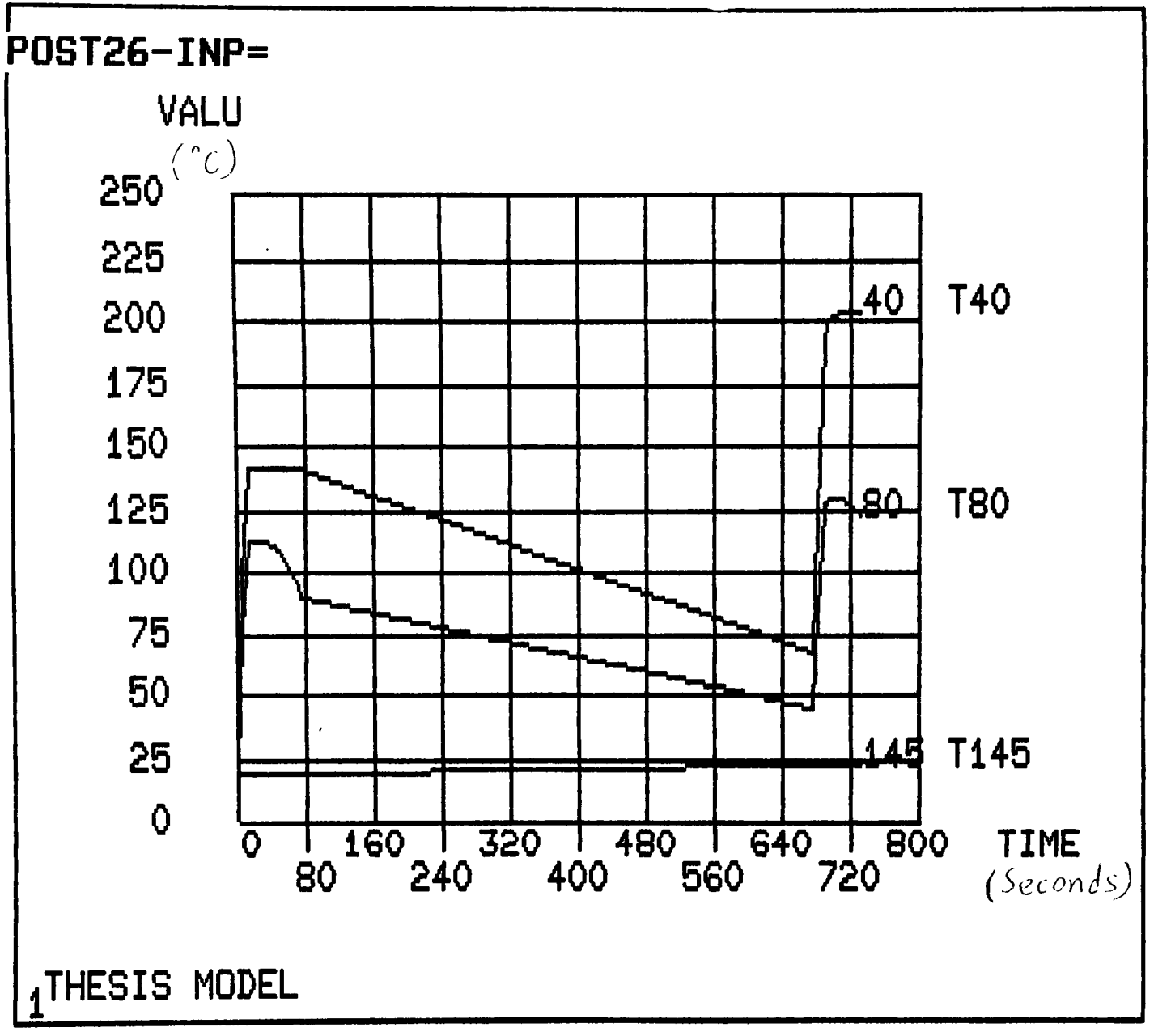

Fig. 4.8 Transient Temperature Distribution of Nodes 40, 80, and 145. (3-step)

the points on the rotor surface in direct contact with the steam. This is attributed to the rapid change in film coefficient, introduced by the initiation and subsequent termination of steam condensation. Fig. 4.9 shows the temperature differential between points of the upper surface of the platform and the rotor center axis, i.e., node 80 and 145. Fig. 4.10 shows the transient temperature distribution of nodes 40, 80, and 145 from 0 to 75 seconds. Fig. 4.11 shows the temperature differential between node 80 and 145 from 0 to 75 seconds. Fig. 4.12 shows the transient temperature distribution of nodes 40, 80, and 145 from 675 to 750 seconds. Fig. 4.13 shows the temperature differential between node 80 and 145 from 675 to 750 seconds.

4.3.2 Structural analysis:

Program 4, in appendix, is the structural analysis program which accompanied with Program 2 would solve thermal stress problem of every time step, i.e., from 0 to 750 seconds. Program 4 is almost identical with program 2 except the command KTEMP. KTEMP,9,69 is used in program four which can make the thermal analysis at time 731 seconds be the input to this structural analysis.

In the three dimensional control stage model, the center of rotor was constrained, allowing no displacement in the x and y directions. Node 141, the end of rotor center axis, was constrained in all directions so as to make the model always in the same place no matter what kind of analysis was applied on it. Finally, corresponding nodes on the lateral surfaces (shaded in Fig. 4.2) of the cover, platform and disk rim were coupled in view of the periodic nature of the boundary

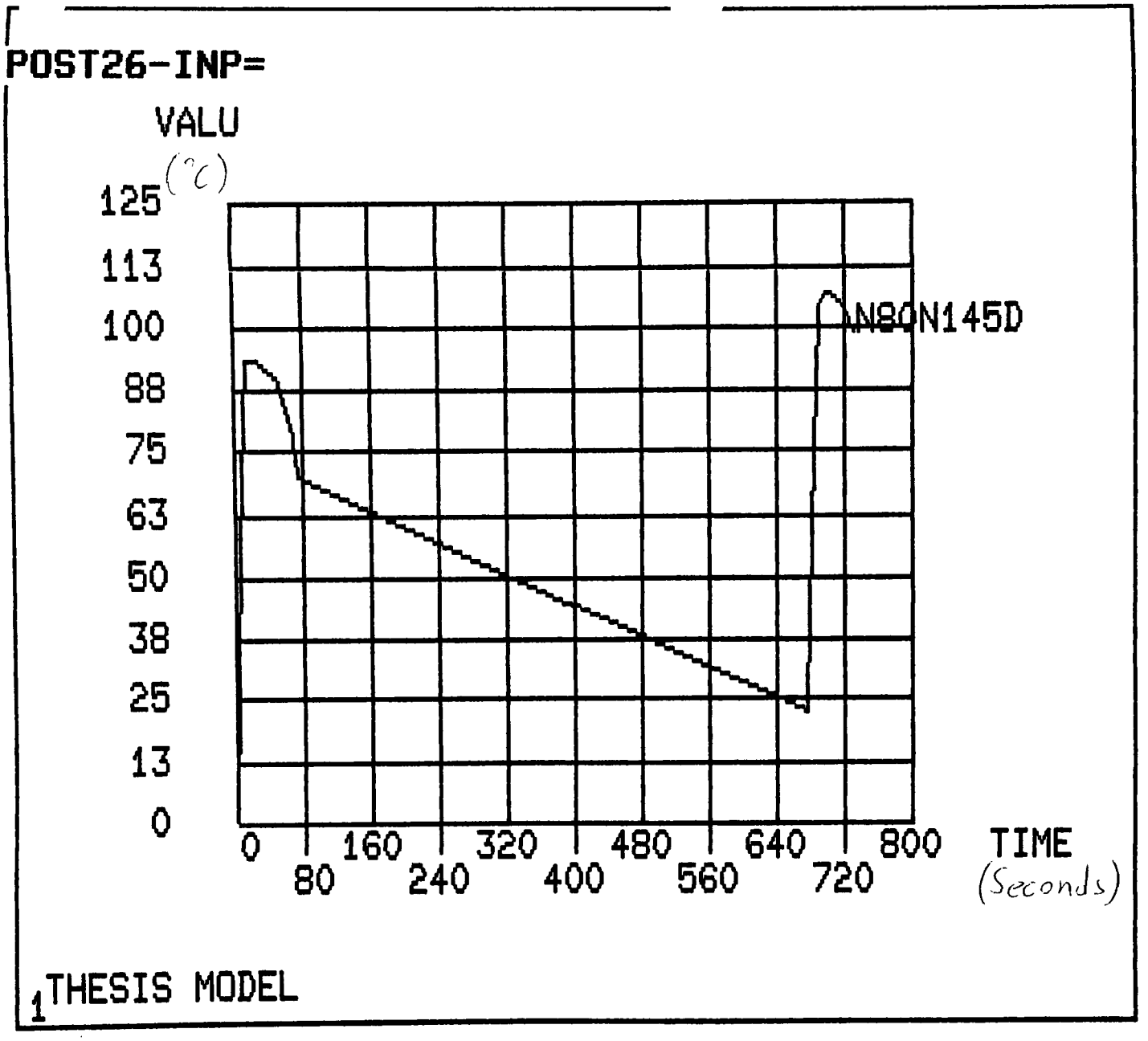

Fig. 4.9 Temperature Difference Between Nodes 80 and 145. (3-step)

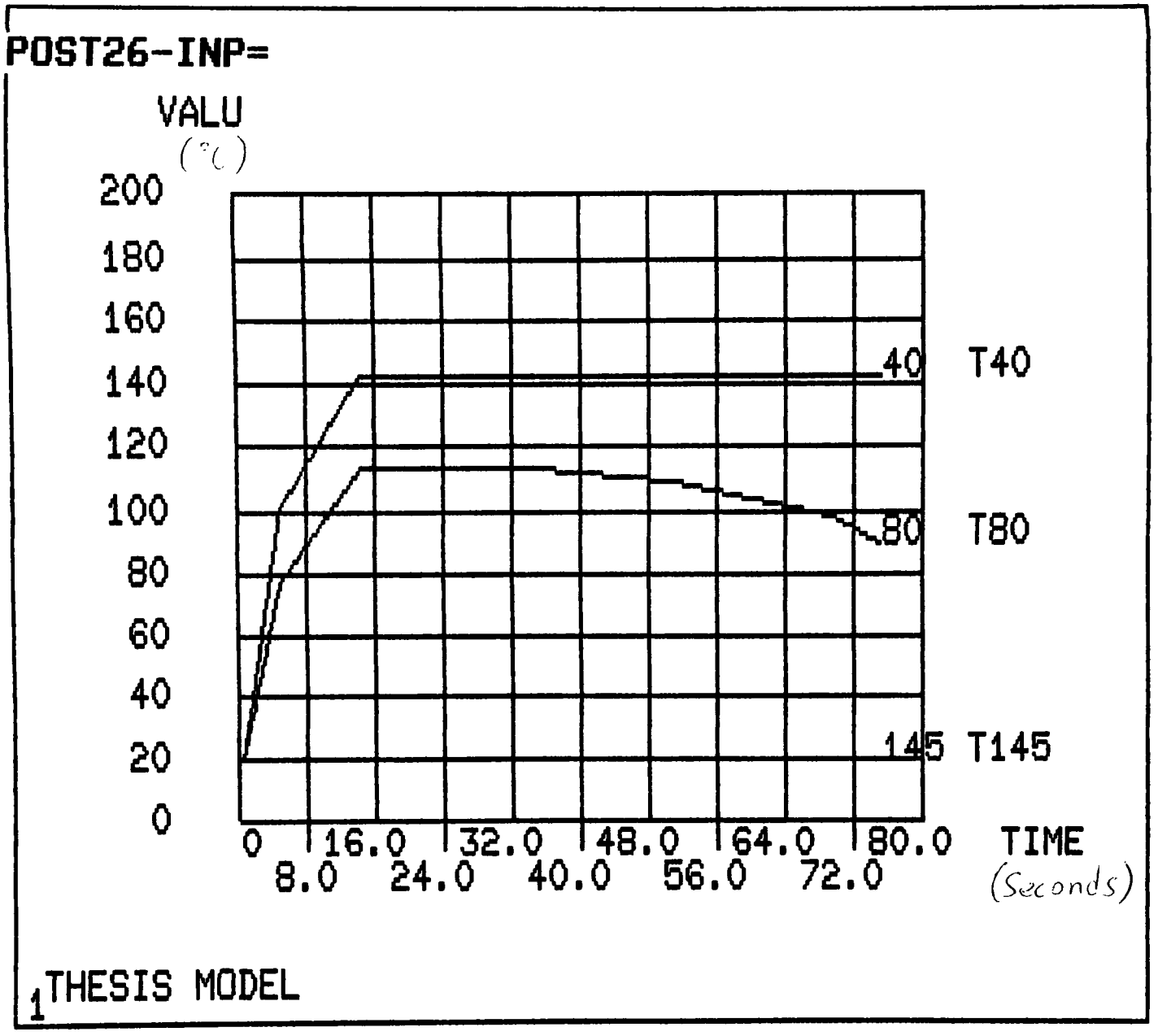

Fig. 4.10 Transient Temperature Distribution of Nodes 40, 80, and 145. (3-step)

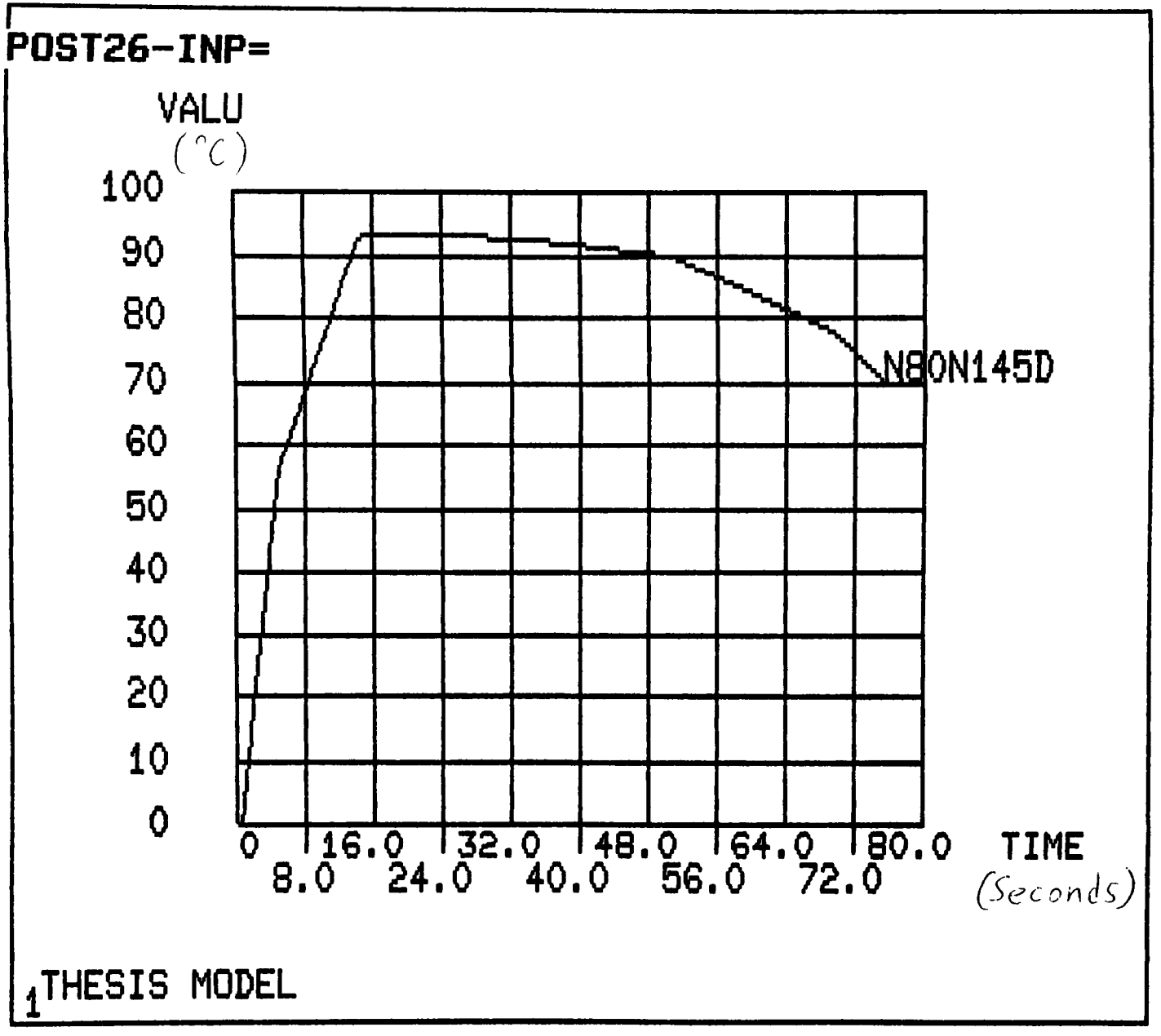

ANSYS 4.3
JAN 18 1988
19:52:48
POST26

ZV=1
DIST=1.48

Fig. 4.11 Temperature Difference Between Nodes 80 and 145. (3-step)

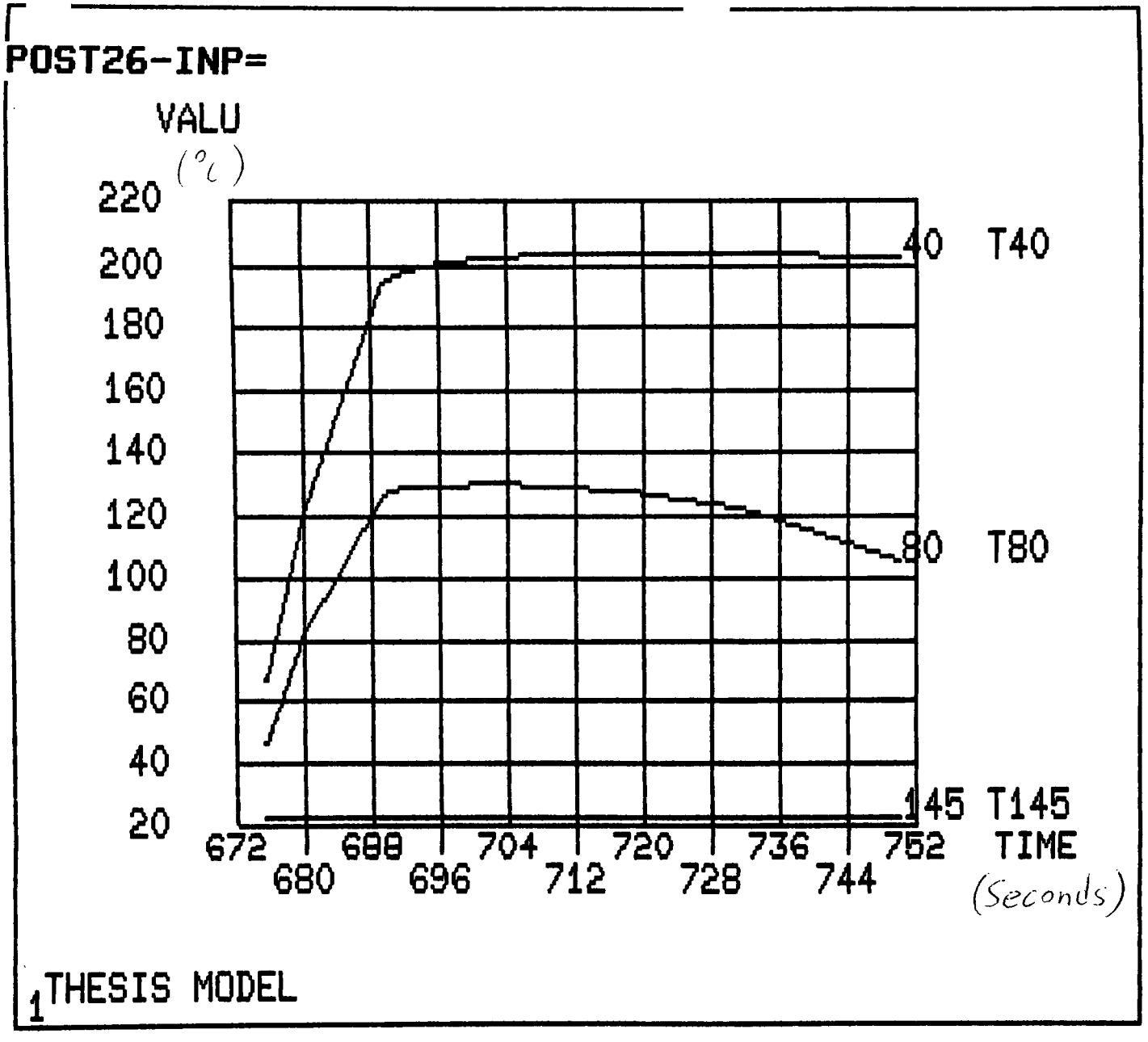

Fig. 4.12 Transient Temperature Distribution of Nodes 40, 80, and 145. (3 step)

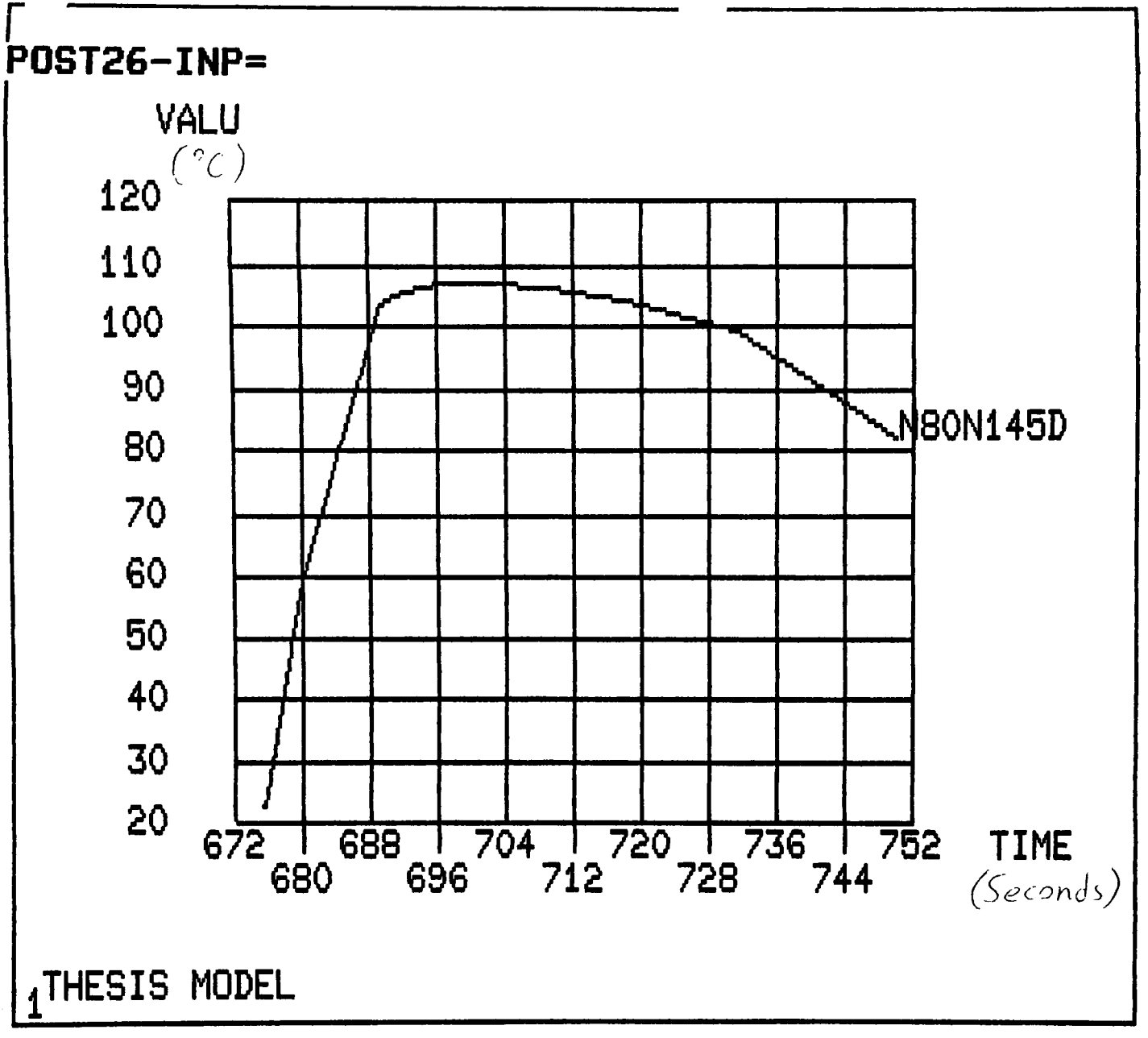

Fig. 4.13 Temperature Difference Between Nodes 80 and 145. (3-step)

conditions and geometry along the circumferential direction.

4.3.3 Results of three-step heating process:

Two thermal equivalent stress peaks can be found in this period of time from 0 to 750 seconds. one is 387 MPA at 731.2 seconds from the starting point. The corresponding maximum hoop stresses for the above two time points are -282 MPA at element 27 and -341 MPA at element 27 respectively.

Fig. 4.14 shows the platform temperature distribution at time 50.8 seconds. The corresponding stress distribution is shown in Fig. 4.15. The maximum thermal stress is on the edge of the platform which corresponds with the two-step heating process (see Fig. 4.5). The maximum stresses of these two analyses occurred approximately 30 seconds later than STI's analysis. The main reason for this situation is the difference in the simplified mesh model used in this project and the actual model generated by STI. The segment gridwork of this simplified model consisted of 92 three dimensional isoparametric elements and approximately 200 nodes. The segment gridwork of STI's real model consisted of 675 three dimensional isoparametric elements and approximately 1000 nodes.

Fig. 4.16 shows the platform temperature distribution at time 731 seconds. The corresponding stress distribution is shown in Fig. 4.17. The maximum equivalent thermal stress can be decreased if the warm up time, time step 5, can be made longer.

4.4 Effect of film coefficient on the maximum thermal stress:

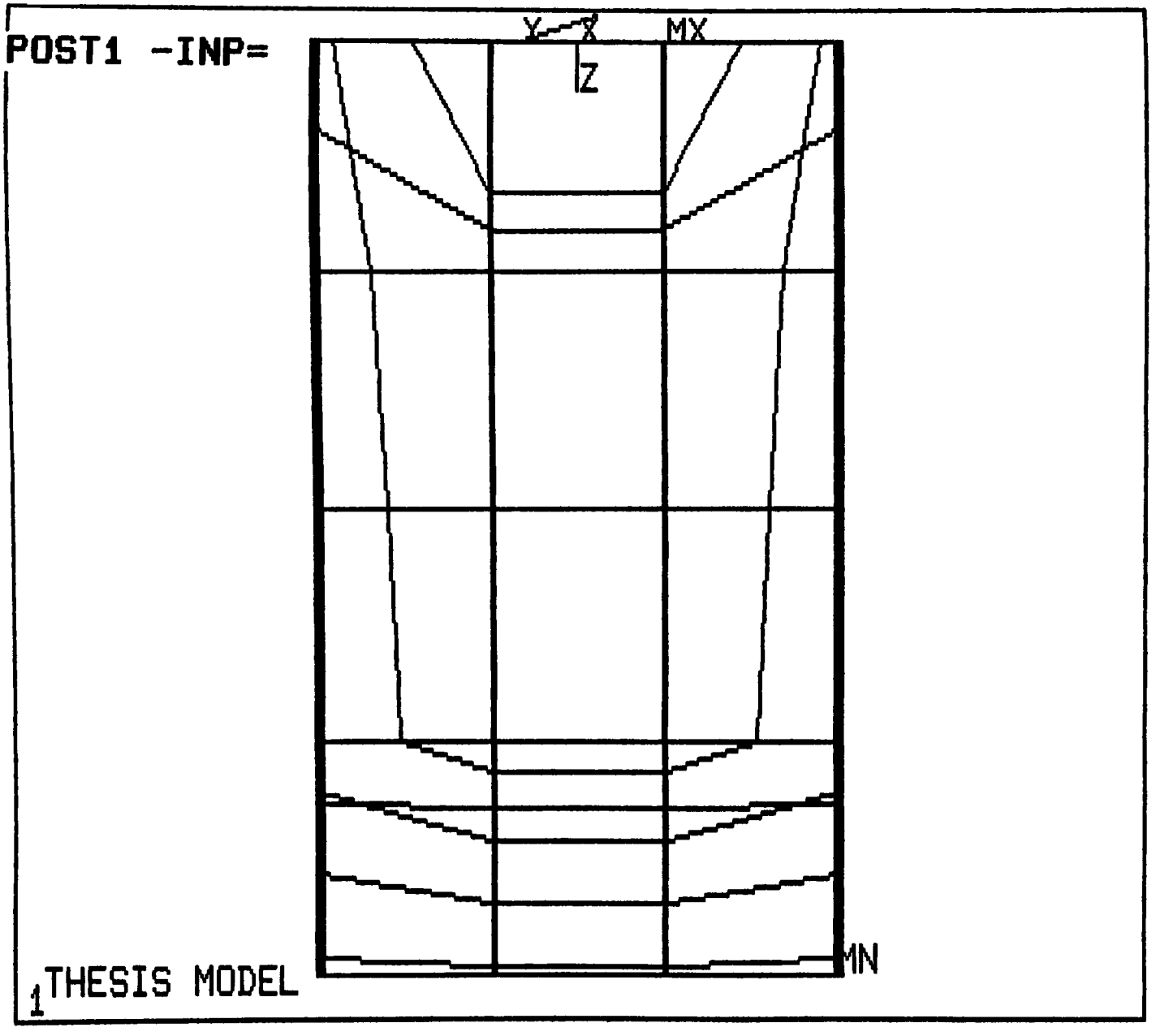

Fig. 4.14 Platform Temperature Distribution, time = 50.8 sec.,
HF = 10000W/m-K. (3-step)

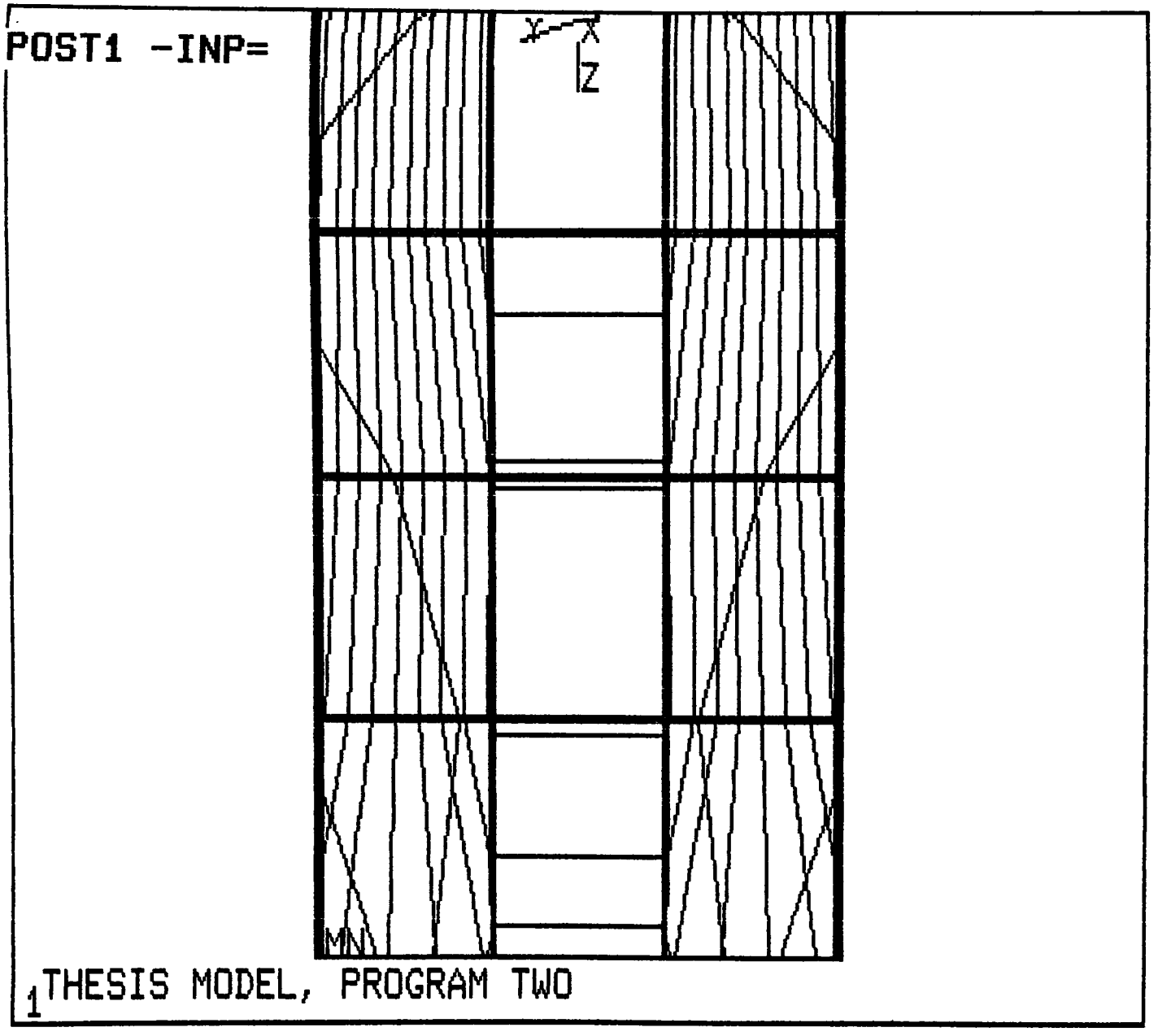

Fig. 4.15 Platform Stress Distribution, Maximum Thermal Stress = 310MPA, time = 50.8sec., HF = 10000W/m-K. (3-plot)

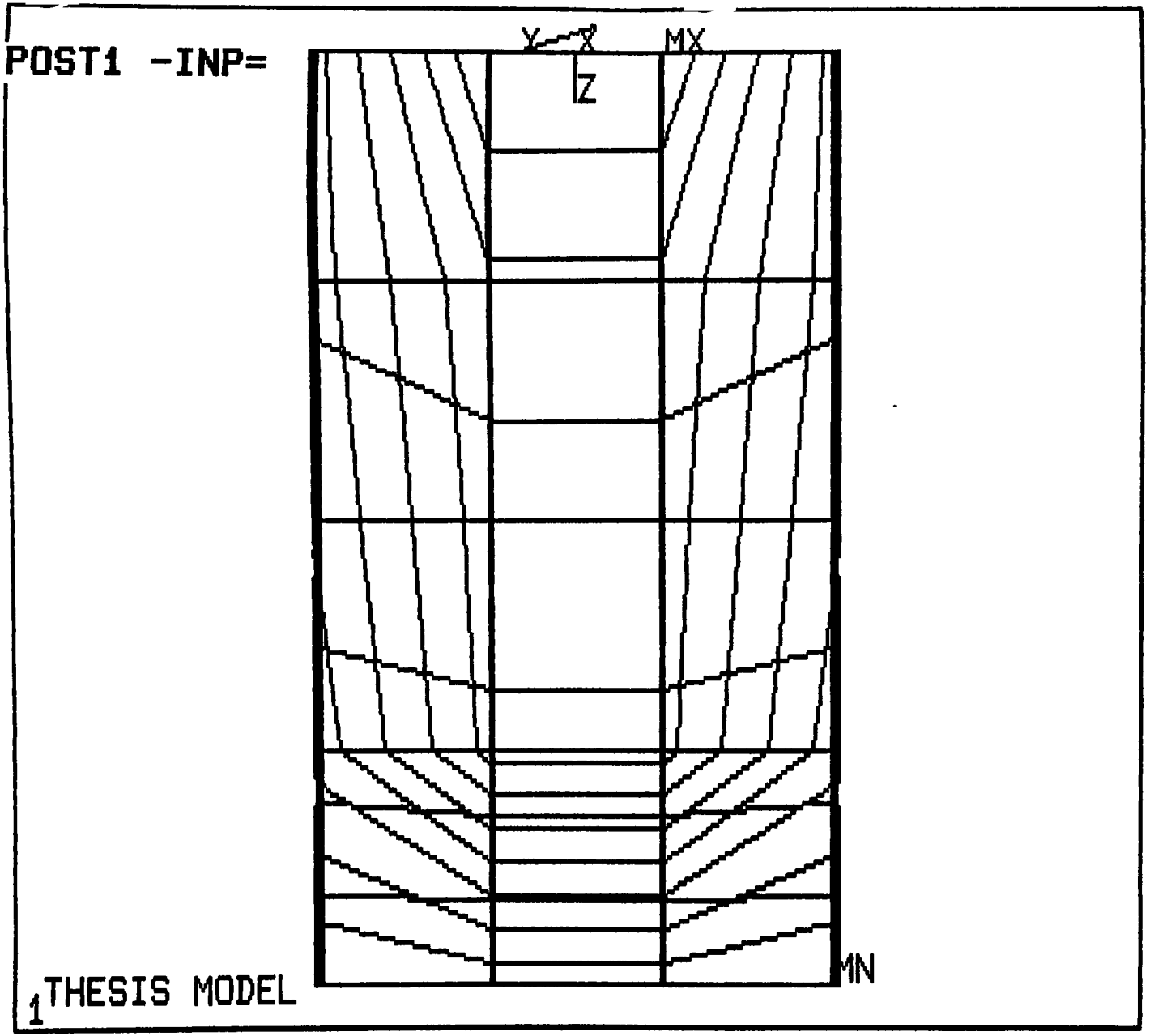

Fig. 4.16 Platform Temperature distribution, time = 731sec.,

HF = 10000W/m-K. (3-step)

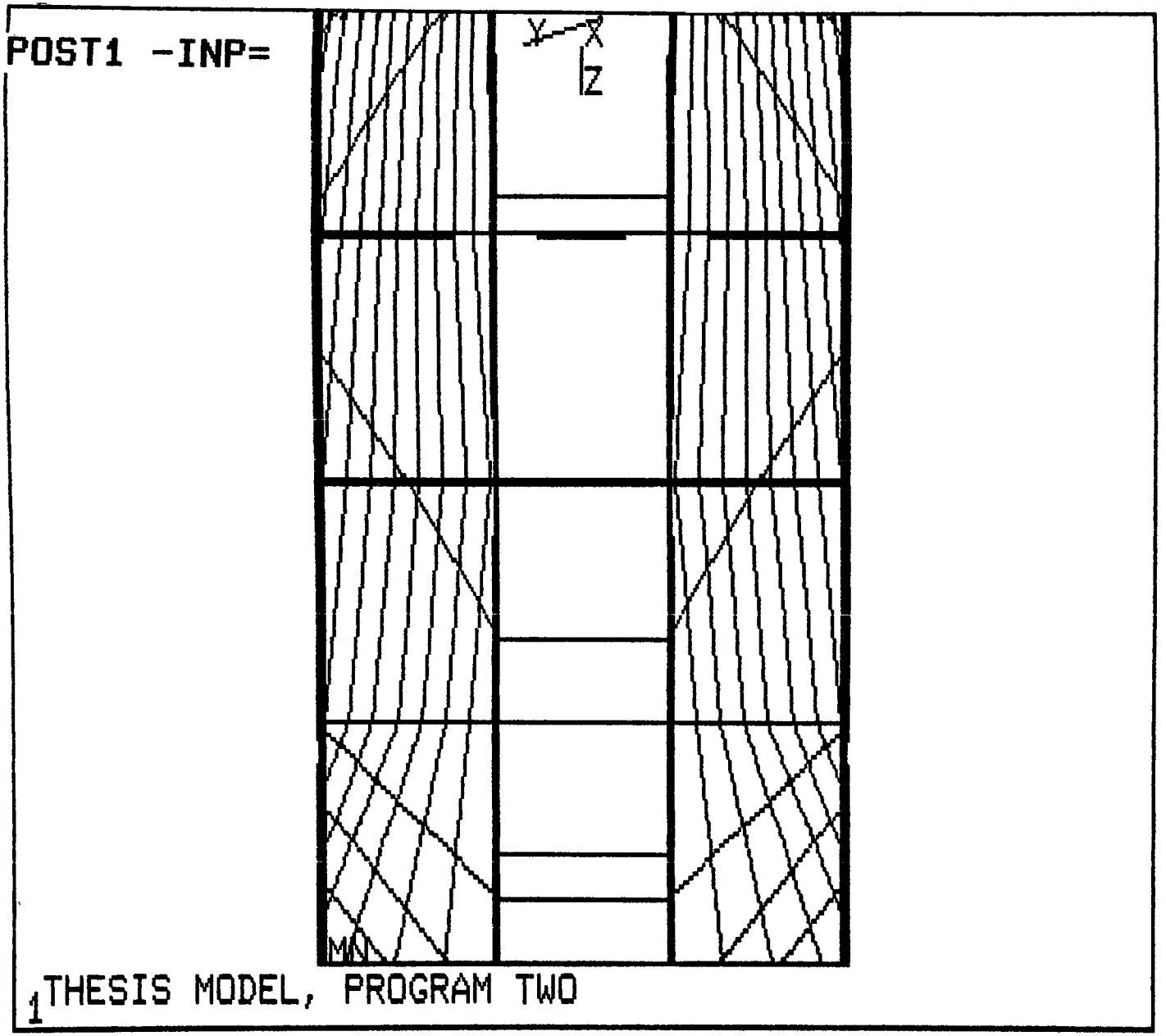

Fig. 4.17 Platform Stress Distribution, Maximum Thermal Stress = 387MPA, time = 731sec., HF = 10000W/m-K. (3-step)

Same operating conditions with different film coefficients will be analysed. These film coefficients are 10000, 5000, 15000, and 1000 W/m^2-K.

The first film coefficient to be studied in this section is 10000 W/m^2-K. The maximum thermal stress, 437 MPA, is shown in the platform stress distribution Fig. 4.5. This analysis has been discussed in section 4.2.

Program 5, in appendix, did the thermal analysis of film coefficient equals 5000 W/m^2-K which was half the magnitude of the first one. Program 5 is similar to Program 1 except the difference of film coefficients between these two programs. Program 2 can be coupled with Program 5 to do the structural analysis.

The maximum thermal stress is 391 MPA at time 53.2 seconds which is due to the analysis with film coefficient of 5000 W/m^2-K. Fig. 4.18 shows the corresponding platform stress distribution at time 53.2 seconds.

The third film coefficient to be analysed is 15000 W/m^2-K. Program 6, in appendix, used 15000 W/m^2-K as the film coefficient to study the thermal response. Program 6 is similar to Program 1 except the difference of film coefficients between these two programs. Program 2 can be coupled with Program 6 to do the structural analysis.

The maximum thermal stress is 464 MPA at time 52.0 seconds which is due to the analysis with film coefficient of 15000 W/m^2-K. Fig. 4.19 shows the corresponding platform stress distribution at time 52.0 seconds.

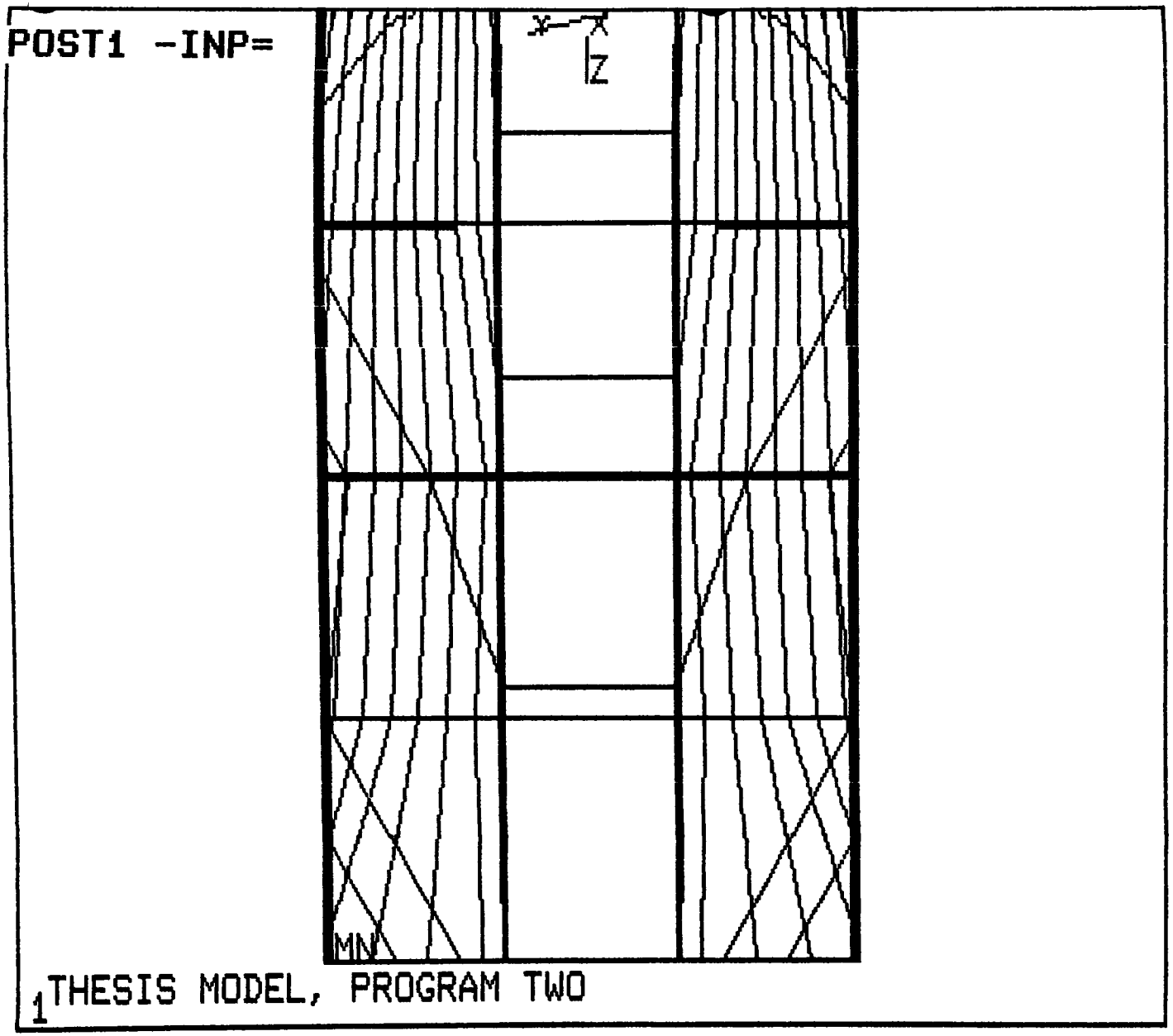

Fig. 4.18 Platform Stress Distribution, Maximum Thermal Stress = 391MPA, time = 53.2sec , HF = 5000W/m-K. (2-step)

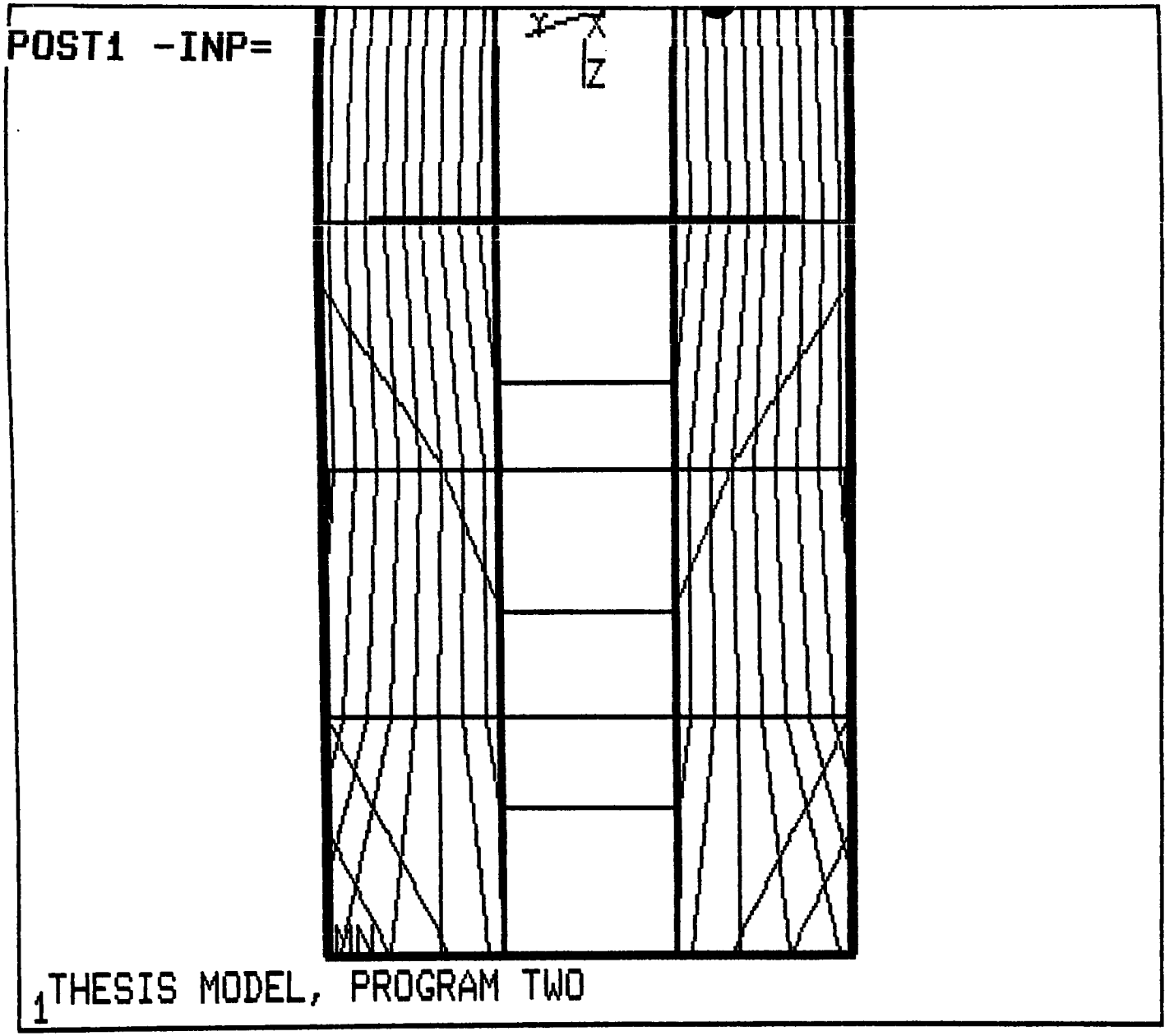

Fig. 4.19 Platform Stress Distribution, Maximum Thermal Stress = 464MPA, time = 53.0sec., HF = 15000W/m-K. (2-step)

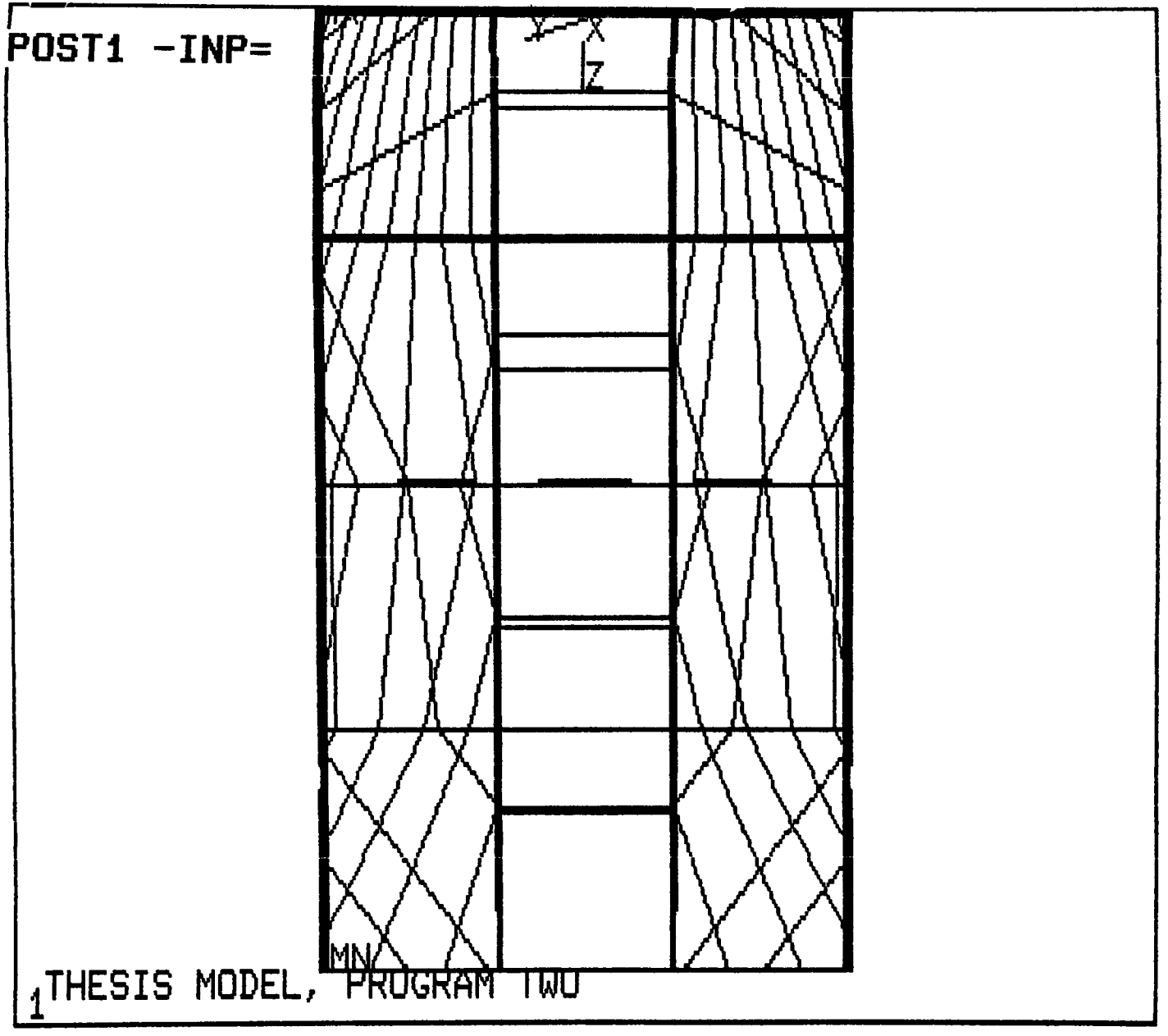

Fig. 4.20 Platform Stress Distribution, Maximum Thermal Stress = 231MPA, time = 81.4sec., HF = 1000W/m-K. (2-step)

The final film coefficient to be analysed is 1000 W/m^2-K. This magnitude is only one tenth of the first one and its maximum thermal stress decreased to 231 MPA. Fig. 4.20 shows the corresponding platform stress distribution at time 51.4 seconds.

Results:

Thermal stress was affected by different film coefficients if these coefficients had significant difference among them. The following table can display the relationship between thermal stress and film coefficient of the above four analyses.

Case	Film coefficient (W/m^2-K)	Maximum stress MPA
I	10,000	437
II	5,000	391
III	15,000	464
IV	1,000	231

5.0 OPTIMIZATION OF THE THREE-STEP HEATING METHOD

5.1 Purpose of work:

This chapter is an extension of the previous chapter. The purpose is to investigate the advantage of a longer warm up time for a steam turbine which has a cold start procedure. The second purpose is to find an optimum heating temperature which can reduce the severity of a thermal shock.

5.2 Warm up time:

Program 7, in appendix, shows the thermal analysis which is similar to Program 3 except the TIME command. In program seven the time step 5 was from 75 seconds to 1275 seconds. But, the time interval 5 in program three was from 75 seconds to 675 seconds. From the chapter 4, the warm up time, time step 5, was ten minutes and the maximum stress was 387 MPA at time 731.2 seconds. An increase in the warm up time to twenty minutes instead of ten minutes resulted in a decrease of the the maximum stress to 422 MPA at time 1328.2 seconds. Figure 5.1 shows the platform temperature distribution at time 1328.2 seconds, the figure 5.2 shows the corresponding platform stress distribution.

5.3 Optimum heating temperature:

Figure 4.7 shows the heating procedure from 20C to 142C and from 142C to 204C and the corresponding stress to be 347 MPA at 50.8 seconds and

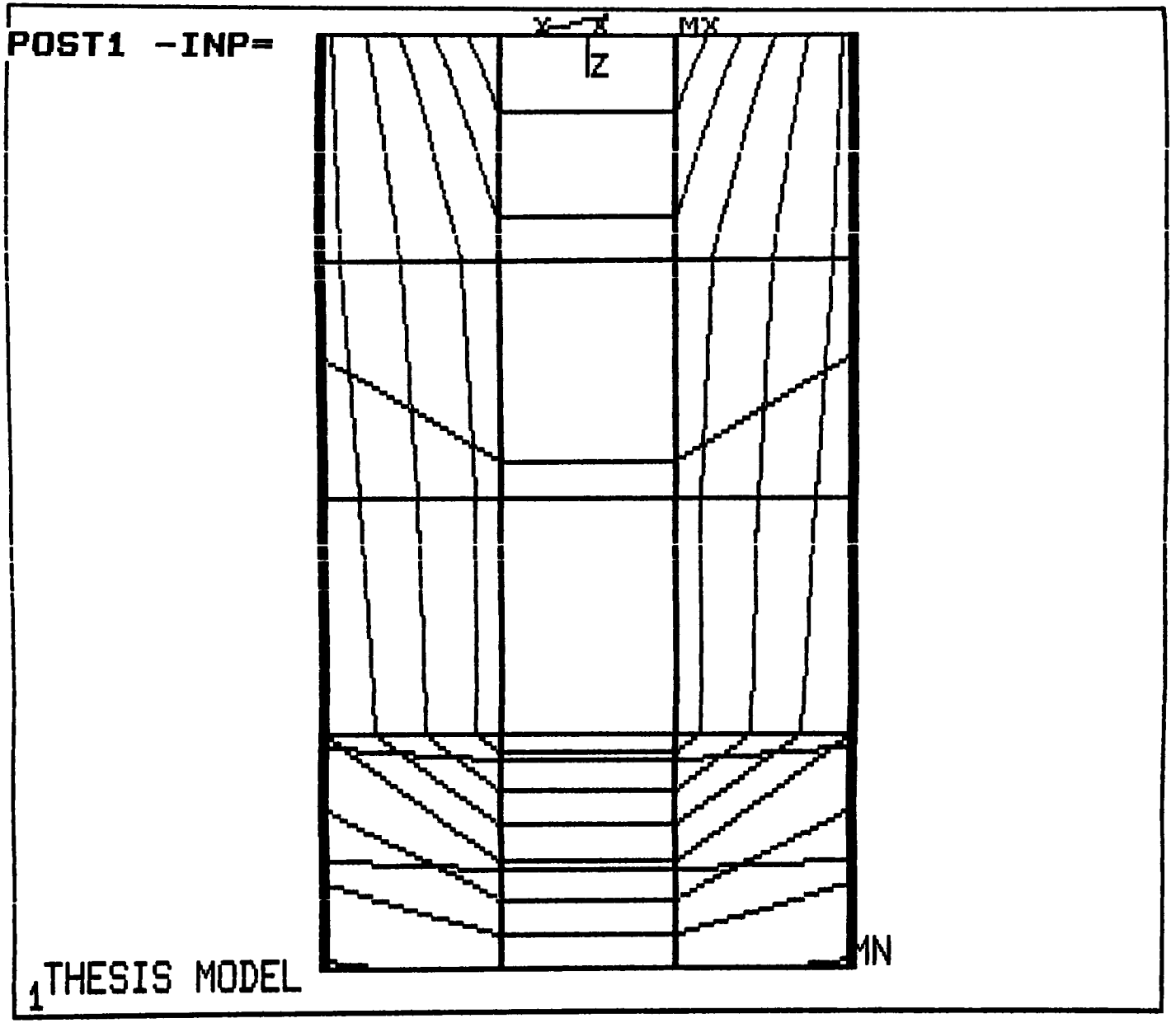

Fig. 5.1 Platform Temperature Distribution, Time Step 5 = 20min.

1st Heating Temp. = 142C, time = 1328sec.

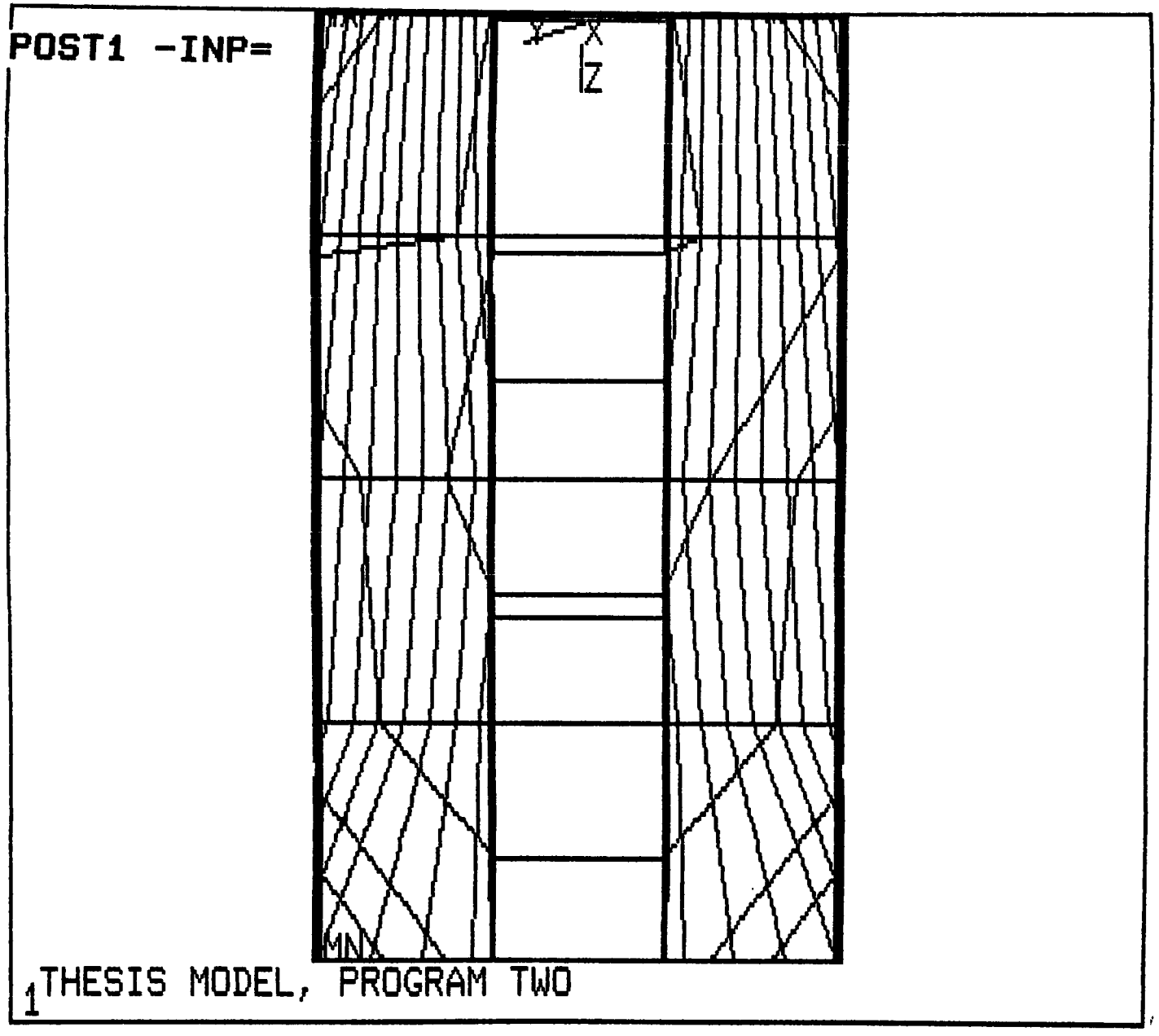

Fig. 5.2 Platform Stress Distribution, Time Step 5 = 20min.

1st Heating Temp. = 142C, time = 1328sec.

427 MPA at 731.2 seconds. For the second heating step, it was found that the corresponding stress was not acceptable because its magnitude is 80 MPA greater than the first one. The optimum way is to make both stresses uniform. Extending the warm up time did not solve the problem in a satisfactory way. The maximum stress difference between step one and step two was still substantial at 75 MPA, even if the warm up time, time interval 5, is increased to twenty minutes. Under this condition, the only way to make stresses uniform is to change the heating temperatures at the intermediate steps.

The first heating temperature increased from 20C to 160C instead of from 20C to 142C. Figures 5.3 and 5.4 show two thermal stress peaks. The first one was 350 MPA at 48.4 seconds and the second one was 360 MPA at 1328.8 seconds from the starting point. Program eight, in appendix, shows the thermal analysis which had 160C as the first heating temperature. Command of KTEMP in program two had been changed in order to conduct the corresponding structural analyses.

By linear interpolation method, the first heating temperature was chosen as 162C instead of 160C so as to do another trial. The first thermal stress peak was 358 MPA which happened at 47.8 seconds, and the second one was 352 MPA at 1328.2 seconds from the starting point. The thermal stress difference between these two peaks was only 6 MPA. Figures 5.5 and 5.6 depict the platform stress distributions of the above two maximum stresses. Figures 5.7 to 5.10 depict stresses happened at 32.7, 64.7, 1317.3, and 1341.5 seconds respectively.

Program 9, in appendix, solved the thermal analysis which had 162C as the first heating temperature. Command of KTEMP in program four had

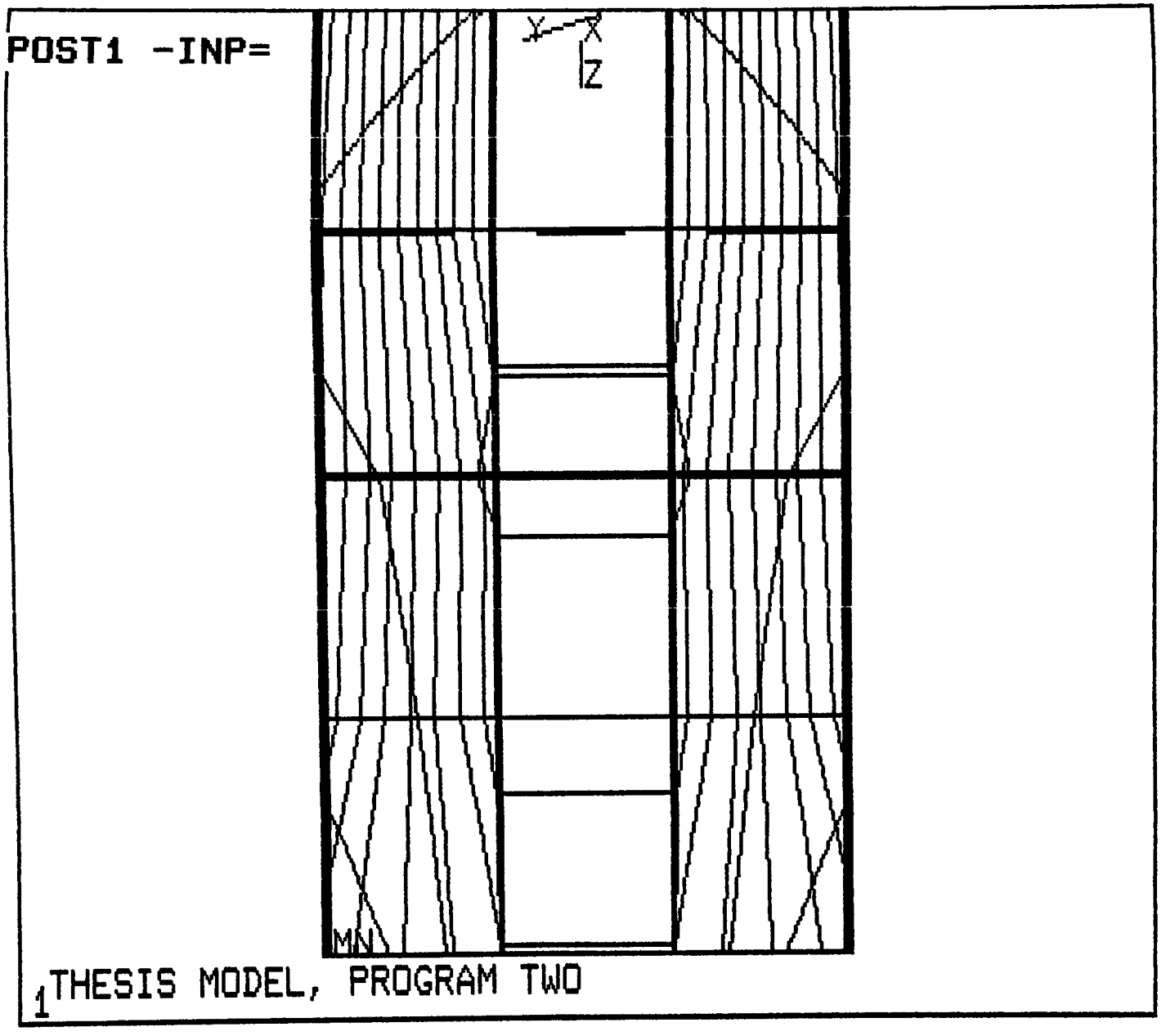

Fig. 5.3 Platform Stress Distribution, Time Step 5 = 20min.

1st Heating Temp. = 160C, time = 48.4sec.

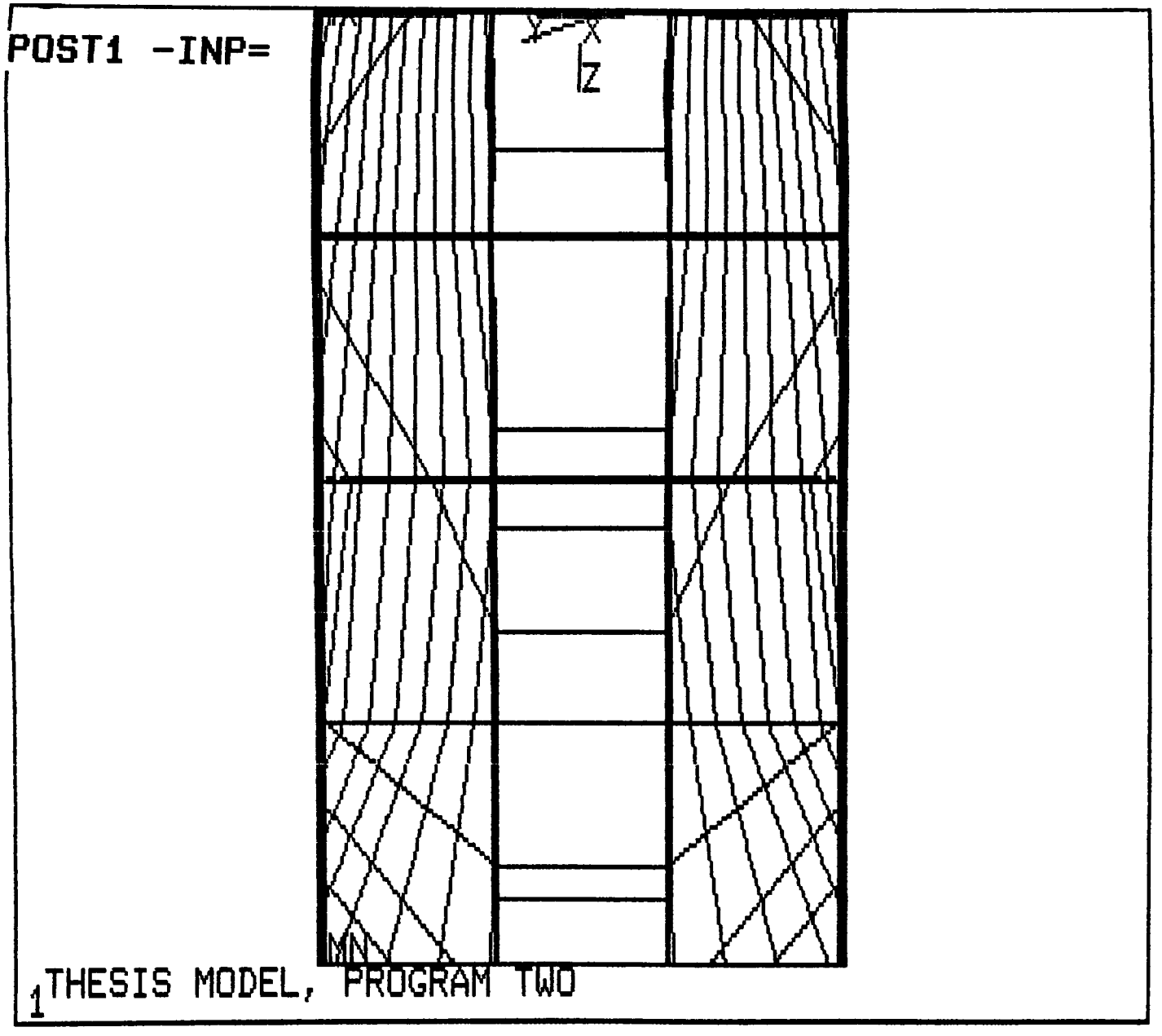

Fig. 5.4 Platform Stress Distribution, Time Step 5 = 20min.

1st Heating Temp. = 160C, time = 1328.8sec.

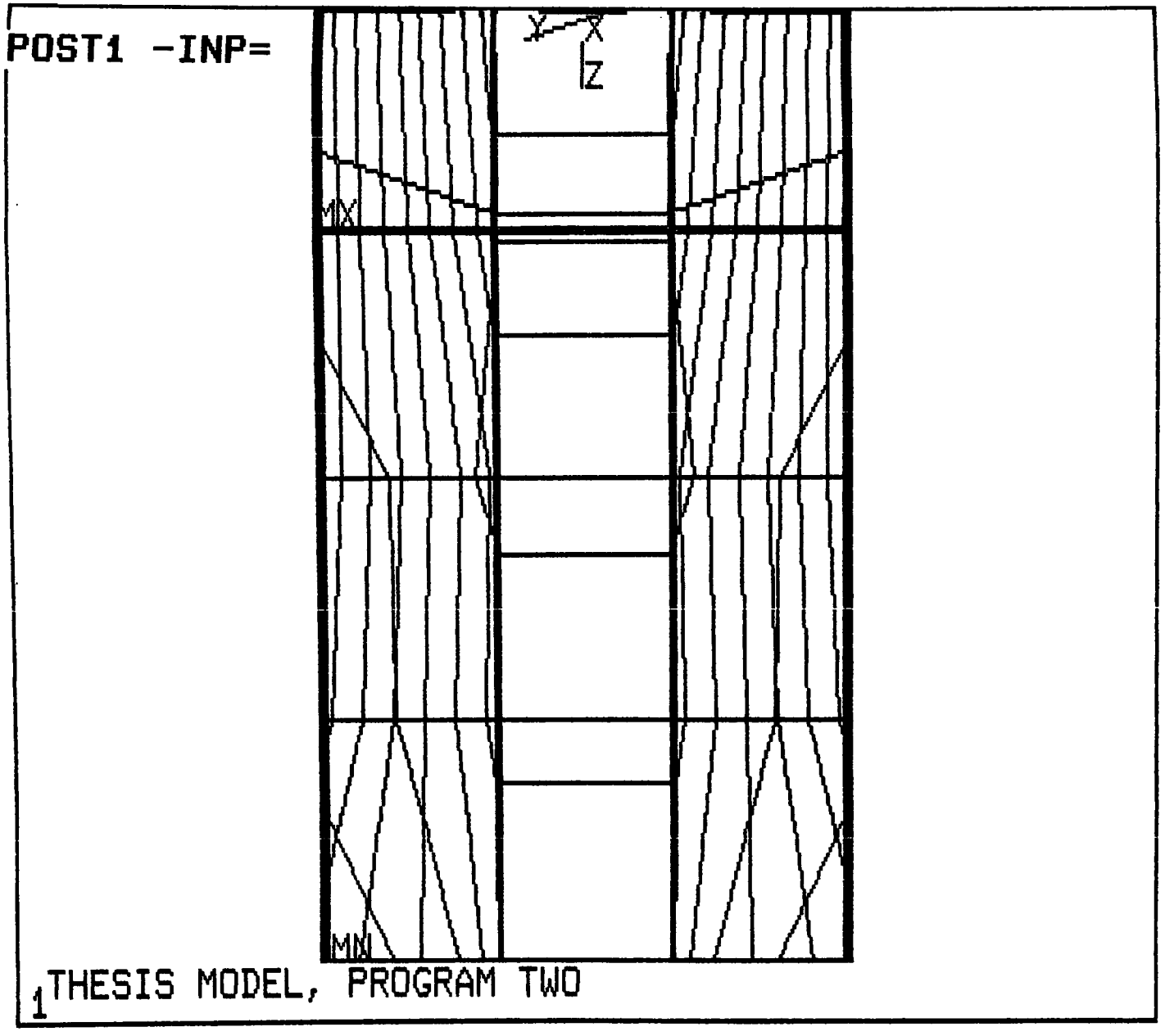

Fig. 5.5 Platform Stress Distribution, Time Step 5 = 20min.

1st Heating Temp. = 162C, time = 47.8sec.

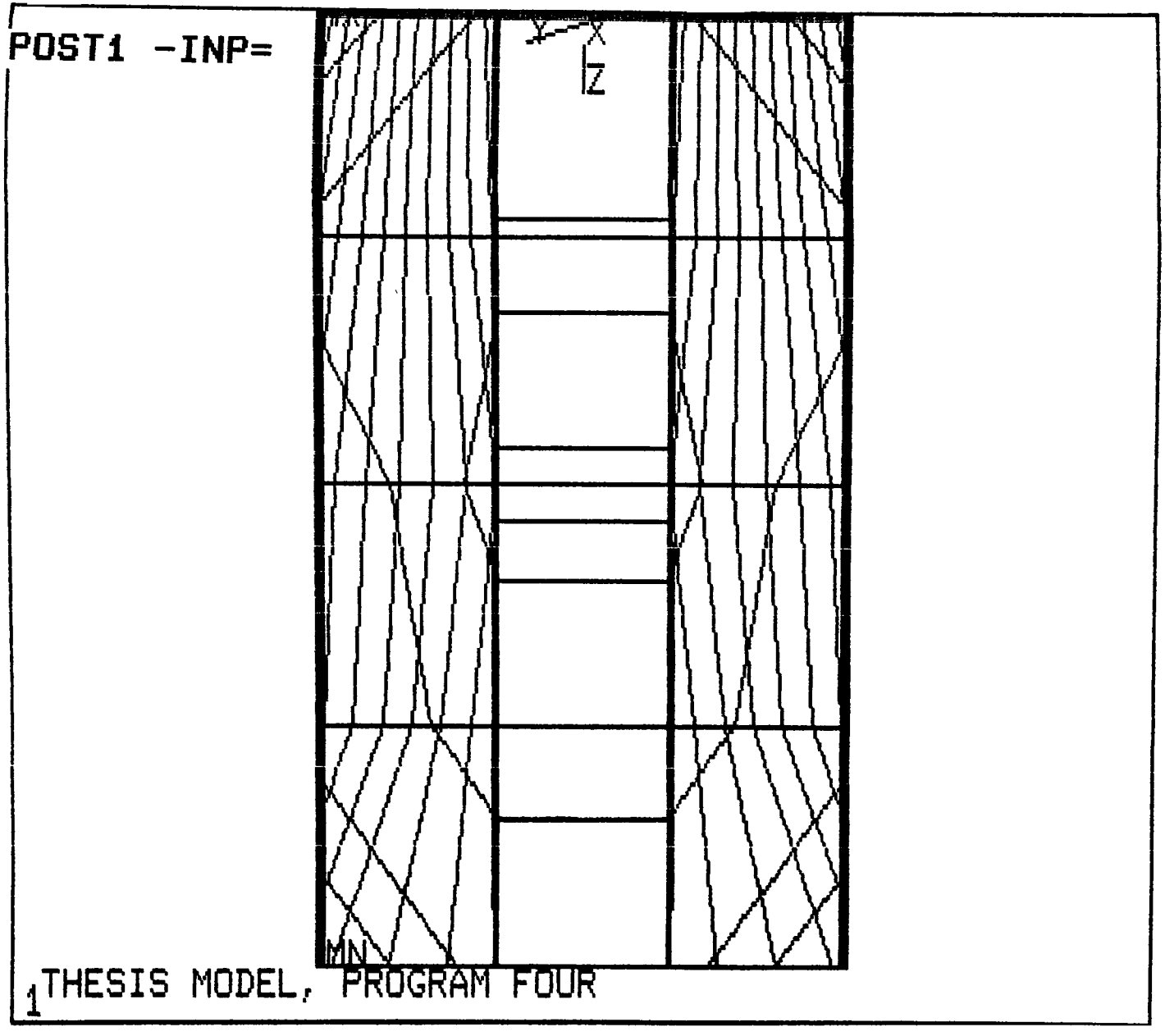

Fig. 5.6 Platform Stress Distribution, Time Step 5 = 20min.

1st Heating Temp. = 163C, time = 1328.2sec.

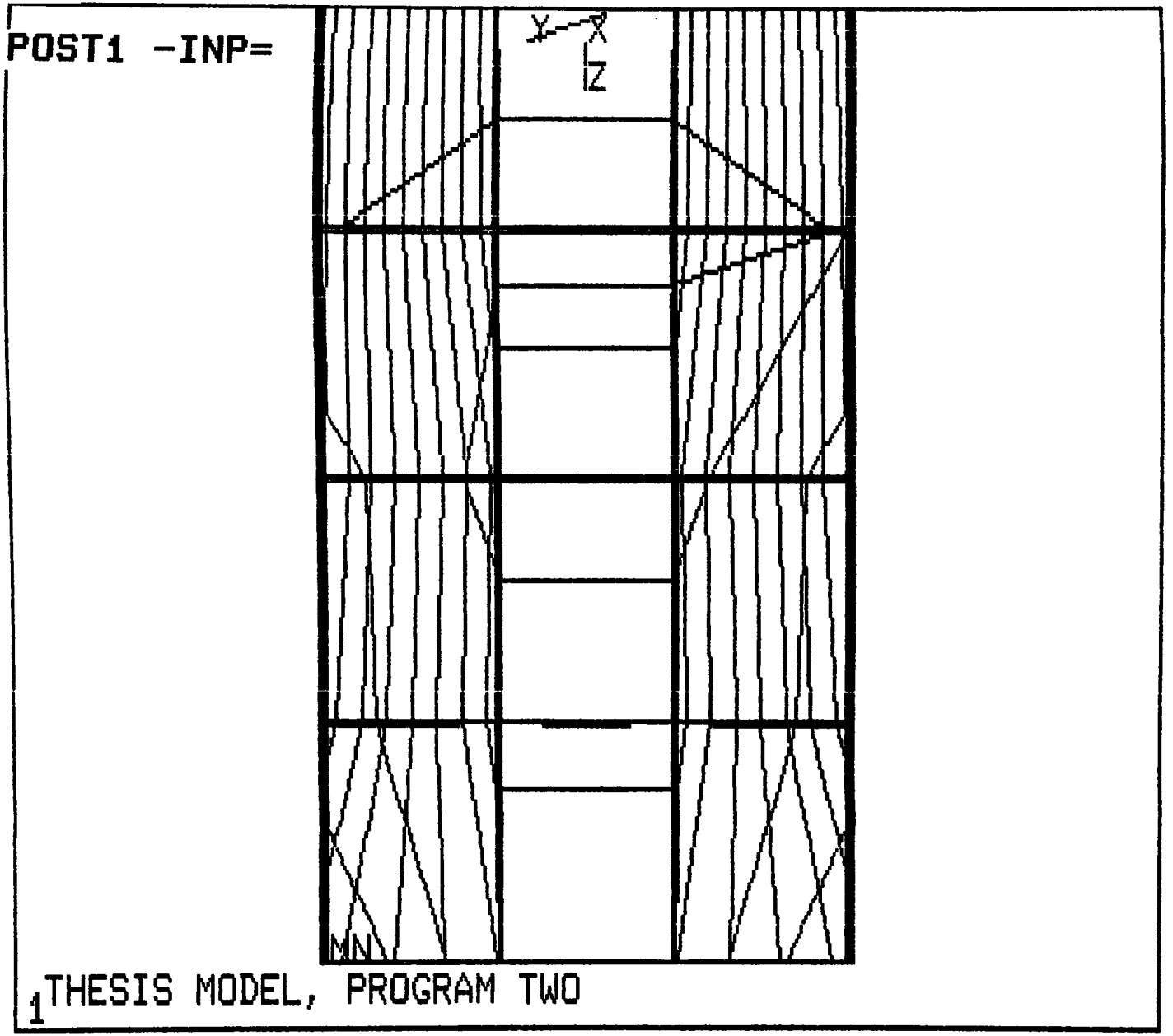

Fig. 5.7 Platform Stress Distribution, Time Step 5 = 20min.

1st Heating Temp. = 1620, time = 32.7sec.

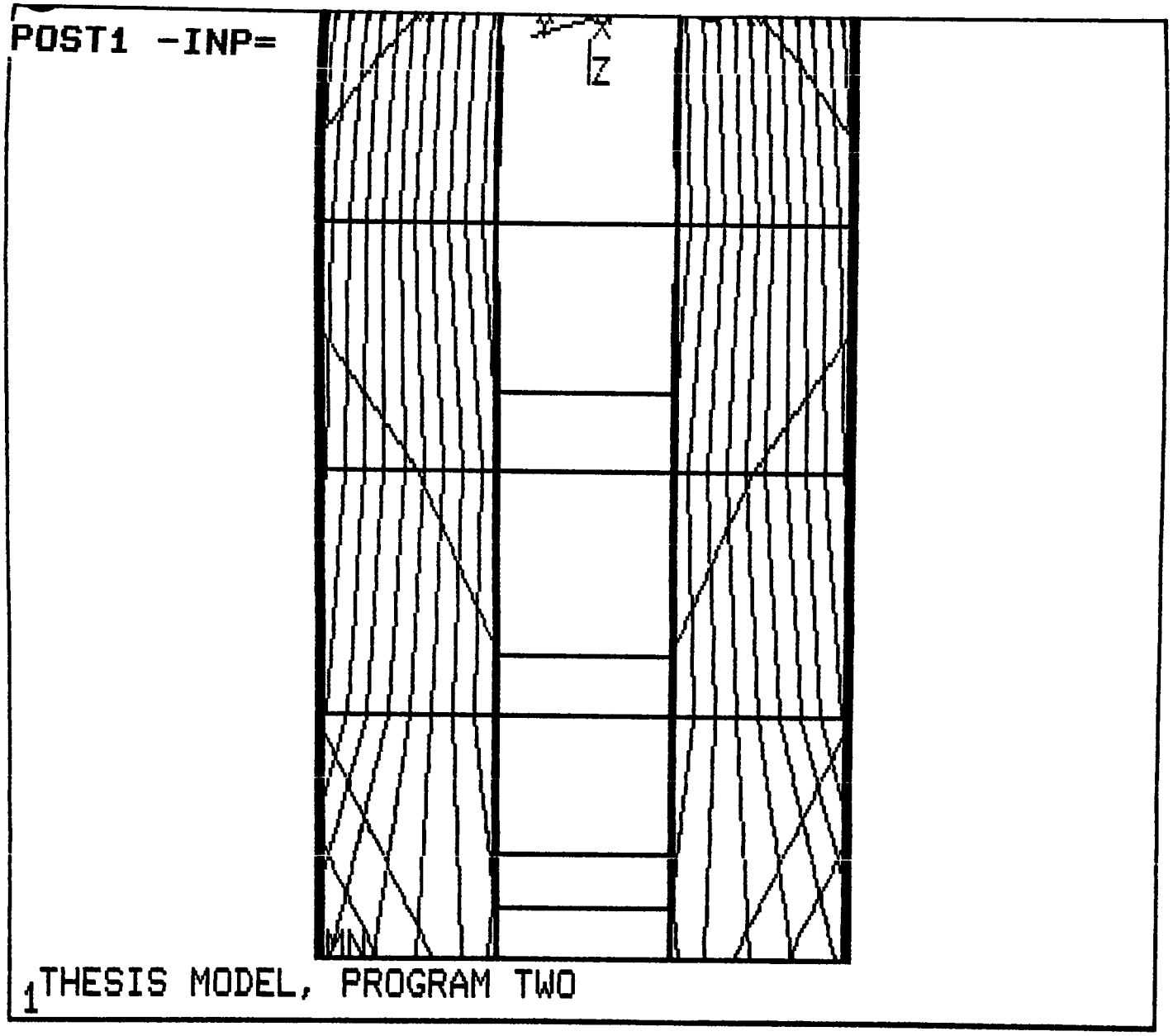

Fig. 5.8 Platform Stress Distribution, Time Step 5 = 20min.

1st Heating Temp. = 162C, time = 54.7sec.

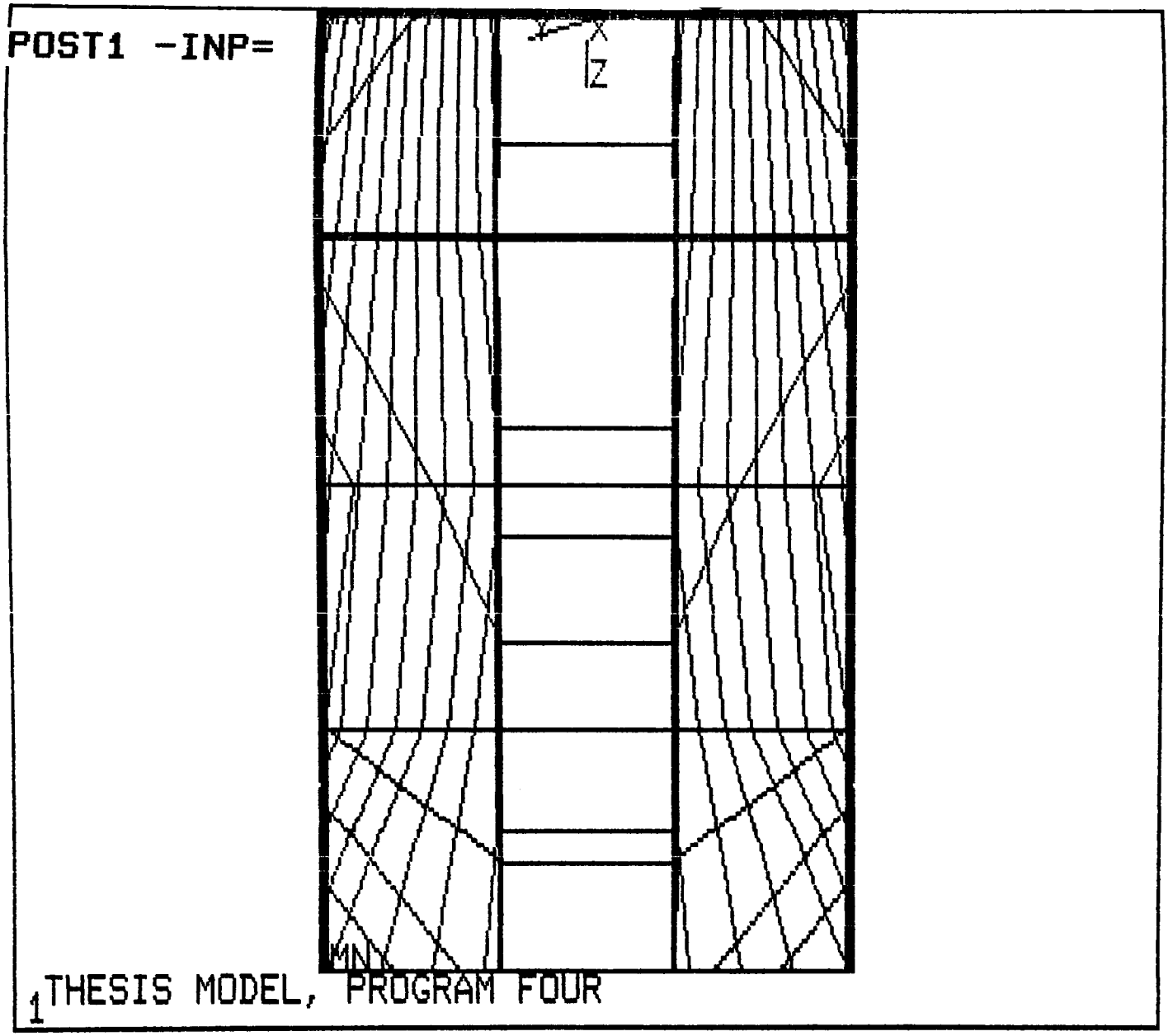

ANSYS 4.3
FEB 3 1988
9:00:41
POST1 STRESS
STEP=1
ITER=1
SIGE (AVG)

XV=1
DIST=.055
XF=.355
ZF=.05
ANGL=90
MX=349231995
MN=168579910
NCON=18
VMIN=178087910
VINC=9508005

Fig. 5.9 Platform Stress Distribution, Time Step 5 = 20min.
1st Heating Temp. = 1620, time = 1317.3sec.

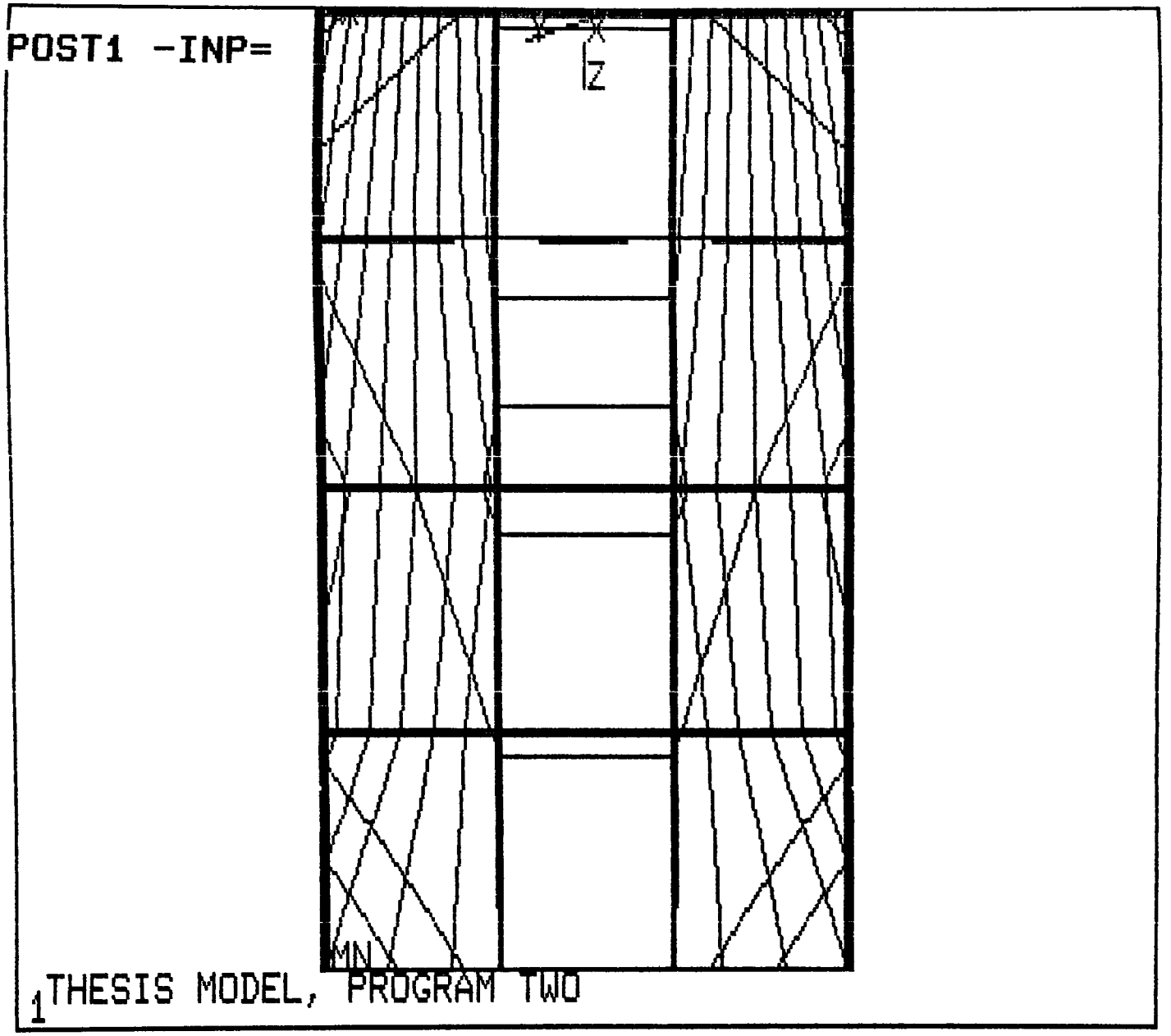

Fig. 5.10 Platform Stress Distribution, Time Step 5 = 20min.

1st Heating temp. = 162C, time = 1341.5sec.

been changed in order to solve the corresponding structural analyses.

Figure 5.11 shows the cover, platform, and rotor center axis, i.e., nodes 40, 80, and 145 transient temperature distribution. A sharp increase in temperature followed by an equally rapid decrease within short periods of time was found to be typical for the nodes 40 and 80 on the rotor surface in direct contact with the steam. This is attributed to the rapid change in film coefficient, introduced by the initiation and subsequent termination of steam condensation. Figure 5.12 shows the temperature differential between points in the control stage model of node 80 and node 145. The peak temperature difference between the top of the platform and the rotor axis occurred at approximately 32.7 seconds from the starting point. Table 8.1 shows that every nodal temperature was at 32.7 seconds.

Transient stresses of three cases with different heating temperatures (142, 160, and 162 C) are shown in Fig. 5.13. The Case 3 with heating temperature as 162 C has the most uniform peaks.

5.4 Results:

Eventually, the maximum thermal stress decreased from 489 MPA to 398 MPA. The total operating time was 22.5 minutes, which was 21.25 minutes longer than the original one. The above optimum method is just a demonstration which can give the turbine designer a clue to decrease the thermal shock problem. It is obvious that the longer warm up time the less thermal shock will be. From the economic point of view, the longer warm up time the less economic will be. A turbine

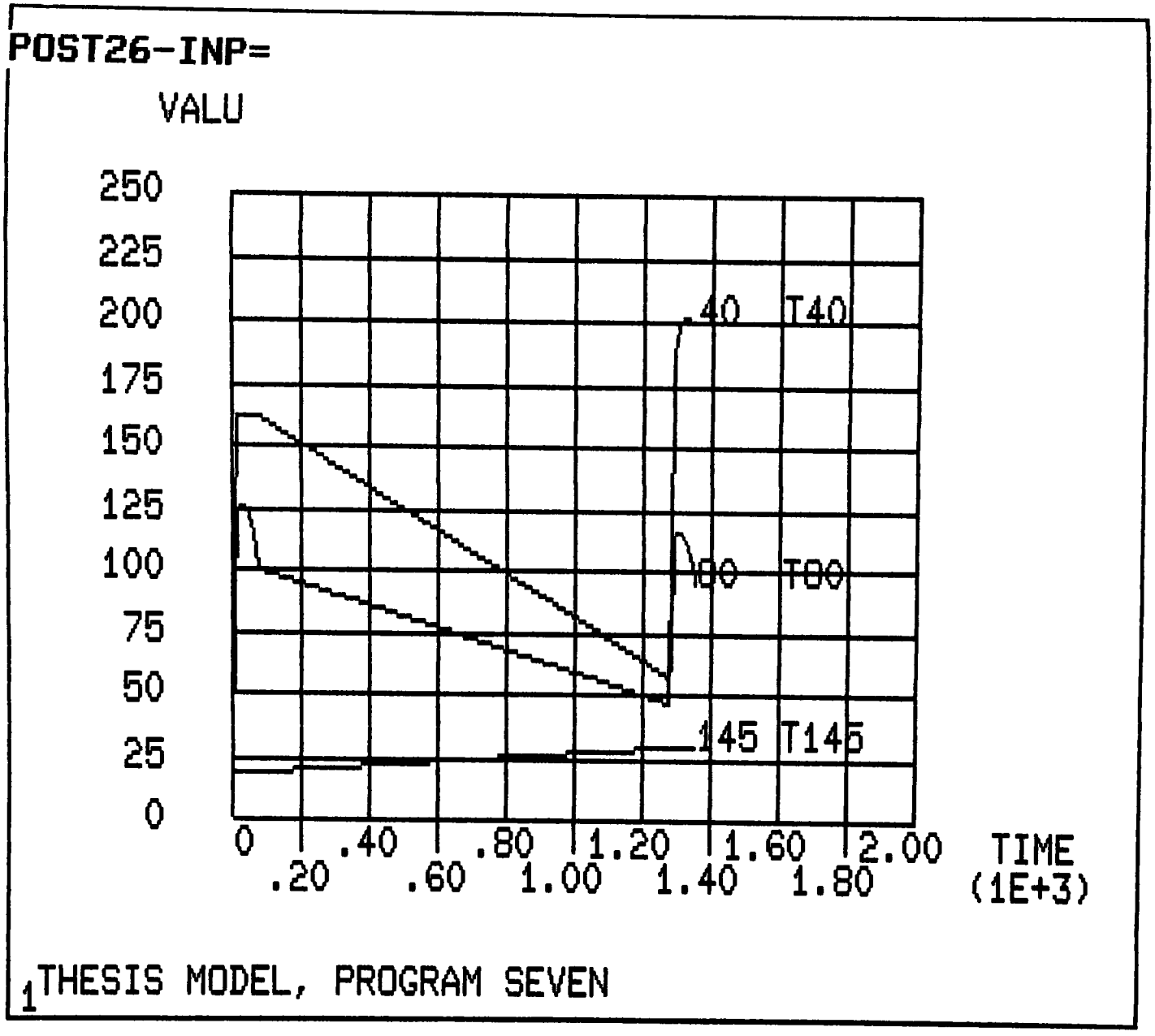

Fig. 5.11 Transient Temperature Distribution of Nodes 40, 80, and 145. 1st Heating Temp. = 162C

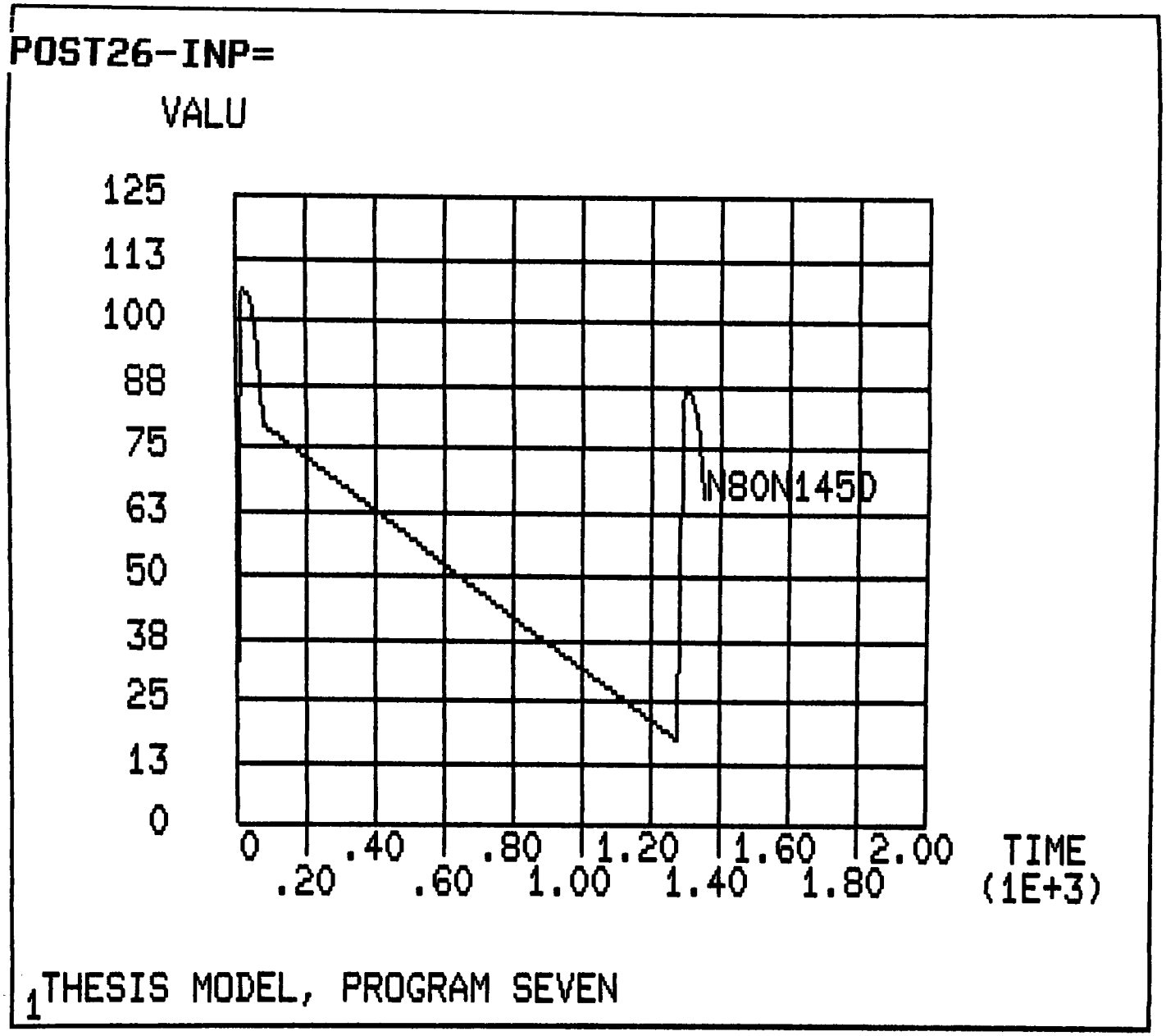

Fig. 5.12 Transient Temperature Difference Between Nodes 80 and 145. 1st Heating Temp. = 162C

FIG. 5.13 STRESS VARIATION WITH TIME

FIRST TWO STEPS OF THE THREE-STEP HEATING PROCESS

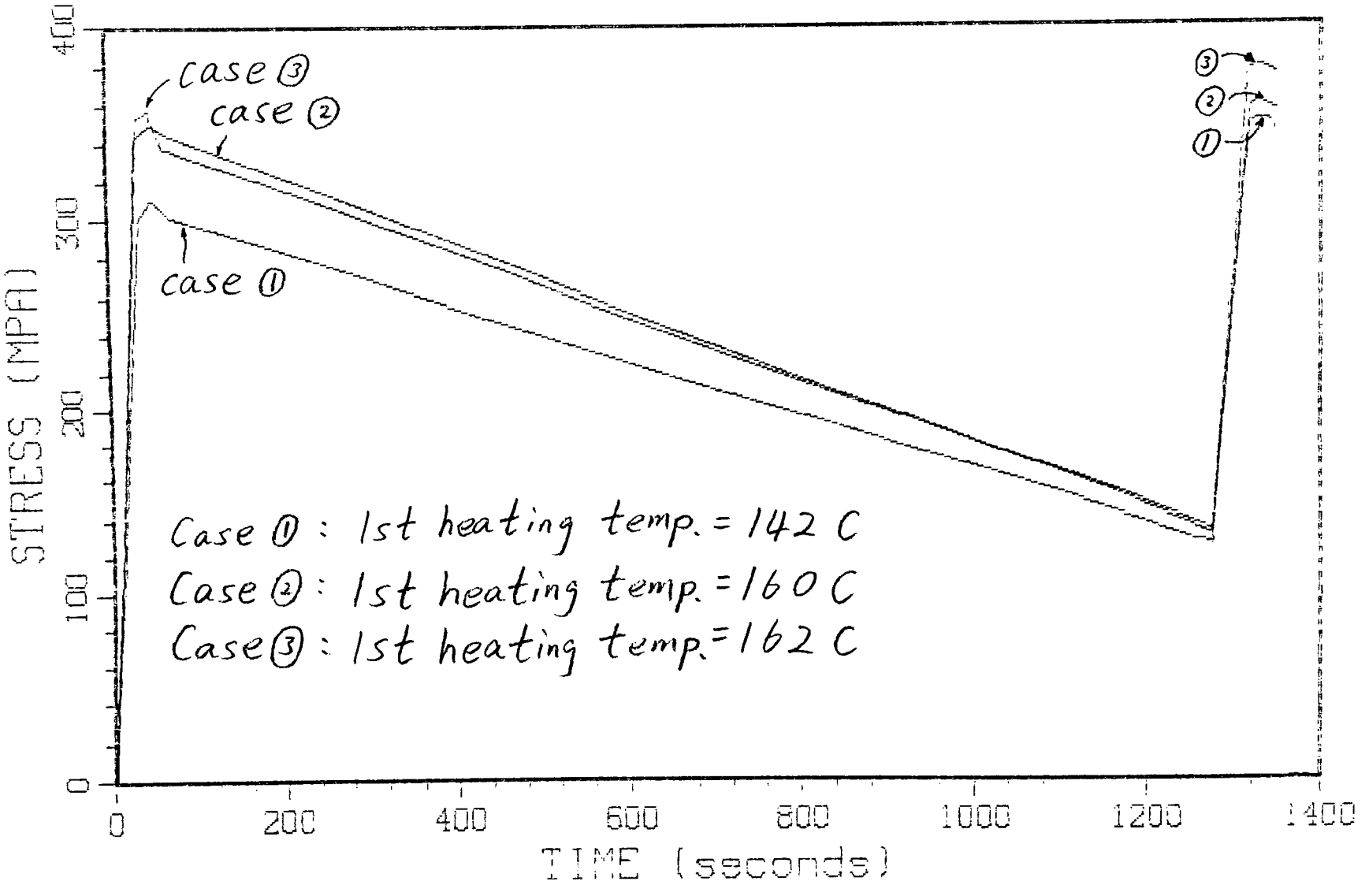

designer should consider both the economic and the thermal shock aspects before making a decision on the starting up strategy of a steam turbine.

6.0 CONCLUSIONS AND RECOMMENDATIONS

Very high stress (437 MPA) was found during the "thermal shock" of the two-step heating process. This compressive stress occurred on the platform surface and might be an important damage mechanism. An improved procedure, three-step heating process, did reduce the thermal shock influence, i.e., the compressive stress on the platform decreased from 437 MPA to 358 MPA at 47.8 seconds and 352 MPA at 1326.2 seconds from the starting point. The thermal stress magnitude of 358 MPA can be decreased if the warm-up time can be longer. The significant reduction of thermal stress would greatly extend the life of a steam turbine. The thermal behavior which was obtained in this project will be useful for a turbine designer to ensure no crack would be formed within the lifetime of the design machine.

Conclusion 1:

Study the thermal stress affected by different film coefficients.

Case	Film Coefficient (W/m^2-K)	Thermal Stress (MPA)
I	1,000	231
II	5,000	391
III	10,000	437
IV	15,000	464

From the above table, the thermal stress was affected by different film coefficients if these coefficients had significant difference in magnitude.

Conclusion 2:

The warm up time interval 5 increased from ten minutes to twenty minutes and the maximum thermal stress decreased from 387 MPA to 379 MPA.

	Time Interval 5 (minutes)	Thermal Stress (MPA) 1st Step	2nd Step
Case			
I	10	310	387
II	20	310	379

The thermal stress difference, 69 MPA, between step one and two was not in a satisfactory magnitude. In order to make both stresses be uniform the following analysis was approached.

Conclusion 3:

The example in chapter five tried to find an optimum heating temperature for the first step with the condition that the total operating time was 22.3 minutes. The maximum thermal stress decreased from the original 437 MPA to 358 MPA. The following table shows the variation of thermal stress according to different heating temperatures of the first step.

Case	Heating Temperature (C)	Thermal Stress (MPA) 1st step	2nd step
I	142	310	379
II	160	350	360
III	162	358	352

The above three cases were all under operating time of 22.5 minutes and the optimum first heating temperature would be 162 C.
In addition, it is recommended that another student be given the charge to do the fracture mechanics work of a propagating crack on the rotor surface due to a severe thermal shock.

7.0 REFERENCES

Akles, A. F., Colborn, J. N., Matchett, J. D. 1967,"A comparison of calculated and measured temperature distributions in forced convection air-cooled gas turbine airfoils", ASME Paper 67-WA/GT-4.

Boley B. A. and Wiener J. H. 1960. "Theory of thermal stresses". Wiley, New York.

Crane, D. M. 1973, "Calculation of temperature distribution in multistage axial gas turbine rotor assemblies when blades are uncooled", ASME Paper 73-GT-3.

Liu, Y.J. and Hsr T.-R. 1982. "On residual stresses/strains in pressure vessels induced by cyclic thermomechanical loads". ASME paper 82-PVP-27

Lockheed-Georgia, "Investigation of stress-strain history modeling at stress risers",
AFFDL-TR-76-130, Phase I, June, 1977,
AFFDL-TR-76-167, Phase II, Dec. 1978.

Manson, S. S. 1966. "Thermal stress and low-cycle fatigue". McGraw-Hill Book Company, Inc. New York.

Puglia Del, A. and Manfredi E. 1978. "High temperature low-cycle fatigue damage". Ch. 9, in creep of engineering materials and structures.

Socie,D. F. 1977, "Fatigue-Life Prediction Using Local Stress-Strain Concepts", Experimental Mechanics, February, 1977, pp. 50-56.

Stepha, F. S. 1980, "Analysis of uncertainties in turbine metal temperature predictions", NASA Technical Paper 1593, April, 1980.

Stodola A. and Loewenstein L. C. 1945. "Steam and gas turbines". McGRAW-HILL book Company, Inc. New York.

Storer J. D. 1969. "A simple history of the steam engine". John Baker Publisher, London.

Walcher, J., Gray, D., and Manson, S. S. 1979, "Aspects of Cumulative Fatigue Damage Analysis of Cold End Rotating Structures", AIAA Paper, pp. 79-1160.

Walcher, J. C. and Finnerty, D. L. 1982, "Titanium fan disk structural life prediction/correlation program", SAE Paper 821437, Oct. 1982.

Wetzell, R. M. 1971, "A method of fatigue damage analysis," PhD. Thesis, University of Waterloo, Canada, also as Sci Res. Staff Rep. SR 71-107, Ford >Motor Co. Dearborn, Michigan.

8.0 APPENDIX

8.1 ANSYS Thermal and Structural Programs

8.1.1 Program One

8.1.2 Program two

8.1.3 Program three

8.1.4 Program four

8.1.5 Program five

8.1.6 Program six

8.1.7 Program seven

8.1.8 Program eight

8.1.9 Program nine

8.2 Nodal Temperature Table of Program nine

```
C*** Program one, Thermal analysis.
C***Film coefficient = 10000 W/m-K,
C*** First heating temperature = 204C.
/PREP7
/TITLE,THESIS MODEL, Program one
KAN,-1
ET,1,70
ET,2,70
MPTEMP,1,20,100,204
MPDATA,EX,1,1,219E9,214E9,207.68E9
MPDATA,EX,2,1,211E9,207E9,199.72E9
MPDATA,ALPX,1,1,9.7E-6,10.1E-6,10.516E-6
MPDATA,ALPX,2,1,9.9E-6,11E-6,12.03E-6
MPDATA,KXX,1,1,27,27,27
MPDATA,KXX,2,1,44,43,41.92
MPDATA,C,1,1,460,480,521.6
MPDATA,C,2,1,460,480,521.6
MPDATA,DENS,1,1,7750,7750,7750
MPDATA,DENS,2,1,7850,7850,7850
TUNIF,20
CSYS,1
N,1,0.4,-4.0909,0
N,5,0.4,-4.0909,0.1
FILL,1,5,3
NGEN,4,5,1,5,1,,2.727
NGEN,2,20,1,20,1,-0.01
NGEN,2,20,26,35,1,-0.015
NGEN,2,40,21,40,1,-0.03
NGEN,2,20,61,80,1,-0.01
NGEN,2,20,81,100,1,-0.05833
NGEN,2,20,101,120,1,-0.11667
NGEN,2,20,121,125,1,-0.175
N,165,0.36,-4.0909,0.967
N,265,0.36,-4.0909,2.76
NGEN,4,5,165,265,100,,2.727
NGEN,2,20,165,180,5,-0.01
NGEN,2,20,265,280,5,-0.01
NGEN,2,20,185,200,5,-0.05833
NGEN,2,20,285,300,5,-0.05833
NGEN,2,20,205,220,5,-0.11667
NGEN,2,20,305,320,5,-0.11667
NGEN,2,20,225,325,100,-0.175
E,1,6,7,2,21,26,27,22
EGEN,3,5,-1
EGEN,4,1,-3
EGEN,3,20,2,11,3
E,61,66,67,62,81,86,87,82
EGEN,3,5,-1
EGEN,4,1,-3
E,65,70,170,165,85,90,190,185
EGEN,3,5,-1
EGEN,2,100,-3
TYPE,2
MAT,2
E,81,86,87,82,101,106,107,102
```

```
EGEN,3,5,-1
EGEN,4,1,-3
EGEN,2,20,-12
E,121,126,141,141,122,127,142,142
E,126,131,141,141,127,132,142,142
E,131,136,141,141,132,137,142,142
EGEN,4,1,-3
E,85,90,190,185,105,110,210,205
EGEN,3,5,-1
EGEN,2,100,-3
EGEN,2,20,-6
E,125,130,145,145,225,230,245,245
E,130,135,145,145,230,235,245,245
E,135,140,145,145,235,240,245,245
EGEN,2,100,-3
NT,265,TEMP,80
RP17,5
KBC,0
TIME,0.5
ITER,-100,100,100
EC,1,1,1000,38.4,12,1
EC,1,2,1000,38.4,3,1
EC,1,6,1000,38.4,10,3
EC,3,6,1000,38.4,12,3
EC,10,4,1000,38.4,12,1
EC,13,2,1000,38.4,17,4
EC,16,4,1000,38.4,20,4
EC,13,5,1000,38.4,20,1
EC,13,3,1000,38.4,20,1
EC,21,1,1000,38.4,30,3
EC,23,1,1000,38.4,32,3
EC,33,1,1000,45.3,35,1
EC,36,1,1000,66.1,38,1
LWRI
TIME,5
ITER,-100,100,100
EC,1,1,10000,204,12,1
EC,1,2,10000,204,3,1
EC,1,6,10000,204,10,3
EC,3,6,10000,204,12,3
EC,10,4,10000,204,12,1
EC,13,2,10000,204,17,4
EC,16,4,10000,204,20,4
EC,13,5,10000,204,20,1
EC,13,3,10000,204,20,1
EC,21,1,10000,204,30,3
EC,23,1,10000,204,32,3
EC,33,1,10000,183,35,1
EC,36,1,10000,121,38,1
LWRI
TIME,14.5
ITER,-100,100,100
EC,1,1,10000,204,12,1
EC,1,2,10000,204,3,1
EC,1,6,10000,204,10,3
```

```
EC,3,6,10000,204,12,3
EC,10,4,10000,204,12,1
EC,13,2,10000,204,17,4
EC,16,4,10000,204,20,4
EC,13,5,10000,204,20,1
EC,13,3,10000,204,20,1
EC,21,1,10000,204,30,3
EC,23,1,10000,204,32,3
EC,33,1,10000,183,35,1
EC,36,1,10000,121,38,1
LWRI
TIME,75
ITER,-100,1,1
EC,1,1,5,204,12,1
EC,1,2,5,204,3,1
EC,1,6,5,204,10,3
EC,3,6,5,204,12,3
EC,10,4,5,204,12,1
EC,13,2,5,204,17,4
EC,16,4,5,204,20,4
EC,13,5,5,204,20,1
EC,13,3,5,204,20,1
EC,21,1,5,204,30,3
EC,23,1,5,204,32,3
EC,33,1,5,183,35,1
EC,36,1,5,121,38,1
LWRI
/PSC,ALL,1
AFWRIT
FINISH
```

```
C*** Program two, Structural analysis
C*** Load step 4, Iteration 70
/PREP7
/TITLE,THESIS MODEL, Program two
KAN,0
ET,1,45
ET,2,45
MPTEMP,1,20,100,204
MPDATA,EX,1,1,219E9,214E9,207.68E9
MPDATA,EX,2,1,211E9,207E9,199.72E9
MPDATA,ALPX,1,1,9.7E-6,10.1E-6,10.516E-6
MPDATA,ALPX,2,1,9.9E-6,11E-6,12.03E-6
MPDATA,KXX,1,1,27,27,27
MPDATA,KXX,2,1,44,43,41.92
MPDATA,C,1,1,460,480,521.6
MPDATA,C,2,1,460,480,521.6
MPDATA,DENS,1,1,7750,7750,7750
MPDATA,DENS,2,1,7850,7850,7850
CSYS,1
N,1,0.4,-4.0909,0
N,5,0.4,-4.0909,0.1
FILL,1,5,3
NGEN,4,5,1,5,1,,2.727
NGEN,2,20,1,20,1,-0.01
NGEN,2,20,26,35,1,-0.015
NGEN,2,40,21,40,1,-0.03
NGEN,2,20,61,80,1,-0.01
NGEN,2,20,81,100,1,-0.05833
NGEN,2,20,101,120,1,-0.11667
NGEN,2,20,121,125,1,-0.175
N,165,0.36,-4.0909,0.987
N,265,0.36,-4.0909,2.76
NGEN,4,5,165,265,100,,2.727
NGEN,2,20,165,180,5,-0.01
NGEN,2,20,265,280,5,-0.01
NGEN,2,20,185,200,5,-0.05833
NGEN,2,20,285,300,5,-0.05833
NGEN,2,20,205,220,5,-0.11667
NGEN,2,20,305,320,5,-0.11667
NGEN,2,20,225,325,100,-0.175
E,1,6,7,2,21,26,27,22
EGEN,3,5,-1
EGEN,4,1,-3
EGEN,3,20,2,11,3
E,61,66,67,62,81,86,87,82
EGEN,3,5,-1
EGEN,4,1,-3
E,65,70,170,165,85,90,190,185
EGEN,3,5,-1
EGEN,2,100,-3
TYPE,2
MAT,2
E,81,86,87,82,101,106,107,102
EGEN,3,5,-1
EGEN,4,1,-3
```

```
EGEN,2,20,-12
E,121,126,141,141,122,127,142,142
E,126,131,141,141,127,132,142,142
E,131,136,141,141,132,137,142,142
EGEN,4,1,-3
E,85,90,190,185,105,110,210,205
EGEN,3,5,-1
EGEN,2,100,-3
EGEN,2,20,-6
E,125,130,145,145,225,230,245,245
E,130,135,145,145,230,235,245,245
E,135,140,145,145,235,240,245,245
EGEN,2,100,-3
KBC,0
KTEMP,4,60
CSYS,1
D,141,ALL
D,142,UX
RP4,1
D,142,UY
RP4,1
D,245,UX
D,245,UY
D,345,UX
D,345,UY
CP,1,UX,1,16
CPSG,2,20,1
CPSG,5,1,1,2,1
CPLG,1,UY,UZ
RP10,1
CP,31,UX,61,76
CPSG,4,20,31
CPSG,5,1,31,34,1
CPLG,31,UY,UZ
RP20,1
CP,91,UX,165,180
CPSG,4,20,91
CPSG,2,100,91,94,1
CPLG,91,UY,UZ
RP8,1
/PBC,ALL,1
AFWRIT
FINISH
```

```
C*** Program three, Film coefficient = 10000 W/m-K
C*** Time step 5 = 10 minutes
C*** First heating temperature = 142C
/PREP7
/TITLE,THESIS MODEL, Program three
KAN,-1
ET,1,70
ET,2,70
MPTEMP,1,20,100,204
MPDATA,EX,1,1,219E9,214E9,207.68E9
MPDATA,EX,2,1,211E9,207E9,199.72E9
MPDATA,ALPX,1,1,9.7E-6,10.1E-6,10.516E-6
MPDATA,ALPX,2,1,9.9E-6,11E-6,12.03E-6
MPDATA,KXX,1,1,27,27,27
MPDATA,KXX,2,1,44,43,41.92
MPDATA,C,1,1,460,480,521.6
MPDATA,C,2,1,460,480,521.6
MPDATA,DENS,1,1,7750,7750,7750
MPDATA,DENS,2,1,7350,7850,7850
TUNIF,20
CSYS,1
N,1,0.4,-4.0909,0
N,5,0.4,-4.0909,0.1
FILL,1,5,3
NGEN,4,5,1,5,1,,2.727
NGEN,2,20,1,20,1,-0.01
NGEN,2,20,26,35,1,-0.015
NGEN,2,40,21,40,1,-0.03
NGEN,2,20,61,80,1,-0.01
NGEN,2,20,81,100,1,-0.05833
NGEN,2,20,101,120,1,-0.11667
NGEN,2,20,121,125,1,-0.175
N,165,0.36,-4.0909,0.987
N,265,0.36,-4.0909,2.76
NGEN,4,5,165,265,100,,2.727
NGEN,2,20,165,180,5,-0.01
NGEN,2,20,265,280,5,-0.01
NGEN,2,20,185,200,5,-0.05833
NGEN,2,20,285,300,5,-0.05833
NGEN,2,20,205,220,5,-0.11667
NGEN,2,20,305,320,5,-0.11667
NGEN,2,20,225,325,100,-0.175
E,1,6,7,2,21,26,27,22
EGEN,3,5,-1
EGEN,4,1,-3
EGEN,3,20,2,11,3
E,61,66,67,62,81,86,87,82
EGEN,3,5,-1
EGEN,4,1,-3
E,65,70,170,165,85,90,190,185
EGEN,3,5,-1
EGEN,2,100,-3
TYPE,2
MAT,2
E,81,86,87,82,101,106,107,102
```

```
EGEN,3,5,-1
EGEN,4,1,-3
EGEN,2,20,-12
E,121,126,141,141,122,127,142,142
E,126,131,141,141,127,132,142,142
E,131,136,141,141,132,137,142,142
EGEN,4,1,-3
E,85,90,190,185,105,110,210,205
EGEN,3,5,-1
EGEN,2,100,-3
EGEN,2,20,-6
E,125,130,145,145,225,230,245,245
E,130,135,145,145,230,235,245,245
E,135,140,145,145,235,240,245,245
EGEN,2,100,-3
NT,265,TEMP,80
RP17,5
KBC,0
TIME,0.5
ITER,-100,100,100
EC,1,1,1000,32.2,12,1
EC,1,2,1000,32.2,3,1
EC,1,6,1000,32.2,10,3
EC,3,6,1000,32.2,12,3
EC,10,4,1000,32.2,12,1
EC,13,2,1000,32.2,17,4
EC,16,4,1000,32.2,20,4
EC,13,5,1000,32.2,20,1
EC,13,3,1000,32.2,20,1
EC,21,1,1000,32.2,30,3
EC,23,1,1000,32.2,32,3
EC,33,1,1000,40.2,35,1
EC,36,1,1000,64.1,38,1
LWRI
TIME,5
ITER,-100,100,100
EC,1,1,10000,142,12,1
EC,1,2,10000,142,3,1
EC,1,6,10000,142,10,3
EC,3,6,10000,142,12,3
EC,10,4,10000,142,12,1
EC,13,2,10000,142,17,4
EC,16,4,10000,142,20,4
EC,13,5,10000,142,20,1
EC,13,3,10000,142,20,1
EC,21,1,10000,142,30,3
EC,23,1,10000,142,32,3
EC,33,1,10000,132,35,1
EC,36,1,10000,101,38,1
LWRI
TIME,14.5
ITER,-100,100,100
EC,1,1,10000,142,12,1
EC,1,2,10000,142,3,1
EC,1,6,10000,142,10,3
```

```
EC,3,6,10000,142,12,3
EC,10,4,10000,142,12,1
EC,13,2,10000,142,17,4
EC,16,4,10000,142,20,4
EC,13,5,10000,142,20,1
EC,13,3,10000,142,20,1
EC,21,1,10000,142,30,3
EC,23,1,10000,142,32,3
EC,33,1,10000,132,35,1
EC,36,1,10000,101,38,1
LWRI
TIME,75
ITER,-100,1,1
EC,1,1,5,142,12,1
EC,1,2,5,142,3,1
EC,1,6,5,142,10,3
EC,3,6,5,142,12,3
EC,10,4,5,142,12,1
EC,13,2,5,142,17,4
EC,16,4,5,142,20,4
EC,13,5,5,142,20,1
EC,13,3,5,142,20,1
EC,21,1,5,142,30,3
EC,23,1,5,142,32,3
EC,33,1,5,132,35,1
EC,36,1,5,101,38,1
LWRI
TIME,1275
ITER,-100,100,100
EC,1,1,5,142,12,1
EC,1,2,5,142,3,1
EC,1,6,5,142,10,3
EC,3,6,5,142,12,3
EC,10,4,5,142,12,1
EC,13,2,5,142,17,4
EC,16,4,5,142,20,4
EC,13,5,5,142,20,1
EC,13,3,5,142,20,1
EC,21,1,5,142,30,3
EC,23,1,5,142,32,3
EC,33,1,5,132,35,1
EC,36,1,5,101,38,1
LWRI
TIME,675.5
ITER,-100,100,100
EC,1,1,1000,148.2,12,1
EC,1,2,1000,148.2,3,1
EC,1,6,1000,148.2,10,3
EC,3,6,1000,148.2,12,3
EC,10,4,1000,148.2,12,1
EC,13,2,1000,148.2,17,4
EC,16,4,1000,148.2,20,4
EC,13,5,1000,148.2,20,1
EC,13,3,1000,148.2,20,1
EC,21,1,1000,148.2,30,3
```

```
EC,23,1,1000,148.2,32,3
EC,33,1,1000,136.8,35,1
EC,36,1,1000,102.7,38,1
LWRI
TIME,680
ITER,-100,100,100
EC,1,1,10000,204,12,1
EC,1,2,10000,204,3,1
EC,1,6,10000,204,10,3
EC,3,6,10000,204,12,3
EC,10,4,10000,204,12,1
EC,13,2,10000,204,17,4
EC,16,4,10000,204,20,4
EC,13,5,10000,204,20,1
EC,13,3,10000,204,20,1
EC,21,1,10000,204,30,3
EC,23,1,10000,204,32,3
EC,33,1,10000,183,35,1
EC,36,1,10000,121,38,1
LWRI
TIME,689.5
ITER,-100,100,100
EC,1,1,10000,204,12,1
EC,1,2,10000,204,3,1
EC,1,6,10000,204,10,3
EC,3,6,10000,204,12,3
EC,10,4,10000,204,12,1
EC,13,2,10000,204,17,4
EC,16,4,10000,204,20,4
EC,13,5,10000,204,20,1
EC,13,3,10000,204,20,1
EC,21,1,10000,204,30,3
EC,23,1,10000,204,32,3
EC,33,1,10000,183,35,1
EC,36,1,10000,121,38,1
LWRI
TIME,750
ITER,-100,1,1
EC,1,1,5,204,12,1
EC,1,2,5,204,3,1
EC,1,6,5,204,10,3
EC,3,6,5,204,12,3
EC,10,4,5,204,12,1
EC,13,2,5,204,17,4
EC,16,4,5,204,20,4
EC,13,5,5,204,20,1
EC,13,3,5,204,20,1
EC,21,1,5,204,30,3
EC,23,1,5,204,32,3
EC,33,1,5,183,35,1
EC,36,1,5,121,38,1
LWRI
/PBC,ALL,1
AFWRIT
FINISH
```

```
C*** Program four, Structural analysis
C*** Load Step 9, Iteration 69
/PREP7
/TITLE,THESIS MODEL, Program four
KAN,0
ET,1,45
ET,2,45
MPTEMP,1,20,100,204
MPDATA,EX,1,1,219E9,214E9,207.68E9
MPDATA,EX,2,1,211E9,207E9,199.72E9
MPDATA,ALPX,1,1,9.7E-6,10.1E-6,10.516E-6
MPDATA,ALPX,2,1,9.9E-6,11E-6,12.03E-6
MPDATA,KXX,1,1,27,27,27
MPDATA,KXX,2,1,44,43,41.92
MPDATA,C,1,1,460,480,521.6
MPDATA,C,2,1,460,480,521.6
MPDATA,DENS,1,1,7750,7750,7750
MPDATA,DENS,2,1,7850,7850,7850
CSYS,1
N,1,0.4,-4.0909,0
N,5,0.4,-4.0909,0.1
FILL,1,5,3
NGEN,4,5,1,5,1,,2.727
NGEN,2,20,1,20,1,-0.01
NGEN,2,20,26,35,1,-0.015
NGEN,2,40,21,40,1,-0.03
NGEN,2,20,61,80,1,-0.01
NGEN,2,20,81,100,1,-0.05833
NGEN,2,20,101,120,1,-0.11667
NGEN,2,20,121,125,1,-0.175
N,165,0.36,-4.0909,0.987
N,265,0.36,-4.0909,2.76
NGEN,4,5,165,265,100,,2.727
NGEN,2,20,165,180,5,-0.01
NGEN,2,20,265,280,5,-0.01
NGEN,2,20,185,200,5,-0.05633
NGEN,2,20,285,300,5,-0.05833
NGEN,2,20,205,220,5,-0.11667
NGEN,2,20,305,320,5,-0.11667
NGEN,2,20,225,325,100,-0.175
E,1,6,7,2,21,26,27,22
EGEN,3,5,-1
EGEN,4,1,-3
EGEN,3,20,2,11,3
E,61,66,67,62,81,86,87,82
EGEN,3,5,-1
EGEN,4,1,-3
E,65,70,170,165,85,90,190,185
EGEN,3,5,-1
EGEN,2,100,-3
TYPE,2
MAT,2
E,81,86,87,82,101,106,107,102
EGEN,3,5,-1
EGEN,4,1,-3
```

```
EGEN,2,20,-12
E,121,126,141,141,122,127,142,142
E,126,131,141,141,127,132,142,142
E,131,136,141,141,132,137,142,142
EGEN,4,1,-3
E,85,90,190,185,105,110,210,205
EGEN,3,5,-1
EGEN,2,100,-3
EGEN,2,20,-6
E,125,130,145,145,225,230,245,245
E,130,135,145,145,230,235,245,245
E,135,140,145,145,235,240,245,245
EGEN,2,100,-3
KBC,0
KTEMP,9,o9
CSYS,1
D,141,ALL
D,142,UX
RP4,1
D,142,UY
RP4,1
D,245,UX
D,245,UY
D,345,UX
D,345,UY
CP,1,UX,1,16
CPSG,2,20,1
CPSG,5,1,1,2,1
CPLG,1,UY,UZ
RP10,1
CP,31,UX,61,75
CPSG,4,20,31
CPSG,5,1,31,34,1
CPLG,31,UY,UZ
RP20,1
CP,91,UX,165,180
CPSG,4,20,91
CPSG,2,100,91,94,1
CPLG,91,UY,UZ
RP8,1
/PBC,ALL,1
AFWRIT
FINISH
```

```
C*** Program five, Film Coefficient = 5000 W/m-K
C*** First heating temperature = 204C
/PREP7
/TITLE,THESIS MODEL, Program five
KAN,-1
ET,1,70
ET,2,70
MPTEMP,1,20,100,204
MPDATA,EX,1,1,219E9,214E9,207.68E9
MPDATA,EX,2,1,211E9,207E9,199.72E9
MPDATA,ALPX,1,1,9.7E-6,10.1E-6,10.516E-6
MPDATA,ALPX,2,1,9.9E-6,11E-6,12.03E-6
MPDATA,KXX,1,1,27,27,27
MPDATA,KXX,2,1,44,43,41.92
MPDATA,C,1,1,460,480,521.6
MPDATA,C,2,1,460,480,521.6
MPDATA,DENS,1,1,7750,7750,7750
MPDATA,DENS,2,1,7850,7850,7850
TUNIF,20
CSYS,1
N,1,0.4,-4.0909,0
N,5,0.4,-4.0909,0.1
FILL,1,5,3
NGEN,4,5,1,5,1,,2.727
NGEN,2,20,1,20,1,-0.01
NGEN,2,20,26,35,1,-0.015
NGEN,2,40,21,40,1,-0.03
NGEN,2,20,61,80,1,-0.01
NGEN,2,20,81,100,1,-0.05833
NGEN,2,20,101,120,1,-0.11667
NGEN,2,20,121,125,1,-0.175
N,165,0.36,-4.0909,0.987
N,265,0.36,-4.0909,2.76
NGEN,4,5,165,265,100,,2.727
NGEN,2,20,165,180,5,-0.01
NGEN,2,20,265,280,5,-0.01
NGEN,2,20,185,200,5,-0.05833
NGEN,2,20,285,300,5,-0.05833
NGEN,2,20,205,220,5,-0.11667
NGEN,2,20,305,320,5,-0.11667
NGEN,2,20,225,325,100,-0.175
E,1,6,7,2,21,26,27,22
EGEN,3,5,-1
EGEN,4,1,-3
EGEN,3,20,2,11,3
E,61,66,67,62,81,86,87,82
EGEN,3,5,-1
EGEN,4,1,-3
E,65,70,170,165,85,90,190,185
EGEN,3,5,-1
EGEN,2,100,-3
TYPE,2
MAT,2
E,81,86,87,82,101,106,107,102
EGEN,3,5,-1
```

```
EGEN,4,1,-3
EGEN,2,20,-12
E,121,126,141,141,122,127,142,142
E,126,131,141,141,127,132,142,142
E,131,136,141,141,132,137,142,142
EGEN,4,1,-3
E,85,90,190,185,105,110,210,205
EGEN,3,5,-1
EGEN,2,100,-3
EGEN,2,20,-6
E,125,130,145,145,225,230,245,245
E,130,135,145,145,230,235,245,245
E,135,140,145,145,235,240,245,245
EGEN,2,100,-3
NT,265,TEMP,80
RP17,5
KBC,0
TIME,0.5
ITER,-100,100,100
EC,1,1,500,38.4,12,1
EC,1,2,500,38.4,3,1
EC,1,6,500,38.4,10,3
EC,3,6,500,38.4,12,3
EC,10,4,500,38.4,12,1
EC,13,2,500,38.4,17,4
EC,16,4,500,33.4,20,4
EC,13,5,500,38.4,20,1
EC,13,3,500,38.4,20,1
EC,21,1,500,33.4,30,3
EC,23,1,500,38.4,32,3
EC,33,1,500,45.3,35,1
EC,36,1,500,66.1,38,1
LWRI
TIME,5
ITER,-100,100,100
EC,1,1,5000,204,12,1
EC,1,2,5000,204,3,1
EC,1,6,5000,204,10,3
EC,3,6,5000,204,12,3
EC,10,4,5000,204,12,1
EC,13,2,5000,204,17,4
EC,16,4,5000,204,20,4
EC,13,5,5000,204,20,1
EC,13,3,5000,204,20,1
EC,21,1,5000,204,30,3
EC,23,1,5000,204,32,3
EC,33,1,5000,183,35,1
EC,36,1,5000,121,38,1
LWRI
TIME,14.5
ITER,-100,100,100
EC,1,1,5000,204,12,1
EC,1,2,5000,204,3,1
EC,1,6,5000,204,10,3
EC,3,6,5000,204,12,3
```

```
EC,10,4,5000,204,12,1
EC,13,2,5000,204,17,4
EC,16,4,5000,204,20,4
EC,13,5,5000,204,20,1
EC,13,3,5000,204,20,1
EC,21,1,5000,204,30,3
EC,23,1,5000,204,32,3
EC,33,1,5000,183,35,1
EC,36,1,5000,121,38,1
LWRI
TIME,75
ITER,-100,1,1
EC,1,1,5,204,12,1
EC,1,2,5,204,3,1
EC,1,6,5,204,10,3
EC,3,6,5,204,12,3
EC,10,4,5,204,12,1
EC,13,2,5,204,17,4
EC,16,4,5,204,20,4
EC,13,5,5,204,20,1
EC,13,3,5,204,20,1
EC,21,1,5,204,30,3
EC,23,1,5,204,32,3
EC,33,1,5,183,35,1
EC,36,1,5,121,38,1
LWRI
/PBC,ALL,1
AFWRIT
FINISH
```

```
C*** Program six, Film coefficient = 15000 W/m-K
C*** First heating temperature = 204C
/PREP7
/TITLE,THESIS MODEL, Program six
KAN,-1
ET,1,70
ET,2,70
MPTEMP,1,20,100,204
MPDATA,EX,1,1,219E9,214E9,207.68E9
MPDATA,EX,2,1,211E9,207E9,199.72E9
MPDATA,ALPX,1,1,9.7E-6,10.1E-6,10.516E-6
MPDATA,ALPX,2,1,9.9E-6,11E-6,12.03E-6
MPDATA,KXX,1,1,27,27,27
MPDATA,KXX,2,1,44,43,41.92
MPDATA,C,1,1,460,480,521.6
MPDATA,C,2,1,460,480,521.6
MPDATA,DENS,1,1,7750,7750,7750
MPDATA,DENS,2,1,7850,7850,7850
TUNIF,20
CSYS,1
N,1,0.4,-4.0909,0
N,5,0.4,-4.0909,0.1
FILL,1,5,3
NGEN,4,5,1,5,1,,2.727
NGEN,2,20,1,20,1,-0.01
NGEN,2,20,26,35,1,-0.015
NGEN,2,40,21,40,1,-0.03
NGEN,2,20,61,80,1,-0.01
NGEN,2,20,81,100,1,-0.05833
NGEN,2,20,101,120,1,-0.11667
NGEN,2,20,121,125,1,-0.175
N,165,0.36,-4.0909,0.987
N,265,0.36,-4.0909,2.76
NGEN,4,5,165,265,100,,2.727
NGEN,2,20,165,180,5,-0.01
NGEN,2,20,265,280,5,-0.01
NGEN,2,20,185,200,5,-0.05833
NGEN,2,20,285,300,5,-0.05833
NGEN,2,20,205,220,5,-0.11667
NGEN,2,20,305,320,5,-0.11667
NGEN,2,20,225,325,100,-0.175
E,1,6,7,2,21,26,27,22
EGEN,3,5,-1
EGEN,4,1,-3
EGEN,3,20,2,11,3
E,61,66,67,62,81,86,87,32
EGEN,3,5,-1
EGEN,4,1,-3
E,65,70,170,165,85,90,190,185
EGEN,3,5,-1
EGEN,2,100,-3
TYPE,2
MAT,2
E,61,36,37,82,101,106,107,102
EGEN,3,5,-1
```

```
EGEN,4,1,-3
EGEN,2,20,-12
E,121,126,141,141,122,127,142,142
E,126,131,141,141,127,132,142,142
E,131,136,141,141,132,137,142,142
EGEN,4,1,-3
E,85,90,190,185,105,110,210,205
EGEN,3,5,-1
EGEN,2,100,-3
EGEN,2,20,-6
E,125,130,145,145,225,230,245,245
E,130,135,145,145,230,235,245,245
E,135,140,145,145,235,240,245,245
EGEN,2,100,-3
NT,205,TEMP,80
RP17,5
KBC,0
TIME,0.5
ITER,-100,100,100
EC,1,1,1500,38.4,12,1
EC,1,2,1500,38.4,3,1
EC,1,6,1500,38.4,10,3
EC,3,6,1500,38.4,12,3
EC,10,4,1500,38.4,12,1
EC,13,2,1500,38.4,17,4
EC,16,4,1500,38.4,20,4
EC,13,5,1500,38.4,20,1
EC,13,3,1500,38.4,20,1
EC,21,1,1500,38.4,30,3
EC,23,1,1500,38.4,32,3
EC,33,1,1500,45.3,35,1
EC,36,1,1500,66.1,38,1
LWRI
TIME,5
ITER,-100,100,100
EC,1,1,15000,204,12,1
EC,1,2,15000,204,3,1
EC,1,6,15000,204,10,3
EC,3,6,15000,204,12,3
EC,10,4,15000,204,12,1
EC,13,2,15000,204,17,4
EC,16,4,15000,204,20,4
EC,13,5,15000,204,20,1
EC,13,3,15000,204,20,1
EC,21,1,15000,204,30,3
EC,23,1,15000,204,32,3
EC,33,1,15000,183,35,1
EC,36,1,15000,121,38,1
LWRI
TIME,14.5
ITER,-100,100,100
EC,1,1,15000,204,12,1
EC,1,2,15000,204,3,1
EC,1,6,15000,204,10,3
EC,3,6,15000,204,12,3
```

```
EC,10,4,15000,204,12,1
EC,13,2,15000,204,17,4
EC,16,4,15000,204,20,4
EC,13,5,15000,204,20,1
EC,13,3,15000,204,20,1
EC,21,1,15000,204,30,3
EC,23,1,15000,204,32,3
EC,33,1,15000,183,35,1
EC,36,1,15000,121,38,1
LWRI
TIME,75
ITER,-100,1,1
EC,1,1,5,204,12,1
EC,1,2,5,204,3,1
EC,1,6,5,204,10,3
EC,3,6,5,204,12,3
EC,10,4,5,204,12,1
EC,13,2,5,204,17,4
EC,16,4,5,204,20,4
EC,13,5,5,204,20,1
EC,13,3,5,204,20,1
EC,21,1,5,204,30,3
EC,23,1,5,204,32,3
EC,33,1,5,183,35,1
EC,36,1,5,121,38,1
LWRI
/PBC,ALL,1
AFWRIT
FINISH
```

```
C*** Program seven, Load step 5 = 20 minutes
C*** First heating temperature = 142C
/PREP7
/TITLE,THESIS MODEL, Program seven
KAN,-1
ET,1,70
ET,2,70
MPTEMP,1,20,100,204
MPDATA,EX,1,1,219E9,214E9,207.68E9
MPDATA,EX,2,1,211E9,207E9,199.72E9
MPDATA,ALPX,1,1,9.7E-6,10.1E-6,10.516E-6
MPDATA,ALPX,2,1,9.9E-6,11E-6,12.03E-6
MPDATA,KXX,1,1,27,27,27
MPDATA,KXX,2,1,44,43,41.92
MPDATA,C,1,1,460,480,521.6
MPDATA,C,2,1,460,480,521.6
MPDATA,DENS,1,1,7750,7750,7750
MPDATA,DENS,2,1,7850,7850,7850
MPDATA,HF,1,1,0,4444.44,10000
TUNIF,20
CSYS,1
N,1,0.4,-4.0909,0
N,5,0.4,-4.0909,0.1
FILL,1,5,3
NGEN,4,5,1,5,1,,2.727
NGEN,2,20,1,20,1,-0.01
NGEN,2,20,26,35,1,-0.015
NGEN,2,40,21,40,1,-0.03
NGEN,2,20,61,80,1,-0.01
NGEN,2,20,81,100,1,-0.05833
NGEN,2,20,101,120,1,-0.11667
NGEN,2,20,121,125,1,-0.175
N,165,0.36,-4.0909,0.987
N,265,0.36,-4.0909,2.76
NGEN,4,5,165,265,100,,2.727
NGEN,2,20,165,180,5,-0.01
NGEN,2,20,265,280,5,-0.01
NGEN,2,20,185,200,5,-0.05833
NGEN,2,20,285,300,5,-0.05833
NGEN,2,20,205,220,5,-0.11667
NGEN,2,20,305,320,5,-0.11667
NGEN,2,20,225,325,100,-0.175
E,1,6,7,2,21,26,27,22
EGEN,3,5,-1
EGEN,4,1,-3
EGEN,3,20,2,11,3
E,61,66,67,62,81,86,87,82
EGEN,3,5,-1
EGEN,4,1,-3
E,65,70,170,165,85,90,190,185
EGEN,3,5,-1
EGEN,2,100,-3
TYPE,2
MAT,2
E,81,86,87,82,101,106,107,102
```

```
EGEN,3,5,-1
EGEN,4,1,-3
EGEN,2,20,-12
E,121,126,141,141,122,127,142,142
E,126,131,141,141,127,132,142,142
E,131,136,141,141,132,137,142,142
EGEN,4,1,-3
E,85,90,190,185,105,110,210,205
EGEN,3,5,-1
EGEN,2,100,-3
EGEN,2,20,-6
E,125,130,145,145,225,230,245,245
E,130,135,145,145,230,235,245,245
E,135,140,145,145,235,240,245,245
EGEN,2,100,-3
NT,265,TEMP,80
RP17,5
KBC,0
TIME,0.5
ITER,-100,100,100
EC,1,1,1000,32.2,12,1
EC,1,2,1000,32.2,3,1
EC,1,6,1000,32.2,10,3
EC,3,6,1000,32.2,12,3
EC,10,4,1000,32.2,12,1
EC,13,2,1000,32.2,17,4
EC,16,4,1000,32.2,20,4
EC,13,5,1000,32.2,20,1
EC,13,3,1000,32.2,20,1
EC,21,1,1000,32.2,30,3
EC,23,1,1000,32.2,32,3
EC,33,1,1000,40.2,35,1
EC,36,1,1000,64.1,38,1
LWRI
TIME,5
ITER,-100,100,100
EC,1,1,10000,142,12,1
EC,1,2,10000,142,3,1
EC,1,6,10000,142,10,3
EC,3,6,10000,142,12,3
EC,10,4,10000,142,12,1
EC,13,2,10000,142,17,4
EC,16,4,10000,142,20,4
EC,13,5,10000,142,20,1
EC,13,3,10000,142,20,1
EC,21,1,10000,142,30,3
EC,23,1,10000,142,32,3
EC,33,1,10000,132,35,1
EC,36,1,10000,101,38,1
LWRI
TIME,14.5
ITER,-100,100,100
EC,1,1,10000,142,12,1
EC,1,2,10000,142,3,1
EC,1,6,10000,142,10,3
```

```
EC,3,6,10000,142,12,3
EC,10,4,10000,142,12,1
EC,13,2,10000,142,17,4
EC,16,4,10000,142,20,4
EC,13,5,10000,142,20,1
EC,13,3,10000,142,20,1
EC,21,1,10000,142,30,3
EC,23,1,10000,142,32,3
EC,33,1,10000,132,35,1
EC,36,1,10000,101,38,1
LWRI
TIME,75
ITER,-100,1,1
EC,1,1,5,142,12,1
EC,1,2,5,142,3,1
EC,1,6,5,142,10,3
EC,3,6,5,142,12,3
EC,10,4,5,142,12,1
EC,13,2,5,142,17,4
EC,16,4,5,142,20,4
EC,13,5,5,142,20,1
EC,13,3,5,142,20,1
EC,21,1,5,142,30,3
EC,23,1,5,142,32,3
EC,33,1,5,132,35,1
EC,36,1,5,101,38,1
LWRI
TIME,1275
ITER,-100,100,100
EC,1,1,5,142,12,1
EC,1,2,5,142,3,1
EC,1,6,5,142,10,3
EC,3,6,5,142,12,3
EC,10,4,5,142,12,1
EC,13,2,5,142,17,4
EC,16,4,5,142,20,4
EC,13,5,5,142,20,1
EC,13,3,5,142,20,1
EC,21,1,5,142,30,3
EC,23,1,5,142,32,3
EC,33,1,5,132,35,1
EC,36,1,5,101,38,1
LWRI
TIME,1275.5
ITER,-100,100,100
EC,1,1,1000,148.2,12,1
EC,1,2,1000,148.2,3,1
EC,1,6,1000,148.2,10,3
EC,3,6,1000,148.2,12,3
EC,10,4,1000,148.2,12,1
EC,13,2,1000,148.2,17,4
EC,16,4,1000,148.2,20,4
EC,13,5,1000,148.2,20,1
EC,13,3,1000,148.2,20,1
EC,21,1,1000,148.2,30,3
```

```
EC,23,1,1000,148.2,32,3
EC,33,1,1000,136.8,35,1
EC,36,1,1000,102.7,38,1
LWRI
TIME,1280
ITER,-100,100,100
EC,1,1,10000,204,12,1
EC,1,2,10000,204,3,1
EC,1,6,10000,204,10,3
EC,3,6,10000,204,12,3
EC,10,4,10000,204,12,1
EC,13,2,10000,204,17,4
EC,16,4,10000,204,20,4
EC,13,5,10000,204,20,1
EC,13,3,10000,204,20,1
EC,21,1,10000,204,30,3
EC,23,1,10000,204,32,3
EC,33,1,10000,183,35,1
EC,36,1,10000,121,38,1
LWRI
TIME,1289.5
ITER,-100,100,100
EC,1,1,10000,204,12,1
EC,1,2,10000,204,3,1
EC,1,6,10000,204,10,3
EC,3,6,10000,204,12,3
EC,10,4,10000,204,12,1
EC,13,2,10000,204,17,4
EC,16,4,10000,204,20,4
EC,13,5,10000,204,20,1
EC,13,3,10000,204,20,1
EC,21,1,10000,204,30,3
EC,23,1,10000,204,32,3
EC,33,1,10000,183,35,1
EC,36,1,10000,121,38,1
LWRI
TIME,1350
ITER,-100,1,1
EC,1,1,5,204,12,1
EC,1,2,5,204,3,1
EC,1,6,5,204,10,3
EC,3,6,5,204,12,3
EC,10,4,5,204,12,1
EC,13,2,5,204,17,4
EC,16,4,5,204,20,4
EC,13,5,5,204,20,1
EC,13,3,5,204,20,1
EC,21,1,5,204,30,3
EC,23,1,5,204,32,3
EC,33,1,5,183,35,1
EC,36,1,5,121,38,1
LWRI
/PBC,ALL,1
AFWRIT
FINISH
```

```
C*** Program eight, Load step 5 = 20 minutes
C*** First heating temperature = 160C
/PREP7
/TITLE,THESIS MODEL, Program eight
KAN,-1
ET,1,70
ET,2,70
MPTEMP,1,20,100,204
MPDATA,EX,1,1,219E9,214E9,207.68E9
MPDATA,EX,2,1,211E9,207E9,199.72E9
MPDATA,ALPX,1,1,9.7E-6,10.1E-6,10.516E-6
MPDATA,ALPX,2,1,9.9E-6,11E-6,12.03E-6
MPDATA,KXX,1,1,27,27,27
MPDATA,KXX,2,1,44,43,41.92
MPDATA,C,1,1,460,480,521.6
MPDATA,C,2,1,460,480,521.6
MPDATA,DENS,1,1,7750,7750,7750
MPDATA,DENS,2,1,7850,7850,7850
TUNIF,20
CSYS,1
N,1,0.4,-4.0909,0
N,5,0.4,-4.0909,0.1
FILL,1,5,3
NGEN,4,5,1,5,1,,2.727
NGEN,2,20,1,20,1,-0.01
NGEN,2,20,26,35,1,-0.015
NGEN,2,40,21,40,1,-0.03
NGEN,2,20,61,80,1,-0.01
NGEN,2,20,81,100,1,-0.05833
NGEN,2,20,101,120,1,-0.11667
NGEN,2,20,121,125,1,-0.175
N,165,0.36,-4.0909,0.987
N,265,0.36,-4.0909,2.76
NGEN,4,5,165,265,100,,2.727
NGEN,2,20,165,180,5,-0.01
NGEN,2,20,265,280,5,-0.01
NGEN,2,20,185,200,5,-0.05833
NGEN,2,20,285,300,5,-0.05833
NGEN,2,20,205,220,5,-0.11667
NGEN,2,20,305,320,5,-0.11667
NGEN,2,20,225,325,100,-0.175
E,1,6,7,2,21,26,27,22
EGEN,3,5,-1
EGEN,4,1,-3
EGEN,3,20,2,11,3
E,61,66,67,62,81,86,87,82
EGEN,3,5,-1
EGEN,4,1,-3
E,65,70,170,165,85,90,190,185
EGEN,3,5,-1
EGEN,2,100,-3
TYPE,2
MAT,2
E,81,86,87,82,101,106,107,102
EGEN,3,5,-1
```

```
EGEN,4,1,-3
EGEN,2,20,-12
E,121,126,141,141,122,127,142,142
E,126,131,141,141,127,132,142,142
E,131,136,141,141,132,137,142,142
EGEN,4,1,-3
E,85,90,190,185,105,110,210,205
EGEN,3,5,-1
EGEN,2,100,-3
EGEN,2,20,-6
E,125,130,145,145,225,230,245,245
E,130,135,145,145,230,235,245,245
E,135,140,145,145,235,240,245,245
EGEN,2,100,-3
NT,265,TEMP,80
RP17,5
KBC,0
TIME,0.5
ITER,-100,100,100
EC,1,1,1000,34,12,1
EC,1,2,1000,34,3,1
EC,1,6,1000,34,10,3
EC,3,6,1000,34,12,3
EC,10,4,1000,34,12,1
EC,13,2,1000,34,17,4
EC,16,4,1000,34,20,4
EC,13,5,1000,34,20,1
EC,13,3,1000,34,20,1
EC,21,1,1000,34,30,3
EC,23,1,1000,34,32,3
EC,33,1,1000,41.7,35,1
EC,36,1,1000,64.7,38,1
LWRI
TIME,5
ITER,-100,100,100
EC,1,1,10000,160,12,1
EC,1,2,10000,160,3,1
EC,1,6,10000,160,10,3
EC,3,6,10000,160,12,3
EC,10,4,10000,160,12,1
EC,13,2,10000,160,17,4
EC,16,4,10000,160,20,4
EC,13,5,10000,160,20,1
EC,13,3,10000,160,20,1
EC,21,1,10000,160,30,3
EC,23,1,10000,160,32,3
EC,33,1,10000,146.7,35,1
EC,36,1,10000,106.7,38,1
LWRI
TIME,14.5
ITER,-100,100,100
EC,1,1,10000,160,12,1
EC,1,2,10000,160,3,1
EC,1,6,10000,160,10,3
EC,3,6,10000,160,12,3
```

```
EC,10,4,10000,160,12,1
EC,13,2,10000,160,17,4
EC,16,4,10000,160,20,4
EC,13,5,10000,160,20,1
EC,13,3,10000,160,20,1
EC,21,1,10000,160,30,3
EC,23,1,10000,160,32,3
EC,33,1,10000,146.7,35,1
EC,36,1,10000,106.7,38,1
LWRI
TIME,75
ITER,-100,1,1
EC,1,1,5,160,12,1
EC,1,2,5,160,3,1
EC,1,6,5,160,10,3
EC,3,6,5,160,12,3
EC,10,4,5,160,12,1
EC,13,2,5,160,17,4
EC,16,4,5,160,20,4
EC,13,5,5,160,20,1
EC,13,3,5,160,20,1
EC,21,1,5,160,30,3
EC,23,1,5,160,32,3
EC,33,1,5,146.7,35,1
EC,36,1,5,106.7,38,1
LWRI
TIME,1275
ITER,-100,100,100
EC,1,1,5,160,12,1
EC,1,2,5,160,3,1
EC,1,6,5,160,10,3
EC,3,6,5,160,12,3
EC,10,4,5,160,12,1
EC,13,2,5,160,17,4
EC,16,4,5,160,20,4
EC,13,5,5,160,20,1
EC,13,3,5,160,20,1
EC,21,1,5,160,30,3
EC,23,1,5,160,32,3
EC,33,1,5,146.7,35,1
EC,36,1,5,106.7,38,1
LWRI
TIME,1275.5
ITER,-100,100,100
EC,1,1,1000,164.4,12,1
EC,1,2,1000,164.4,3,1
EC,1,6,1000,164.4,10,3
EC,3,6,1000,164.4,12,3
EC,10,4,1000,164.4,12,1
EC,13,2,1000,164.4,17,4
EC,16,4,1000,164.4,20,4
EC,13,5,1000,164.4,20,1
EC,13,3,1000,164.4,20,1
EC,21,1,1000,164.4,30,3
EC,23,1,1000,164.4,32,3
```

```
EC,33,1,1000,137.0,35,1
EC,36,1,1000,103.1,38,1
LWRI
TIME,1280
ITER,-100,100,100
EC,1,1,10000,204,12,1
EC,1,2,10000,204,3,1
EC,1,6,10000,204,10,3
EC,3,6,10000,204,12,3
EC,10,4,10000,204,12,1
EC,13,2,10000,204,17,4
EC,16,4,10000,204,20,4
EC,13,5,10000,204,20,1
EC,13,3,10000,204,20,1
EC,21,1,10000,204,30,3
EC,23,1,10000,204,32,3
EC,33,1,10000,183,35,1
EC,36,1,10000,121,38,1
LWRI
TIME,1289.5
ITER,-100,100,100
EC,1,1,10000,204,12,1
EC,1,2,10000,204,3,1
EC,1,6,10000,204,10,3
EC,3,6,10000,204,12,3
EC,10,4,10000,204,12,1
EC,13,2,10000,204,17,4
EC,16,4,10000,204,20,4
EC,13,5,10000,204,20,1
EC,13,3,10000,204,20,1
EC,21,1,10000,204,30,3
EC,23,1,10000,204,32,3
EC,33,1,10000,183,35,1
EC,36,1,10000,121,38,1
LWRI
TIME,1350
ITER,-100,1,1
EC,1,1,5,204,12,1
EC,1,2,5,204,3,1
EC,1,6,5,204,10,3
EC,3,6,5,204,12,3
EC,10,4,5,204,12,1
EC,13,2,5,204,17,4
EC,16,4,5,204,20,4
EC,13,5,5,204,20,1
EC,13,3,5,204,20,1
EC,21,1,5,204,30,3
EC,23,1,5,204,32,3
EC,33,1,5,183,35,1
EC,36,1,5,121,38,1
LWRI
/PBC,ALL,1
AFWRIT
FINISH
```

```
C*** Program nine, Load step 5 = 20 minutes
C*** First heating temperature = 162C
/PREP7
/TITLE,THESIS MODEL, Program nine
KAN,-1
ET,1,70
ET,2,70
MPTEMP,1,20,100,204
MPDATA,EX,1,1,219E9,214E9,207.68E9
MPDATA,EX,2,1,211E9,207E9,199.72E9
MPDATA,ALPX,1,1,9.7E-6,10.1E-6,10.516E-6
MPDATA,ALPX,2,1,9.9E-6,11E-6,12.03E-6
MPDATA,KXX,1,1,27,27,27
MPDATA,KXX,2,1,44,43,41.92
MPDATA,C,1,1,460,480,521.6
MPDATA,C,2,1,460,480,521.6
MPDATA,DENS,1,1,7750,7750,7750
MPDATA,DENS,2,1,7850,7850,7850
MPDATA,HF,1,1,0,4444.44,10000
TUNIF,20
CSYS,1
N,1,0.4,-4.0909,0
N,5,0.4,-4.0909,0.1
FILL,1,5,3
NGEN,4,5,1,5,1,,2.727
NGEN,2,20,1,20,1,-0.01
NGEN,2,20,26,35,1,-0.015
NGEN,2,40,31,40,1,-0.03
NGEN,2,20,61,80,1,-0.01
NGEN,2,20,81,100,1,-0.05833
NGEN,2,20,101,120,1,-0.11667
NGEN,2,20,121,125,1,-0.175
N,165,0.36,-4.0909,0.987
N,265,0.36,-4.0909,2.76
NGEN,4,5,165,265,100,,2.727
NGEN,2,20,165,180,5,-0.01
NGEN,2,20,265,280,5,-0.01
NGEN,2,20,185,200,5,-0.05833
NGEN,2,20,285,300,5,-0.05833
NGEN,2,20,205,220,5,-0.11667
NGEN,2,20,305,320,5,-0.11667
NGEN,2,20,225,325,100,-0.175
E,1,6,7,2,21,26,27,22
EGEN,3,5,-1
EGEN,4,1,-3
EGEN,3,20,2,11,3
E,61,66,67,62,81,86,87,82
EGEN,3,5,-1
EGEN,4,1,-3
E,65,70,170,165,85,90,190,185
EGEN,3,5,-1
EGEN,2,100,-3
TYPE,2
MAT,2
E,81,86,87,82,101,106,107,102
```

```
EGEN,3,5,-1
EGEN,4,1,-3
EGEN,2,20,-12
E,121,126,141,141,122,127,142,142
E,126,131,141,141,127,132,142,142
E,131,136,141,141,132,137,142,142
EGEN,4,1,-3
E,85,90,190,185,105,110,210,205
EGEN,3,5,-1
EGEN,2,100,-3
EGEN,2,20,-6
E,125,130,145,145,225,230,245,245
E,130,135,145,145,230,235,245,245
E,135,140,145,145,235,240,245,245
EGEN,2,100,-3
NT,265,TEMP,80
RP17,5
KBC,0
TIME,0.5
ITER,-100,100,100
EC,1,1,1000,34.2,12,1
EC,1,2,1000,34.2,3,1
EC,1,6,1000,34.2,10,3
EC,3,6,1000,34.2,12,3
EC,10,4,1000,34.2,12,1
EC,13,2,1000,34.2,17,4
EC,16,4,1000,34.2,20,4
EC,13,5,1000,34.2,20,1
EC,13,3,1000,34.2,20,1
EC,21,1,1000,34.2,30,3
EC,23,1,1000,34.2,32,3
EC,33,1,1000,41.7,35,1
EC,36,1,1000,64.7,38,1
LWRI
TIME,5
ITER,-100,100,100
EC,1,1,10000,162,12,1
EC,1,2,10000,162,3,1
EC,1,6,10000,162,10,3
EC,3,6,10000,162,12,3
EC,10,4,10000,162,12,1
EC,13,2,10000,162,17,4
EC,16,4,10000,162,20,4
EC,13,5,10000,162,20,1
EC,13,3,10000,162,20,1
EC,21,1,10000,162,30,3
EC,23,1,10000,162,32,3
EC,33,1,10000,146.8,35,1
EC,36,1,10000,106.8,38,1
LWRI
TIME,14.5
ITER,-100,100,100
EC,1,1,10000,162,12,1
EC,1,2,10000,162,3,1
EC,1,6,10000,162,10,3
```

```
EC,3,6,10000,162,12,3
EC,10,4,10000,162,12,1
EC,13,2,10000,162,17,4
EC,16,4,10000,162,20,4
EC,13,5,10000,162,20,1
EC,13,3,10000,162,20,1
EC,21,1,10000,162,30,3
EC,23,1,10000,162,32,3
EC,33,1,10000,146.8,35,1
EC,36,1,10000,106.8,38,1
LWRI
TIME,75
ITER,-100,1,1
EC,1,1,5,162,12,1
EC,1,2,5,162,3,1
EC,1,6,5,162,10,3
EC,3,6,5,162,12,3
EC,10,4,5,162,12,1
EC,13,2,5,162,17,4
EC,16,4,5,162,20,4
EC,13,5,5,162,20,1
EC,13,3,5,162,20,1
EC,21,1,5,162,30,3
EC,23,1,5,162,32,3
EC,33,1,5,146.8,35,1
EC,36,1,5,106.8,38,1
LWRI
TIME,1275
ITER,-100,100,100
EC,1,1,5,162,12,1
EC,1,2,5,162,3,1
EC,1,6,5,162,10,3
EC,3,6,5,162,12,3
EC,10,4,5,162,12,1
EC,13,2,5,162,17,4
EC,16,4,5,162,20,4
EC,13,5,5,162,20,1
EC,13,3,5,162,20,1
EC,21,1,5,162,30,3
EC,23,1,5,162,32,3
EC,33,1,5,146.8,35,1
EC,36,1,5,106.8,38,1
LWRI
TIME,1275.5
ITER,-100,100,100
EC,1,1,1000,166.2,12,1
EC,1,2,1000,166.2,3,1
EC,1,6,1000,166.2,10,3
EC,3,6,1000,166.2,12,3
EC,10,4,1000,166.2,12,1
EC,13,2,1000,166.2,17,4
EC,16,4,1000,166.2,20,4
EC,13,5,1000,166.2,20,1
EC,13,3,1000,166.2,20,1
EC,21,1,1000,166.2,30,3
```

```
EC,25,1,1000,166.2,32,3
EC,33,1,1000,137.1,35,1
EC,36,1,1000,103.2,38,1
LWRI
TIME,1280
ITER,-100,100,100
EC,1,1,10000,204,12,1
EC,1,2,10000,204,3,1
EC,1,6,10000,204,10,3
EC,3,6,10000,204,12,3
EC,10,4,10000,204,12,1
EC,13,2,10000,204,17,4
EC,16,4,10000,204,20,4
EC,13,5,10000,204,20,1
EC,13,3,10000,204,20,1
EC,21,1,10000,204,30,3
EC,23,1,10000,204,32,3
EC,33,1,10000,183,35,1
EC,36,1,10000,121,38,1
LWRI
TIME,1289.5
ITER,-100,100,100
EC,1,1,10000,204,12,1
EC,1,2,10000,204,3,1
EC,1,6,10000,204,10,3
EC,3,6,10000,204,12,3
EC,10,4,10000,204,12,1
EC,13,2,10000,204,17,4
EC,16,4,10000,204,20,4
EC,13,5,10000,204,20,1
EC,13,3,10000,204,20,1
EC,21,1,10000,204,30,3
EC,23,1,10000,204,32,3
EC,33,1,10000,183,35,1
EC,36,1,10000,121,38,1
LWRI
TIME,1350
ITER,-100,1,1
EC,1,1,5,204,12,1
EC,1,2,5,204,3,1
EC,1,6,5,204,10,3
EC,3,6,5,204,12,3
EC,10,4,5,204,12,1
EC,13,2,5,204,17,4
EC,16,4,5,204,20,4
EC,13,5,5,204,20,1
EC,13,3,5,204,20,1
EC,21,1,5,204,30,3
EC,23,1,5,204,32,3
EC,33,1,5,183,35,1
EC,36,1,5,121,38,1
LWRI
/PSC,ALL,1
AFWRIT
FINISH
```

TABLE 8.1

LOAD STEP 4 ITERATION= 55 SECTION= 1
TIME= 32.775 LOAD CASE= 1

NODE	TEMP
1	162.0
2	162.0
3	162.0
4	162.0
5	162.0
6	162.0
7	162.0
8	162.0
9	162.0
10	162.0
11	162.0
12	162.0
13	162.0
14	162.0

NODE	TEMP
15	162.0
16	162.0
17	162.0
18	162.0
19	162.0
20	162.0
21	162.0
22	162.0
23	162.0
24	162.0
25	162.0
26	161.8
27	161.9
28	161.8

NODE	TEMP
29	161.8
30	161.7
31	161.8
32	161.9
33	161.8
34	161.8
35	161.7
36	162.0
37	162.0
38	162.0
39	162.0
40	162.0
46	159.3
47	158.7

NODE	TEMP

48	158.6
49	158.1
50	158.8
51	159.8
52	158.7
53	158.6
54	158.1
55	158.8
61	134.4
62	134.4
63	134.2
64	133.9
65	122.9
66	140.9

NODE	TEMP
67	136.4
68	136.4
69	136.3
70	123.2
71	140.9
72	136.4
73	136.4
74	136.3
75	123.2
76	134.4
77	134.4
78	134.2
79	133.9
80	122.9

NODE	TEMP
81	86.65
82	86.10
83	85.59
84	84.07
85	78.76
86	87.01
87	86.26
88	85.69
89	84.17
90	78.78
91	87.01
92	86.26
93	85.69
94	84.17

NODE	TEMP
95	78.78
96	86.65
97	86.10
98	85.59
99	84.07
100	78.76
101	24.21

102	24.23
103	24.13
104	23.85
105	23.51
106	24.17
107	24.23
108	24.13

NODE	TEMP
109	23.85
110	23.51
111	24.17
112	24.23
113	24.13
114	23.85
115	23.51
116	24.21
117	24.23
118	24.13
119	23.85
120	23.51
121	20.07
122	20.06

NODE	TEMP
123	20.06
124	20.06
125	20.05
126	20.08
127	20.06
128	20.06
129	20.06
130	20.05
131	20.08
132	20.06
133	20.06
134	20.06
135	20.05
136	20.07

NODE	TEMP
137	20.06
138	20.06
139	20.06
140	20.05
141	20.00
142	20.00
143	20.00
144	20.00
145	20.00
165	102.3
170	102.3
175	102.3
180	102.3
185	62.25

NODE	TEMP
190	62.25
195	62.25
200	62.25
205	22.26
210	22.26
215	22.26
220	22.26
225	20.05
230	20.05
235	20.05
240	20.05
245	20.02
265	80.00
270	80.00

NODE	TEMP
275	80.00
280	80.00
285	80.00
290	80.00
295	80.00
300	80.00
305	80.00
310	80.00
315	80.00
320	80.00
325	80.00
330	80.00
335	80.00
340	80.00

NODE	TEMP
345	80.00

MAXIMUMS

NODE	21
VALUE	162.0